Mississippi State University
Scholars Junction

Theses and Dissertations | Theses and Dissertations

1-1-2018

Detailed Beta-Decay Studies of Neutron-Rich 74-77Ga Isotopes

Umesh Silwal

Follow this and additional works at: https://scholarsjunction.msstate.edu/td

Recommended Citation
Silwal, Umesh, "Detailed Beta-Decay Studies of Neutron-Rich 74-77Ga Isotopes" (2018). *Theses and Dissertations*. 1326.
https://scholarsjunction.msstate.edu/td/1326

This Dissertation - Open Access is brought to you for free and open access by the Theses and Dissertations at Scholars Junction. It has been accepted for inclusion in Theses and Dissertations by an authorized administrator of Scholars Junction. For more information, please contact scholcomm@msstate.libanswers.com.

www.manaraa.com

Detailed β-decay studies of neutron-rich $^{74-77}$Ga isotopes

By

Umesh Silwal

A Dissertation
Submitted to the Faculty of
Mississippi State University
in Partial Fulfillment of the Requirements
for the Degree of Doctor of Philosophy
in Engineering/Applied Physics
in the Bagley College of Engineering

Mississippi State, Mississippi

December 2018

www.manaraa.com

Copyright by

Umesh Silwal

2018

www.manaraa.com

Detailed β-decay studies of neutron-rich $^{74-77}$Ga isotopes

By

Umesh Silwal

Approved:

Jeffry A. Winger
(Major Professor)

James A. Dunne
(Committee Member)

Dipangkar Dutta
(Committee Member)

Benjamin P. Crider
(Committee Member)

Yaroslav Koshka
(Committee Member)

Hendrik F. Arnoldus
(Graduate Coordinator)

Jason M. Keith
Dean
Bagley College of Engineering

www.manaraa.com

Name: Umesh Silwal

Date of Degree: December , 2018

Institution: Mississippi State University

Major Field: Engineering/Applied Physics

Major Professor: Dr. Jeffry Allen Winger

Title of Study: Detailed β-decay studies of neutron-rich $^{74-77}$Ga isotopes

Pages of Study: 193

Candidate for Degree of Doctor of Philosophy

The National Nuclear Data Center (NNDC) contains a compilation of information on the β decays of Gallium isotopes. In the mass range A = 74 to 77, the Germanium daughters lie close to or at the valley of stability leading us to believe the decays would have been well studied. However, closer inspection indicates significant conflict for placement of γ-rays and energy levels between different measurements, especially for upper-lying states. Detailed β-decay studies for the $^{74-77}$Ga isotopes were performed using a high resolution four clover Hyper-Pure Germanium (HPGe) detector system with two β scintillators in the Holifield Radioactive Ion Beam Facility (HRIBF) at Oak Ridge National Lab (ORNL) to better understand the structure of the corresponding $^{74-77}$Ge daughter nuclei. In our experiments, use of a high-resolution mass separator greatly improved the purity of the samples in comparison to previous measurements. Besides that, the efficiency of the detector system we utilized was much higher than used in previous studies. We also

www.manaraa.com

established a method to determine statistically significant $\gamma\gamma$ coincidence relationships to add reliability to the placement of γ rays to energy levels and avoid experimental biases.

From our analysis, we have established comprehensive decay schemes for all four Germanium nuclei in this study. In most cases, we have extended the energy levels to cover more of the energy window available for β decay. Our proposed ^{74}Ge decay scheme contains 44 energy levels occupying up to 4.36 MeV with the placement of 99 γ rays. Similarly, ^{75}Ga decay scheme contains 71 γ rays with 30 energy levels occupying up to 2.75 MeV. The ^{76}Ga decay scheme has 48 excited states with 100 γ rays occupying up to 4.81 MeV. And, the ^{77}Ge decay scheme has 67 γ rays and 33 energy levels occupying up to 3.14 MeV. Based on the expanded level schemes, β-feeding intensity and $\log(ft)$ value lower limits were calculated and attempts were made to assign the spin-parity of the observed states. The resulting level schemes were then compared with the Nushellx theoretical predictions.

Key words: Exotic nuclei, Shell model, High-resolution, Statistically significant, β-feeding, $\log(ft)$, Nushellx result

www.manaraa.com

DEDICATION

To my loving grandmother,

Late Padma Kumari Silwal

To my parents,

Padam Prasad Silwal and Dil Kumari Silwal

My wife,

Sweta

And

Brothers

Milan and Sushil

www.manaraa.com

ACKNOWLEDGEMENTS

I would like to express my sincere gratitude to my advisor Dr. Jeffry Allen Winger for his continuous support, encouragement, and guidance throughout my Ph.D and research. I am thankful to him for providing me the opportunity to work in different projects at the Holifield Radioactive Ion Facility (HRIBF) in Oak Ridge National Lab (ORNL).

I would like to thank my dissertation committee members Dr. James Dunne, Dr. Dipangkar Dutta, Dr. Ben Crider, and Dr. Yaroslav Koshka for their insightful comments and valuable time.

I would like to thank the Department of Physics and Astronomy, Mississippi State University and all its staff for their constant support throughout my graduate study.

I am grateful to the HRIBF, especially Dr. Krzysztof Rykaczwski for helping us during our work at ORNL.

I would like to acknowledge Dr. Robert Grzywacz for providing the computing facility and guidance for Nushellx calculations.

Thanks to my research group mates Dr. James L Tracy, Jr and Durga P. Siwakoti. It was an immense pleasure working with them.

Thanks to all the friends and Nepalese community at Starkville for their continuous encouragement during the challenges of graduate school.

At last but not the least, I would also like to thank my family for their love, faith, support,

www.manaraa.com

and inspiration. I am especially thankful to my wife Sweta and brother Sushil for continued help and support.

www.manaraa.com

TABLE OF CONTENTS

www.manaraa.com

www.manaraa.com

www.manaraa.com

LIST OF TABLES

www.manaraa.com

LIST OF FIGURES

www.manaraa.com

www.manaraa.com

www.manaraa.com

LIST OF SYMBOLS, ABBREVIATIONS, AND NOMENCLATURE

Symbols used

N: Total number of neutrons in a nucleus.

Z: Total number of protons in a nucleus.

A: Mass number of the nucleus, which is the sum of the total protons and neutrons.

MeV: Mega electron volt, 1 MeV = 10^6 electron Volt.

keV: Kilo electron volt, 1keV = 10^3 electron Volt.

$\pi d_{5/2}$: Shell model configuration for the proton energy level with angular momentum $l = 2$ and total angular momentum $j = 5/2$. For neutron π is replaced with ν.

$\pi f_{5/2}$: Shell model configuration for the proton energy level with angular momentum $l = 3$ and total angular momentum $j = 5/2$. For neutrons, π is replaced with ν.

$\nu g_{9/2}$: Shell model configuration for the neutron energy level with angular momentum $l = 4$ and total angular momentum $j = 9/2$.

$\pi p_{1/2}$: Proton energy level with angular momentum $l = 1$ and total angular momentum $j = 1/2$. For neutron π is replaced with ν.

$\pi p_{3/2}$: Proton energy level with angular momentum $l = 1$ and total angular momentum $j = 3/2$. For neutron π is replaced with ν.

δ: Pairing force term coefficient in Bethe-Weizsacker formula.

www.manaraa.com

$^{A}_{Z}\mathbf{X}_{N}$: Symbol used to represent atomic information for nuclide of element **X** with Z protons, N neutrons and total mass A.

β^{+}: Symbol for β decay process in which an excess proton converts to neutron.

β^{-}: Symbol for β decay process in which an excess neutron converts to proton.

EC: Electron Capture where an inner shell electron is captured by the nucleus converting a proton into a neutron.

γ: Symbol representing a γ-ray radiation.

Q_{β}: Energy difference between the ground states of the parent and daughter nuclei involved in a β decay.

FWHM: Full width at half maximum for a γ-ray peak, represents the resolution.

β_{skew}: Parameter representing the skew Gaussian shape of a γ-ray peak.

I_{γ}: Gamma feeding intensity to a particular state of interest.

I_{β}: Beta feeding intensity to a particular state of interest.

S_{n}: Neutron separation energy.

Definitions

AME2012: Atomic Mass Evaluation 2012.

BR: Branching Ratio.

CARDS: Clarion Array for Radioactive Decay Spectroscopy.

DAMM: Display Manipulation Module, Linux-based package developed at ORNL for data analysis.

DEP: Double Escape Peak, a γ-ray peak whose energy is two electron masses lower than the full-energy real peak.

www.manaraa.com

DGF-XIA: Digital Gamma Finder produced by X-ray Instrumentation Associates.

ESPE: Effective Single Particle Energy.

GERDA: Germanium Detector Array collaboration.

gf3: Linux-based software program within the RadWare package for fitting γ-ray spectra.

ISOL: Isotope Separation Online, a technique to produce the nuclei of interest.

log (ft): Logarithm value of comparative half-life for particular levels.

rp-process: Rapid-proton capture process: one of the primary nucleosynthesis processes.

r-process: Rapid-neutron capture processes: one of the primary nucleosynthesis processes.

HPGe: High-Purity Germanium detector for γ-ray spectroscopy.

HRIBF: Holifield Radioactive Ion Beam Facility.

LeRIBSS: Low-energy Radioactive Ion Beam Spectroscopy Station.

MTAS: Modular Total Absorption Spectrometer.

MTC: Moving Tape Collector.

NNDC: National Nuclear Data Center.

ORIC: Oak Ridge Isochronous Cyclotron.

ORNL: Oak Ridge National Lab.

RO: Ranging Out method.

SEP: Single Escape Peak, a γ-ray peak whose energy is one electron mass lower

www.manaraa.com

than the original full energy peak.

TAGS: Total Absorption γ-ray Spectroscopy.

www.manaraa.com

CHAPTER I

INTRODUCTION

Our present knowledge of atomic nuclei suggests that around 6000 to 7000 distinct nuclei are predicted to exist, of which some 3000 nuclei can be produced and studied in the laboratory. The less than 300 nuclei which are stable (or especially long-lived) [50, 87] are indicated by black squares on the nuclear chart shown in Fig. 1.1. The region represented by black squares are also known as the valley of stability which is a characterization of the stability of nuclides to radioactivity based on their binding energy. The remaining nuclei are radioactive and undergo some decay process to form the stable nuclei. A tremendous effort throughout the history of nuclear physics has been to understand the nuclear force: a force that acts between the nucleons which are responsible for the observed characteristics of atomic nuclei. Although the major properties of nucleon-nucleon interactions for the nuclei near stability are well-known [62], questions such as the evolution of single-particle states as one moves away from the valley of stability remain unanswered [111].

Many theoretical models have been proposed to understand nuclear structure and interactions, but none of them completely describe the structure of all nuclei. The Shell Model is quite successful for predicting nuclear features and interactions for a large number of well-tested nuclei near stability. This model accurately describes the structure of low-lying

www.manaraa.com

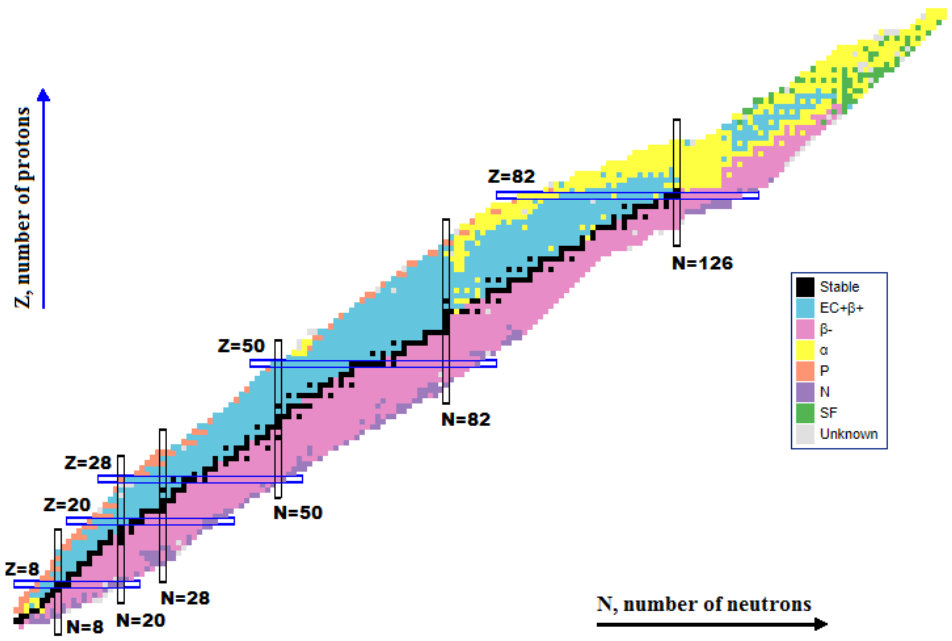

Figure 1.1: Segre chart or chart of nuclides [6].

levels in non-deformed nuclei in terms of the coupling of nucleon particles outside a closed core, or of nucleon holes insides of a closed core. These closed cores are represented by the empirically known magic numbers 2, 8, 20, 28, 50, 82 and 126 [115]. Even-even nuclei which have a proton or a neutron numbers equal to a magic number have a relatively high energy first excited state energy, while those having a both magic number of protons and neutrons, the so-called doubly magic nuclei, exhibit enhanced stability including an especially high first excited state energy, enhanced binding (lower relative mass), and a smaller relative size. However, it is unclear how this theory applies, or even if the predicted magic numbers really exist for nuclei which lie far away from the valley of stability where experimental data is either very limited or non-existent. To obtain a further insight, exper-

www.manaraa.com

imental data needs to be gathered in this unexplored region to test the various theoretical models [15, 109, 111].

There are still many neutron-rich nuclei above proton number Z = 20 which remain beyond the reach of any current facility, and any information about their properties comes totally from theoretical predictions. Generally, the properties of nuclei near stability are well known and have been used to extrapolate to nuclei near the particle drip lines. However, it has been experimentally shown that the general trends expected are not always followed, requiring some new aspect of the nuclear force to be considered. For example, the proton-neutron interaction across the major shells as well as interactions with continuum states leads to the migration of the single-particle states for nuclei with proton number near Z = 28 and neutron number from N = 28 to 50, hence approaching ^{78}Ni [27, 29, 37, 53, 54, 61, 78, 111, 117]. Shells and sub-shells are seen to appear and disappear with the addition of neutrons. This dynamic aspect of reappearance and disappearance of shell closures for nuclei occupying the $pf_{5/2}g_{9/2}$ shell are an area of current interest as they exhibit anomalous behaviors like deformation and shape co-existence which are important in understanding the evolution of nuclear structure [22, 56, 113].

The primary goal of this research is to use β-decay spectroscopy as a tool to understand the evolution of nuclear structure as well as the astrophysical processes involving atomic nuclei far from the valley of stability. However, there are more practical applications as well. In recent years, the development of clean nuclear power is considered as an alternative electrical energy source which is free from greenhouse gases [2, 8, 9]. However, the same concerns toward nuclear energy are present today as they were in the past when the

www.manaraa.com

construction of new nuclear reactors began to fall off. These concerns include the issues of safety, nuclear waste management, nuclear weapons proliferation, and cost. The fission of nuclear fuel produces a wide range of neutron-rich radioactive products having excess neutrons which require β decay to go back to stability. During β decay, one of the excess neutrons converts to a proton with the emission of a β particle, an electron anti-neutrino, and γ rays. Each of these contributes to the overall heat generation in the nuclear fuel cycle [113]. About 8% of the total heat generated during the nuclear fuel cycle comes from the β decay of the fission products which is known as decay heat. This decay heat continues to be generated after the shut-down of the nuclear reactor and varies as a function of time. Thus, coolant needs to be maintained even after the termination of the neutron-induced fission process in the reactor, and precise decay heat calculations are essential for the proper design and operation of the nuclear facilities [17].

For fissioning nuclei like ^{238}U, decay heat can be estimated from summation calculations using the inventory of nuclei present in the NNDC database. In general, these estimations of decay heat worked well, but a significant discrepancy has been observed between the predicted and observed decay heat in the 300-3000 s cooling time after the reactor has been shut down [17]. This indicates the accuracy of the presently available decay data is not high enough, and nuclear facilities require higher safety margins implying larger economic costs. The compiled data in the NNDC database are from the evaluation of different measurements, which basically used Ge detectors, i.e. the high-resolution technique. Due to the poor detection efficiency of the Ge detectors, and the fact that the γ-ray detection efficiency decreases with the energy, it is highly probable that the γ-ray energy actually

www.manaraa.com

released by the decaying nuclei is not accounted fully. The decay scheme is developed by the detection of the γ rays and the detection of coincidences between them. In most of the cases, decay schemes developed from these studies are not complete and the feeding patterns are incorrectly determined because many weak γ-ray transitions are not clearly observed. This lack complete assignment of γ ray is known as the pandemonium effect [48]. As the Q_{β^-} value increases for neutron-rich nuclei, a large number of excited states are fed at high excitation energy through allowed β-decay transitions. These states will decay either by the emission of high-energy γ rays with small intensities or β delayed neutron emission. The unobserved high-energy or weak γ-ray transitions cause an overestimation of β feeding intensity to low lying states and underestimation of the total γ-ray energy released, which propagates the uncertainty in the decay heat calculation [17, 48, 89, 119].

Experiments done in the past used the best technology and techniques available at that time. But, for β-decay spectroscopy, low detection efficiency, and beam contamination severely limited the information which could be obtained. This certainly has led to a lack in knowledge on the detection and placement of weak transitions. A major limitation was that most of the initial studies didn't have $\gamma\gamma$ coincidence data. These early studies used only energy sums and intensity balance for observed γ rays to develop a decay scheme in which incorrect placement of transitions based on inferior data caused serious problems. This dissertation will cover more complete β-decay studies of four neutron-rich Gallium isotopes near the ^{78}Ni doubly magic nuclide using a purified beam, high-efficiency Ge clover detectors, and better data analysis techniques along with $\gamma\gamma$ coincidence information to propose new decay schemes. In general, we observed a shift in β feeding to higher

www.manaraa.com

energy thus affecting our understanding of the total decay heat produced by fission products.

Medium-mass neutron-rich isotopes can be produced in different ways including neutron- or proton-induced fission of an actinide target, fragmentation of a stable heavy ion beam by a thick low-Z stable target, or spallation of a thick heavy (high-Z) target by an intense light-ion beam. Although the Holifield Radioactive Ion Beam Facility (HRIBF) closed several years ago, data was available from before the closure along with date from several experiments performed using the Oak Ridge National Laboratory (ORNL) Tandem accelerator to use proton-induced fission of Uranium to produce neutron-rich nuclides. All four experiments covered in this dissertation utilized the Isotope Separation Online (ISOL) technique [4] to obtain the nuclei of interest.

The nuclei around ^{78}Ni, especially Ga and Ge, are interesting from both experimental as well as theoretical points of view. Medium-mass even-even Ge isotopes show unexpected shape transition behavior with shell structure evolution and collectivity in the vicinity of N = 40 [46, 56, 67, 101]. For nuclei having many valance nucleons, nuclear transitions involving many nucleons together induce the collectivity. These nuclei also exhibit unique features like low-level triaxial deformation and shape co-existence [44, 104], i.e. within a very narrow energy range these nuclei show two or more well-defined states or bands of states with distinctly different structure.

With the addition of neutrons in the even-mass Ge isotopes for mass number A = 70 to 82 (N = 38 to 50), an increase of collectivity near the middle of the $\nu g_{9/2}p_{1/2}$ subshell has been observed which lowers the first few excited states as shown in the Fig. 1.2. The grad-

www.manaraa.com

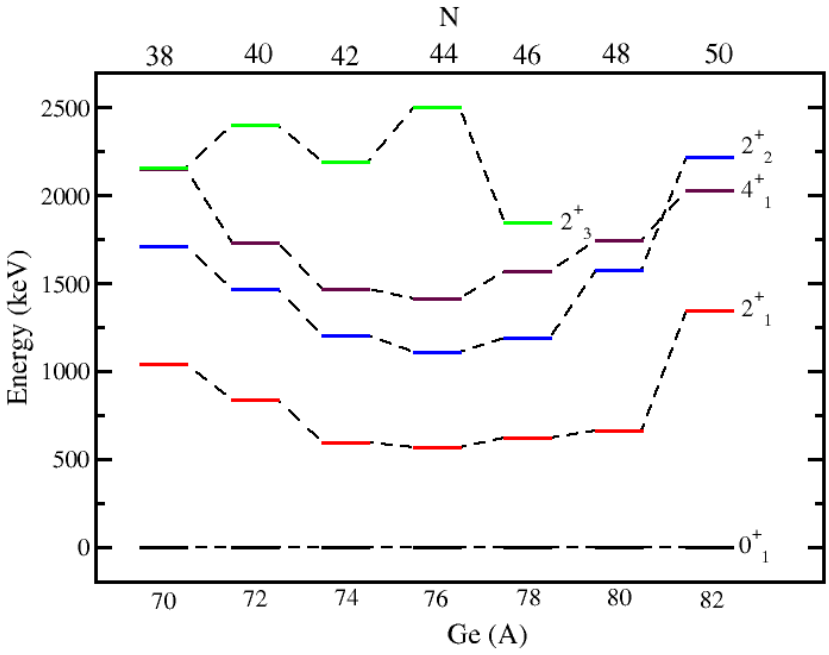

Figure 1.2: Level energy systematics of even Ge isotopes for A = 70 to 82 [11, 12, 34, 45, 95, 97, 99].

ual shape transition of the Ge isotopes is observed with the low-lying second 2^+ excited γ band-head indicating the presence of triaxiality. For the odd-mass Ge isotopes in the same region, there is a change in the order of the states observed with the addition of neutrons as shown in Fig. 1.3. All of the Ge isotopes through A = 64 to 84 already have sets of β-decay information available in the NNDC database. However, a closer inspection indicates significant discrepancies in the observed γ rays as well as the established energy levels between various experiments, especially for higher-lying states. Our current study shows that the NNDC database [6] lacks some details because most of the previous experiments were done in the early years of high-resolution γ-ray spectroscopy and had issues of source

www.manaraa.com

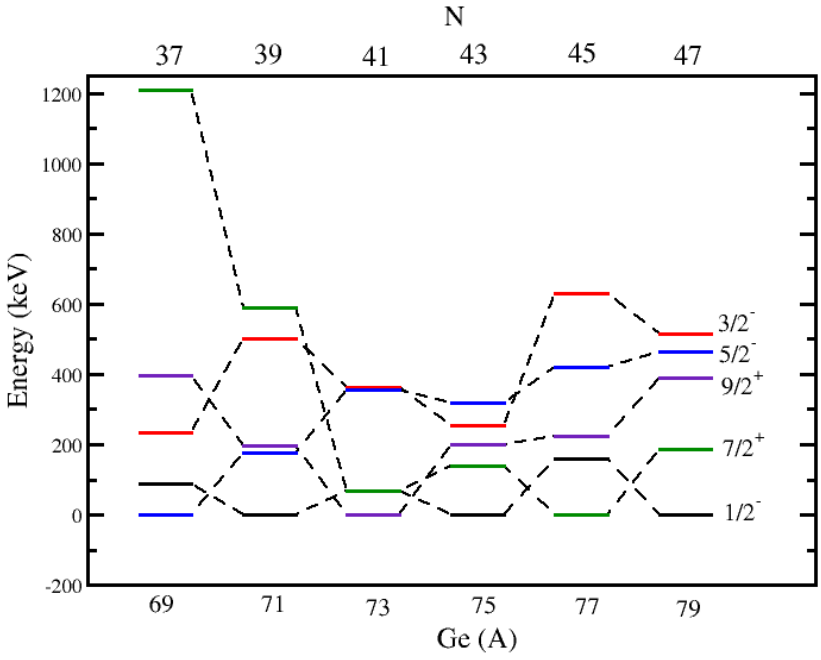

Figure 1.3: Level energy systematics of odd Ge isotopes for A = 69 to 80 [13, 76, 77, 96, 98, 100].

contamination, low detector efficiency and a lack of γ-ray coincidence data. Therefore, we assume that better experimental data will lead to more precise theoretical models which are needed to provide a better picture of these nuclei. In addition, a more complete understanding of the structure of these nuclei and feeding to the higher energy levels will help with power production calculations in design and operation of future generation nuclear reactors, as well as the transportation and waste management of radioisotopes [43].

From our detailed β-decay studies of $^{74-77}$Ga isotopes, we expect to provide the most comprehensive level schemes and β-feeding data for all four Ge nuclei. Furthermore, we expect to extend the decay schemes to higher energy levels through a better understanding

www.manaraa.com

of γ-ray coincidences. Although studying a few nuclei will not answer all the questions, this study will provide us with a better understanding of the pandemonium effect and how it relates to other nuclei which need to be studied. In addition, this study will fill the gaps in our knowledge of the evolution of nuclear structure for nuclei far from the stability by providing new information on weak transitions to enhance the quality of evaluated data on these nuclei.

www.manaraa.com

CHAPTER II

THEORETICAL BACKGROUND

2.1 Nuclear Shell Model

The electronic structure of the atom is well described by the filling of electronic shells which are derived from the observed discontinuities in the ionization energy of the electron as a function of Z. The closing of atomic shells leads to the noble gases which have very low reactivity. Adding or removing just one electron from the shell results in a highly reactive element. With the atomic structure, one only deals with the valence electrons, i.e. those outside an inert noble gas core. Similar to electronic structure, the study of neutron separation energies (S_n) for a large number of nuclei near the valley of stability, as shown in Fig. 2.1, indicates the existence of shell closures in the nucleus. Those nuclei whose nucleon numbers for protons or neutrons are among 2, 8, 20, 28, 50, 82 and 126, the magic numbers, have been found to exhibit enhanced stability in their structure. Just after a magic number, a sudden drop in the neutron separation energy is observed [65].

Shortly after the discovery of the nucleus and the beginning of nuclear physics research, the potential inside the nucleus was poorly understood and many theoretical models developed to explore the behavior of nuclei, ultimately this research lead to the development of the nuclear shell model [69]. A few simple potentials, like square well and harmonic oscillator, were tried in an attempt to reproduce the observed magic numbers. The time-

www.manaraa.com

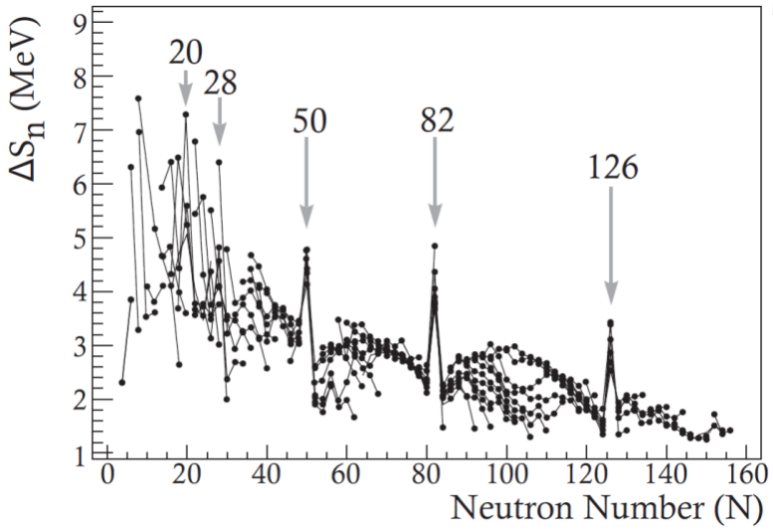

Figure 2.1: Graph of neutron separation energy as a function of neutron number showing peaks at the neutron magic numbers [36].

independent Schrödinger equation was solved to get the energy levels and spin of the nuclear states. Although both potentials were able to reproduce the shell closures up to nucleon number 20, they were identified as non-realistic since the potential goes to infinity for large radii. A more realistic mean field potential is the intermediate form of a square well and a harmonic oscillator potential, also known as the Woods-Saxon potential, was introduced. This potential was again successful in reproducing the shell closures only up to nucleon number 20. This problem was finally solved with the introduction of a spin-orbit interaction force which breaks the degeneracy between the pairs of states with orbital angular momentum $l > 0$ which is discussed in detail below.

A nucleus is a many-body system of interacting particles. There is no analytical solution of Schrödinger equation. We can only calculate the approximate solution for such a system. To simplify the problem, we assume interactions between nucleons in the nuclei

www.manaraa.com

average out and produce the position dependent average potential also known as mean a field potential.

Let's start by considering the average nuclear potential to be a harmonic oscillator potential,

$$V(r) = \frac{1}{2}mw^2r^2, \tag{2.1}$$

where m is the mass, w is the frequency of the oscillator potential and r is the distance from the center of the nucleus. The solution of the three dimensional Schrödinger equation with the harmonic oscillator potential gives:

$$E_N = \hbar w(N + \frac{3}{2}), N = 0, 1, 2, \ldots \tag{2.2}$$

where N is the principal quantum number. The orbital quantum number (l) can be at most equal to N and can take on only even or odd values as N is odd or even. For each l value, there is a $2(2l + 1)$ degeneracy resulting in a total degeneracy for level N of $(N + 1)(N + 2)$. Closed shells correspond to each value of N, so the model predicting closed shells for nucleon numbers 2, 8, 20, 40, 70, 12 and 168 (Fig. 2.2). Thus the model was able to reproduce the observed magic number for first three closed shells up to 20, but not for the rest.

As mentioned previously, to overcome this discrepancy a more realistic mean field potential known as the Wood-Saxon potential was introduced. This potential is given by:

$$V(r) = \frac{-V_0}{1 + exp[(r - R)/a]}, \tag{2.3}$$

where V_0 is the depth of the potential, r is the radial distance of the nucleon from the center of the potential, and a and R are the mean radii and surface thickness of the nucleus.

www.manaraa.com

This potential was able to remove the energy degeneracy for different l states of a given principle quantum number but was still unable to produce the observed magic numbers above 20 (see Fig. 2.2).

Like electrons in the electronic shell model, nucleons also have an intrinsic spin. To produce the observed nuclear magic numbers, a strong spin-orbit interaction term was added to the mean field potential. The total potential becomes:

$$V_T(r) = V(r) - v_s(r)\vec{L}\cdot\vec{S}, \tag{2.4}$$

where $V(r)$ is a mean field or Wood-Saxon potential, $v_s(r)$ is the spin-orbit interaction radial functions and $\vec{L}$ and $\vec{S}$ are orbital and spin angular momenta respectively. The total angular momentum ($\vec{J}$) is given by:

$$\vec{J} = \vec{L} + \vec{S}. \tag{2.5}$$

Since, the spin and orbital angular momentum operators commute with each other, their inner product becomes:

$$\vec{L}\cdot\vec{S} = \frac{1}{2}(J^2 - L^2 - S^2), \tag{2.6}$$

and their expectation value is,

$$< \vec{L}\cdot\vec{S} >= \frac{1}{2}(< J^2 > - < L^2 > - < S^2 >) = \frac{\hbar^2}{2}[j(j+1) - l(l+1) - s(s+1)], \tag{2.7}$$

where $s = \frac{1}{2}$ and $j = l \pm \frac{1}{2}$. Then the spin-orbit interaction becomes:

$$< \vec{L}\cdot\vec{S} >= \begin{cases} \frac{\hbar^2}{2}l, & j = l + \frac{1}{2} \\ \frac{\hbar^2}{2}(l+1), & j = l - \frac{1}{2}. \end{cases} \tag{2.8}$$

www.manaraa.com

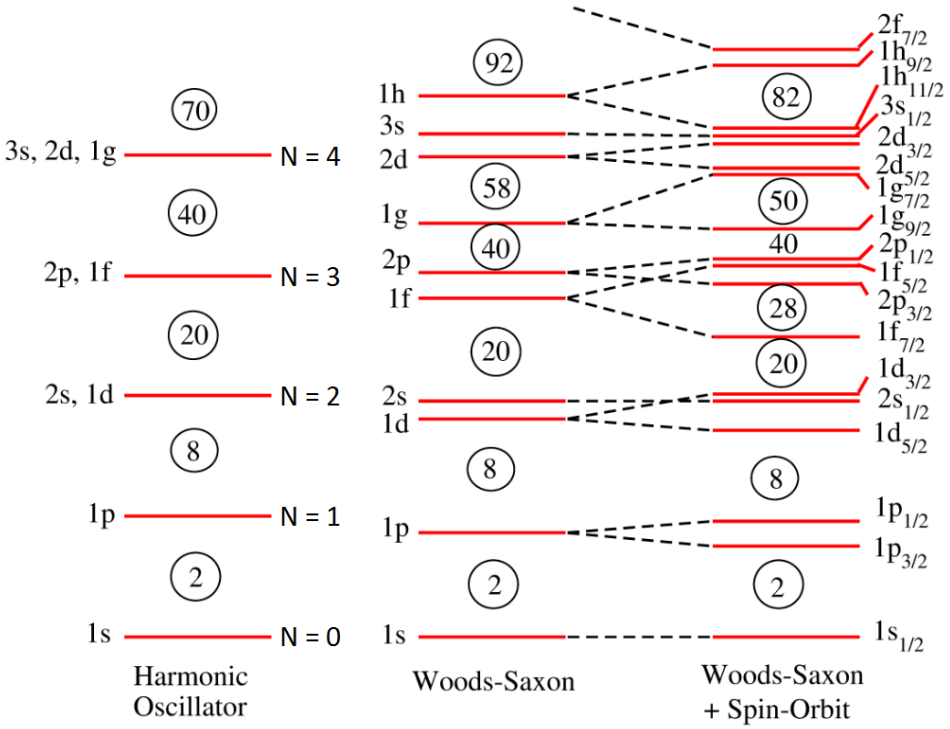

Figure 2.2: Nuclear shell level structure. The Wood-Saxon potential with spin-orbit coupling exactly reproduces the traditional magic numbers.

Equation 2.8 shows that nuclear energy levels with $l > 0$ split into two states with energy gap $\frac{\hbar^2}{2}(2l+1)$. Addition of the spin-orbit coupling term to the mean field potential potential successfully reproduces the magic numbers as seen in Fig. 2.1. For example, the observed large shell gaps for nucleon numbers 28 and 50, shown in Fig. 2.2, come as a result of the splitting the $f_{7/2} - f_{5/2}$ and $g_{9/2} - g_{7/2}$ orbitals, respectively [65].

Furthermore, like atomic structure, we can simplify the problem by dividing the nucleus into an inert core, containing most of the nucleons coupled to a 0^+ state using the known shell closures, and a small number of valence nucleons outside the core. The reason the core gives a 0^+ state is that all the nucleons are coupled in pairs of opposite spin (j).

www.manaraa.com

Let's take as an example application of the shell model for $^{17}_{8}O_9$. In this nucleons, eight protons and eight neutrons completely fill the first two major shells (second magic shell closure), and only a single neutron in the $1\nu d_{5/2}$ orbital determines the properties of the nucleus causing in the ground state spin-parity to be $\frac{5}{2}^+$. We use jj coupling to give states for odd-odd nuclei and nuclei with more than one nucleon outside the core. The parity is given by the product of the parties of the coupled states where odd l gives negative parity while even l gives positive parity. Another example is for $^{18}_{9}F_9$, which has an unpaired proton and neutron in the $1d_{5/2}$ orbitals which are coupled. The total angular momentum (spin) is in the range $|j_p - j_n| \leq j \leq j_n + j_p$, giving the possibility of the spin to be 0, 1, 2, 3, 4, 5 with positive parity (parity = $(-1)^{l_n+l_p}$). Experimentally it is observed to be 1^+ which agrees with one of the shell model predictions.

Thus, the Shell Model description of nuclear structure from the average Wood-Saxon potential with spin-orbit interactions has been very successful in describing the structure of nuclei near the valley of stability [65]. The major question is, does this model work for the nuclei which lie far from stability as they do not have clear description of the mean field, hence the effective interactions, of the nucleus?

2.2 Question About the Nuclear Shell Model

Although nuclear shell patterns are well described by the mean-field model, some of the results observed from experiments cannot be explained by this approach. A few examples include:

www.manaraa.com

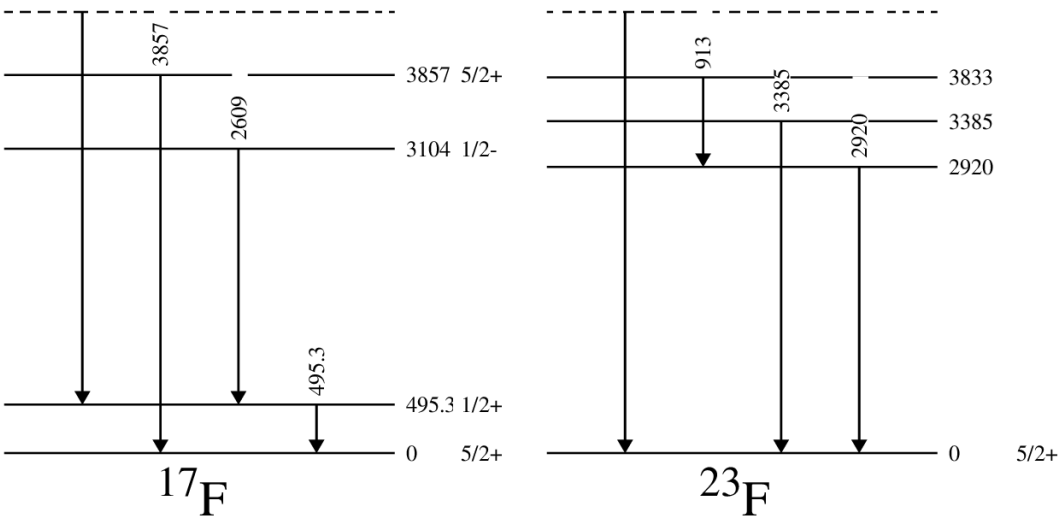

Figure 2.3: Level diagram showing the structure of ^{17}F and ^{23}F nuclei [6, 35, 107].

- Single-particle states for Fluorine are observed to be located at higher excitation energies than predicted by the shell model. The valance proton in ^{23}F (N = 14) is found much more deeply bound than in ^{17}F (N = 8) [72] as shown in Fig. 2.3. This result is surprising since N = 8 corresponds to the major shell closure predicted by shell model while N = 14 does not.

- For the nuclei in the range ^{68}Ni to ^{78}Ni, as neutrons fills the $\nu 1g_{9/2}$ orbits, the $Z = 28$ shell gap is predicted to become smaller with crossing of the $\pi 2p_{3/2}$ and $\pi 1f_{5/2}$ states as shown in Fig. 2.4 (a). Dropping of π1f$_{5/2}$ orbital below π2p$_{3/2}$ orbital for Z = 29 ^{77}Cu^{g} is experimentally observed [51].

- The energy difference between the lowest two single-particle orbitals outside the Z = 50 closed proton shell in Antimony isotopes, $\pi 1h_{11/2}$ and $\pi 1g_{7/2}$ increases with the excess neutron number and the trends is consistently followed with a decrease in the

www.manaraa.com

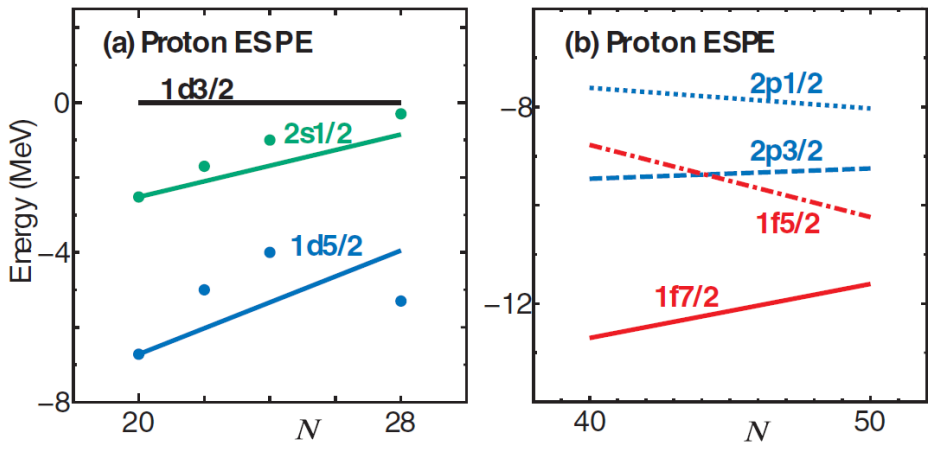

Figure 2.4: Evolution of Effective Single-Particle Energies (ESPE) as a function of neutron number taken from Ref. [78].

nuclear spin-orbit interaction. The experimental result for Antimony isotopes [91] is shown in Fig. 2.4 (b).

- The measured single particle energies for $\nu 1f_{7/2}$ and $\nu 1f_{5/2}$, and first $\nu 2p_{3/2}$ and $\nu 2p_{1/2}$ states in ^{49}Ca and ^{47}Ar indicate a reduction in the N = 28 shell gap from the *fp* spin-orbit splitting. The mean field calculations with finite range interactions predict the disappearance of the N = 28 spherical shell closure for nuclei with N, Z $>$ 10 but do not find any spin-orbit variations [39].

The migration of the proton or neutron orbitals effects the β-decay strength function above the neutron or proton separation energy affecting the conditions for β-delayed nucleon emission. The examples given above clearly suggest that there is something missing in the shell model calculation which needs to be considered.

www.manaraa.com

2.3 Evolution of Single-Particle States

Understanding the processes behind the evolution of single particle states for neutron-rich nuclei is important for evaluating the decay behavior of these nuclei. There might be several reasons why shell structure varies as the shells are filled. The tensor force has been identified as one of the characteristic parts of the nuclear force responsible for driving the mechanism for the evolution of single-particle states [78]. Nucleon-nucleon interactions are believed to occur through multiple meson exchanges, which depends on the relative position and spinning motion of the nucleus. This interaction creates an attractive or repulsive force which contributes to the spin-orbit splitting. Additionally, there is a dominant effect on the single particle energies from the single pion exchange which is responsible for the modification of the splitting of the orbitals from the spin-orbit coupling via spin-isospin interactions, known as the tensor force. It has been observed that the tensor force has a specific, robust and systematic effect on the evolution of the single particle energies of nuclei, breaking or creating new magic numbers [78].

The tensor force can be written as,

$$V_T = (\vec{\tau_1}.\vec{\tau_2})([\vec{s_1}\vec{s_2}]^{(2)}\cdot Y^{(2)} f(r), \tag{2.9}$$

where $\vec{\tau}_{1,2}(\vec{s}_{1,2})$ is the isospin (spin) of nucleons 1 and 2, the symbol $[\ ]^{(K)}$ indicates the coupling of the two operators in the brackets to the angular momentum K, and Y is the spherical harmonics for Euler's angles of the relative coordinate.

The spherical single particle energy of an orbit j can be calculated by its kinetic energy and the effect from the closed shell on the orbit j. When nucleons are added to another

www.manaraa.com

orbit j', the single particle energy of the orbit j changes. If the neutron occupies the j' orbit while the protons are in orbit j ($j \neq j'$), the shift of the single particle energy is

$$\Delta\epsilon_p(j) = \frac{1}{2}(V^{T=0}_{j,j'} + V^{T=1}_{j,j'})n_n(j'), \tag{2.10}$$

where $n_n(j')$ is neutron number in the orbit j'. $V_{j,j'}{}^T$ are the effective single particle energies which depend on both occupation number and isospin structure. They can be written as:

$$V^T_{j,j'} = \frac{\sum_J (2J+1) < jj'|V|ij >_{JT}}{\sum_J (2J+1)}, \tag{2.11}$$

where $< ij|V|ij >_{JT}$ is the two body interaction coupling two nucleons to an angular momentum J and isospin T. This is a monopole interaction.

For l and l' being orbital angular momentum, let us consider the case shown in Fig. 2.5 with protons in orbitals

$$j_{>,<} = l \pm \frac{1}{2} \tag{2.12}$$

and neutrons in orbitals

$$j'_{>,<} = l \pm \frac{1}{2}, \tag{2.13}$$

the following equation can be derived [78],

$$(2j_> + 1)V^T_{j_>,j'} + (2j_< + 1)V^T_{j_<,j'} = 0. \tag{2.14}$$

Equation 2.14 indicates that if both orbital $j_>$ and $j_<$ are fully occupied, the tensor effect is zero. Also, the proton-neutron monopole interaction is twice as strong then as either the proton-proton or neutron-neutron interaction. The detailed explanation of this derivation is in Ref. [78].

www.manaraa.com

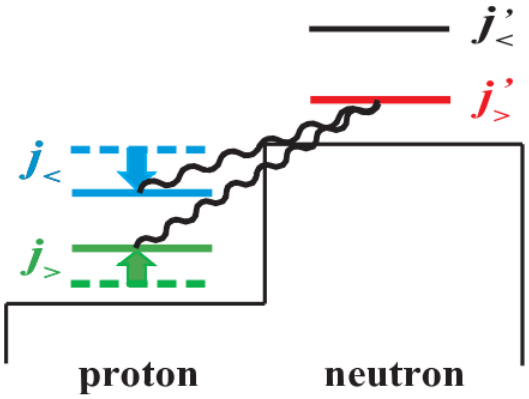

Figure 2.5: Schematic diagram of monopole interaction produced by the tensor force between a proton in $j_{>,<} = l \pm \frac{1}{2}$ and neutron in $j'_{>,<} = l' \pm \frac{1}{2}$ from Ref. [78].

For the protons in the $j_<$ orbital and neutrons in the $j'_>$ orbital, because of the high relative momentum between them, the spatial wave function of their relative motion is narrowly distributed in the direction of the interactions. In this case as represented in Fig. 2.6 (a), the spin of the two nucleons are parallel and added to give S = 1, which causes an attraction between the orbitals j and j'. This holds true for nucleons in $j_>$ and $j'_<$ orbitals as well.

On the other hand, the protons in the $j_>$ orbital and neutron in the $j'_>$ orbitals, as shown in Fig. 2.6 (b), a repulsive interaction is observed. This predicted phenomena from the addition of the tensor force can describe the evolution of the single particle states observed in Figure 2.4.

Figure 2.4 (a) shows the effective single particle energies of the proton pf-shell orbitals ($1f_{7/2}$, $1f_{5/2}$, $2p_{3/2}$ and $2p_{1/2}$ states) as a function of neutron number for nuclei in the range from ^{68}Ni to ^{78}Ni. As more neutrons occupy the $1g_{9/2}$ orbits ($j'_>$), the proton orbits are

www.manaraa.com

shifted due to the tensor interaction force. As shown in the Fig. 2.6, proton $1f_{7/2}$ orbital ($j_>$) is lifted up while the $1f_{5/2}$ ($j_<$) is pushed downward as neutron number increases resulting in the decrease in the $Z = 28$ shell gap between ^{68}Ni to ^{78}Ni.

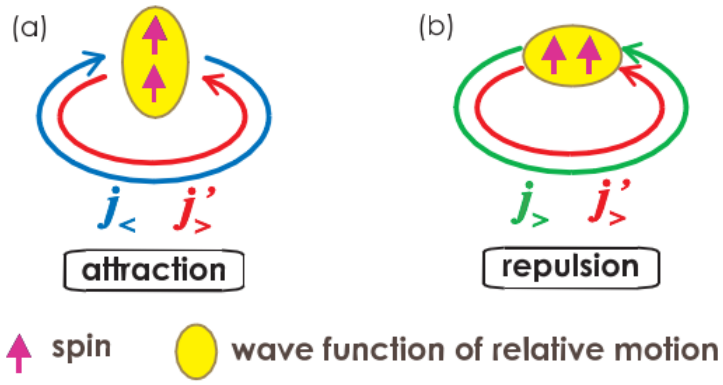

Figure 2.6: Intutive picture of the tensor force acting two nucleions on orbits j and j' from Ref. [78].

Other factors affecting shell evolution include many-body correlations due to pairing which is important for weakly bound system. As the nuclear potential diffuses near the extreme of β-stability, new nuclear structure, and excitation modes can be observed which explains some unique nuclear properties like the nuclear halo.

To confirm the physical aspects responsible for the nuclear structural changes, particle configurations and interactions in neutron-rich environments, a detailed level-structure measurement, and direct information about the single particle states is essential.

www.manaraa.com

2.4 β-Decay: A Tool to Understand Nuclear Structure

As explained in Chapter 1, the less than 300 stable nuclei represented by black squares in Fig. 1.1, form the valley of stability which are stretches along the N = Z line then moves steadily to the neutron-rich sides due to the repulsive Coulomb force. The rest of the nuclei having proton-neutron asymmetry are radioactive and undergo decay processes to form the stable nuclei. There are different modes for the decay process like α-decay, β-decay, γ-ray emission, particle emission and so on, by which unstable nuclei move towards the valley of stability. So, we can think that the balance of the proton and neutron number in the nuclei determines whether the nuclei is stable or unstable. Too many protons or neutrons in the nuclei spoil the balance by disturbing the binding energy from the nuclear forces and makes the nuclei unstable.

There are basically two ways of studying the nuclear properties: reactions and radioactive decay. The prompt radiation from reactions and delayed radiations from decay complement each other. For the β-decay study, we measure the radiation released following β-particle emission. Although many things might have happened prior to the formation of the β-decaying states of nuclei, if we can physically or chemically separate the nuclei of interest, then the β-decay measurement is insensitive to what has happened in the past.

Most of the nuclear ground states decay by the β-decay process. It is a slow process governed by weak interactions whose half-life ranges from ms to 10^{15} years. The probability for this decay process depends on the relation between the wave-functions of the initial and final nuclear states. As the observed β-energy spectrum is continuous, extracting the

www.manaraa.com

structure information is not so straightforward. Although the radioactive decay is limited for studying properties of nuclei, the main advantages of β-decay studies are:

- β decay is a primary source of information for the newly identified nuclei. Even knowing the rough estimates of Q_β values and half-lives gives the important clues to their properties.
- The β-decay properties are important in understating the creation of heavier elements in the explosive stellar r-process.
- Understanding the β-decay properties are essential for the proper design of nuclear reactors and associated questions of the shielding.
- There are some medical applications of β decay like Positron Emission Tomography.

There are three different types of the β-decay process, namely β^-, β^+ and Electron Capture (EC) capture which are explained in detail below:

1. β^--decay: This is favorable on the neutron-rich side of the nuclear chart in which one of the excess neutrons converts into a proton with the emission of an electron, electron antineutrino and γ rays. The simple equation governing this decay is:

$$\beta^- : n \rightarrow p + e^- + \bar{\nu}. \tag{2.15}$$

2. β^+-decay: This is favorable on the neutron-deficient side of the nuclear chart in which one of the excess protons converts into a neutron with the emission of a

www.manaraa.com

positron, electron neutrino and γ rays. The simple equation governing this decay is:

$$\beta^+ : p \rightarrow n + e^+ + \nu. \tag{2.16}$$

3. Electron Capture (EC): This is very similar to the β^+-decay process and populates the same daughter nuclei. In this process, the nucleus captures an atomic electron and converts an excess proton into a neutron with the emission of an electron neutrino, X rays and γ rays. The simple equation governing this decay is:

$$EC : p + e^- \rightarrow n + \nu + X_{ray}. \tag{2.17}$$

The EC process cannot occur for nuclei which are fully ionized. All the above-mentioned processes of general nuclei are given by:

$$\beta^- : {}^A_Z X_N \rightarrow {}^A_{Z+1} X_{N-1} + e^- + \bar{\nu_e}, \tag{2.18}$$

$$\beta^+ : {}^A_Z X_N \rightarrow {}^A_{Z-1} X_{N+1} + e^+ + \nu_e, \tag{2.19}$$

$$EC : {}^A_Z X_N + e^- \rightarrow {}^A_{Z-1} X_{N+1} + \nu_e + X_{ray}, \tag{2.20}$$

where ${}^A_Z X_N$ represents the nuclei having chemical symbol X, proton Z, neutron N and total mass A. X_{ray} is the X-ray emitted during the electron capture process as atomic electrons cascade down to refill the space left by the captured electron.

The Fermi theory of β decay states that the β-decay rate (λ) depends on the nuclear matrix element (M_{fi}) and the density of final states in daughter nucleus ($\rho(E_f)$) which is known as Fermi Golden Rule and given by:

$$\lambda = \frac{2\pi}{\hbar} \mid V_{fi} \mid^2 \rho(E_f), \tag{2.21}$$

www.manaraa.com

where $V_{fi} = gM_{fi}$, g is the β-decay strength constant. The matrix element M_{fi} represents the overlap between the initial ψ_i and final ψ_f states wave function.

$$M_{fi} =< \psi_f^* | V | \psi_i >, \tag{2.22}$$

where V is the β-decay operator. The final state wave function includes the wave functions of daughter nucleus, electron and anti-neutrino.

The β-decay spectrum depends on the number of final states accessible to the emitted particles, Fermi Function ($F(Z', p)$) and the nuclear matrix element. Hence, total decay rate can be written as:

$$\lambda = \frac{g^2 \mid M_{fi} \mid^2}{2\pi^3 \hbar^7 c^3} \int_0^{p_{max}} F(Z', p) p^2 (Q - T_e)^2 dp, \tag{2.23}$$

where p is the electron momentum (which is integrated up to p_{max}). The term Q in the equation is the mass difference of parent and daughter nucleus while the T_e is the electron energy. The integral term in the Equation 2.23 depends on the $Z^{'}$ and maximum electron total energy (E_0), also known as Fermi integral ($f(Z', E_0)$).

$$\lambda = \frac{g^2 \mid M_{fi} \mid^2}{2\pi^3 \hbar^7 c^3} f(Z', E_0). \tag{2.24}$$

Using the decay constant

$$\lambda = \frac{0.693}{t_{1/2}}, \tag{2.25}$$

the Equation 2.24 becomes:

$$f t_{1/2} = 0.693 \frac{2\pi^3 \hbar^7}{g^2 m_e^5 c^4 \mid M_{fi} \mid^2}. \tag{2.26}$$

www.manaraa.com

Table 2.1: Selection rules [81]

Types of Transition	Selection rules	*ft*	$\log(ft)$
Superallowed	$\Delta J = 0, \pm 1 (no)$	$1000 - 4000$	3.0-3.6
Allowded	$\Delta J = 0, \pm 1 (no)$	$2 \times 10^4 - 10^6$	4.3-6.0
First Forbidden	$\Delta J = 0, \pm 1 (yes)$	$10^6 - 10^8$	6.0-8.0
Unique first forbidden	$\Delta J = \pm 2 (yes)$	$10^8 - 10^9$	8.0-9.0
Second forbidden	$\Delta J = \pm 2 (no)$	$2 \times 10^{10} - 10^{13}$	10.3-13.3
Unique second forbidden	$\Delta J = \pm 3 (no)$	10^{12}	12.0
Third forbidden	$\Delta J = \pm 3 (yes)$	10^{18}	18.0
Unique third forbidden	$\Delta J = \pm 4 (yes)$	4×10^{15}	15.6
Fourth forbidden	$\Delta J = \pm 4 (no)$	10^{23}	23.0
Unique fourth forbidden	$\Delta J = \pm 5 (no)$	10^{19}	19.0

The quantity on the left of the above Equation 2.26 is the comparative half-life, which gives a way to compare the β-decay probability. The *ft* value ranges from about 10^3 to 10^{20} and generally represented in $\log_{10}$ scale. As indicated by above equation, the less the $\log(ft)$ value, the more the overlap of the nuclear wave function leading the higher probability for the decay [62]. When we know the $\log(ft)$ value for particular state of the daughter nuclei, using the Table 2.1, we can estimate the β-transitions strength to that level. The β decay is found to occur at a faster rate if the produced lepton carries away $l = 0$ momentum corresponding allowed transitions known as Fermi decay ($S = 0$, electron-neutrino intrinsic spins anti-align). If the lepton carries away $l > 1$ momentum, this is a forbidden decay (less likely to happen) and known as a Gamow-Teller transition ($S = 1$, electron-neutrino intrinsic spins align). The detail of the explanation is in Ref. [62].

www.manaraa.com

CHAPTER III

EXPERIMENTAL SETUP

All experiments reported in this dissertation were performed at the Holifield Radioactive Ion Beam Facility (HRIBF) at the Oak Ridge National Laboratory (ORNL). The HRIBF can provide both accelerated and unaccelerated radioactive ion beams for many nuclei of varying intensity from less than 1ion/s to thousands of ions/s as shown in Fig. 3.1. The experiments used in this dissertation focused on studies of the copper isotopes, so the system was tuned to maximize their production relative to other members of the mass chain. The gallium isotopes studied here either came as a mass contaminant in the beam or were fed by the β decays of the corresponding copper and zinc isotopes in the mass chain. Each gallium isotope β decays to a germanium isotope. A schematic diagram of the HRIBF facility is shown in Fig. 3.2 whose components will be discussed in detail in the following sections.

3.1 Isotope Separation On-Line Technique

The HRIBF has the capability to produce medium mass, short-lived radioactive isotopes utilizing the Isotope Separation On-line (ISOL) technique. This process starts with the high-energy proton beam from the Oak Ridge Isochronous Cyclotron (ORIC) and ends

www.manaraa.com

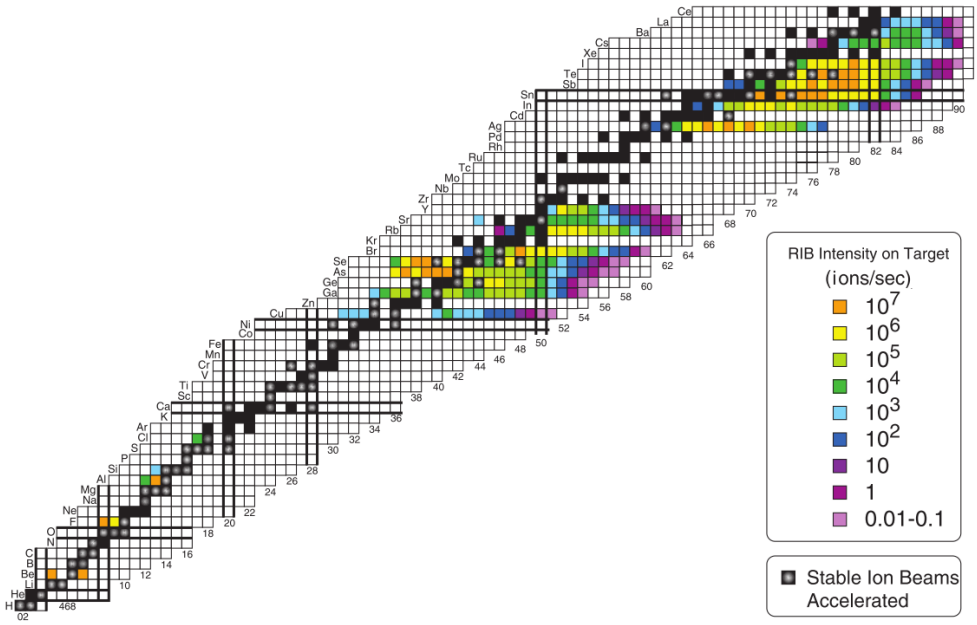

Figure 3.1: Available beam facility at HRIBF, ORNL. The beam production rates are color coded [21].

with the implantation of the desired beam of radioactive nuclei at the Moving Tape Collector (MTC). Details on the ISOL technique are presented below.

3.1.1 ORIC

The Oak Ridge Isochronous Cyclotron (ORIC) at Oak Ridge National Laboratory (ORNL) was constructed in 1962 and initially was used for light ion research (A $<$ 40). Later it was upgraded making it able to produce heavy ions up to A = 200 as a light ion driver for Radioactive Ion Beam (RIB) production [105]. Currently, ORIC is a k = 100 cyclotron having the capability to produce 50-100 MeV energy proton beams with intensity up to 20 μA. The magnetic field of the ORIC is provided by three sectors of irons which are specially designed to provide an increase in the field by 8% at the larger radii. The

www.manaraa.com

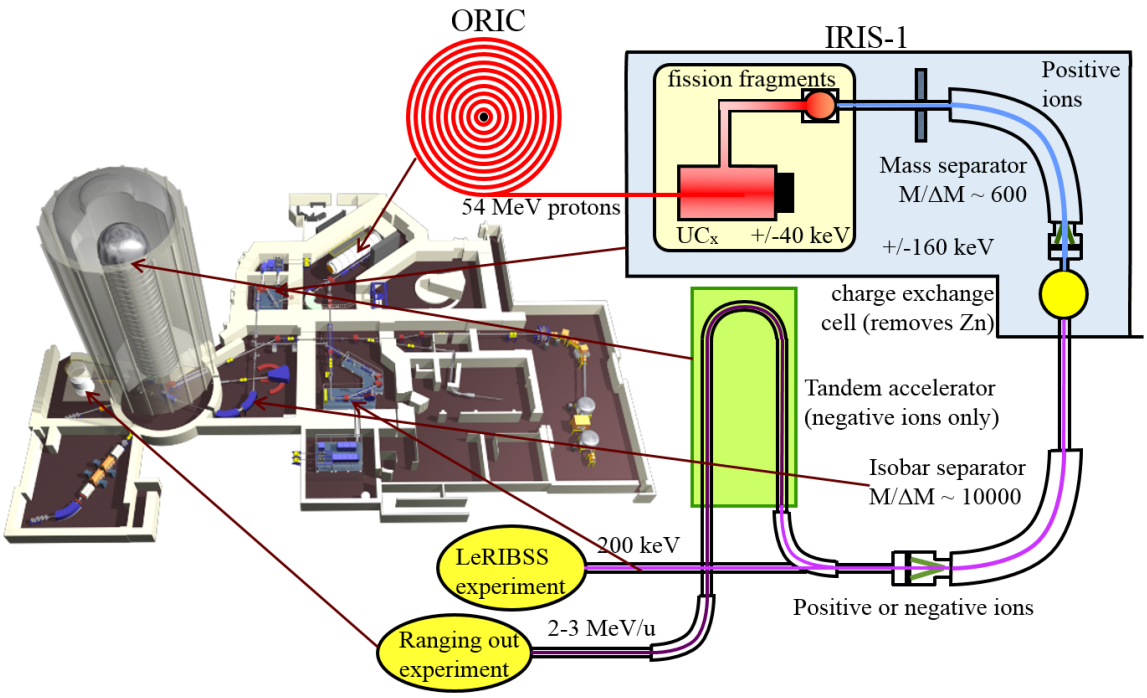

Figure 3.2: Schematic diagram of ISOL facility at HRIBF [79].

major advantage of this synchrocyclotron is it can provide a continuous beam with large beam current. For these studies, after extraction of a beam from the ORIC, proton beam was delivered to the production target.

3.1.2 Target

The high energy proton beams from ORIC were impinged on a carbon matrix target weighting ∼6 - 7 grams with a thin layer of uranium carbide ($UC_x \sim 10\mu$m) coated over it (Fig. 3.3). Interaction of the proton beam with the uranium in the target produces a broad range of fission fragments. Uranium carbide was used in the target over pure uranium due to its high dispersivity and porosity which decrease the release time of the produced fission fragments through the effusion and diffusion processes. Successful production of

www.manaraa.com

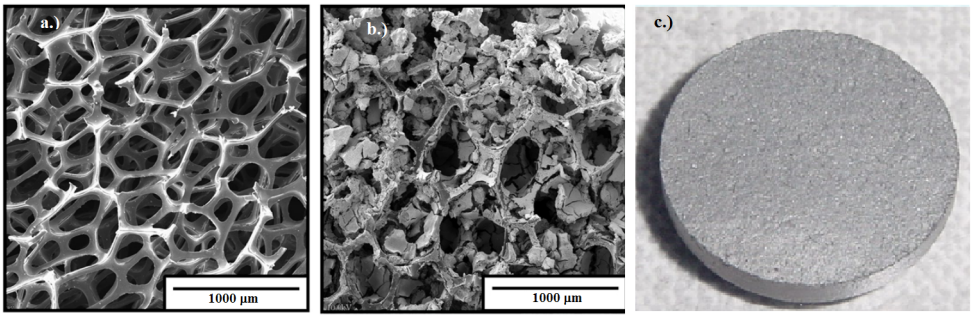

Figure 3.3: Targets used in HRIBF experiments. The left and middle panel shows the microscopic view of uranium un-coated and coated carbon matrix respectively, while right panel shows the actual view of a uranium carbide pallet [103].

a radioactive ion beam depends on the delays associated with diffusion, release time and effusive transport which should be within the half-life of the radioisotope of the interest.

3.1.3 Ion source

The fission fragments were transported to the hot plasma ion source which was designed to operate at temperature $\leqslant 2200\ ^0$C [18]. The ion source was optimized to produce specific radioisotopes of interest which exhibit high efficiency, low energy spread, and chemical selectivity. Fission products are subsequently ionized to charge $+1$ states in a hot plasma ion source then extracted, and accelerated to an energy of about 100 keV, and injected into the low-resolution mass separator.

www.manaraa.com

3.1.4 Mass Separator

The Radioactive Ion Beam (RIB) produced by the target/ion source contains a wide range of nuclei, with several species having nearly identical mass-to-charge ratios. The radius of curvature for an ion beam in a uniform magnetic field given by

$$r = \sqrt{\frac{2mV}{qB^2}}, \tag{3.1}$$

where r is the radius of path produced by magnetic field B, V is the accelerating voltage and m is a mass of ion having charge q. Since the radius of curvature is mass dependent, an aperture slit can be used to select the mass of interest as long as the resolution of the dipole magnet is sufficient. Isobaric separation of the desired mass was achieved using the low-resolution mass separator with mass resolving power M/ΔM$\sim$ 600. After the first stage mass analysis, the radioactive ion beam was directed to the charge exchange cell.

3.1.5 Charge Exchange Cell

The charge exchange cell contains Cesium vapor with a density of 10^{15} atoms/cm^3. When the mass separated beam from the mass separator passes through the cell, about 5 - 10$\%$ of the positive ions pick up electrons to become negative ions. This process takes place by at least two collisions with the Cesium vapor. The first collision neutralizes the positive ion while the second collision converts the neutral ions into negative ions. The positive ions can be deflected by applying electric/magnetic fields which leaves a relatively pure negative ion beam.

The primary purpose for using the charge exchange cell is to create the negative ions needed for injection into the tandem accelerator. The charge exchange cell does not need to

www.manaraa.com

be used for the non-accelerated beams unless it is important to remove particular elements. However, passing a radioactive ion beam through the charge exchange cell broadens the beam effectively reducing the mass resolving power of the subsequent isobar separator. Nevertheless, using the charge exchange cell for unaccelerated beams has some additional benefits. Some elements like Zn and Cd which have negative electron affinity cannot form negative ions. These elements are then easily removed during the subsequent magnetic stages of the separation. For our experiment, removal of the zinc ions from the beam was generally the goal.

3.1.6 Isobar Separator

The radioactive ion beam from the charge exchange cell was further separated by passing it through the high-resolution isobar separator with mass resolving power M/ΔM $\sim 10,000$, which is achieved through two 55-degree bending dipole magnets with a bending radius of 2.8 m. This process removes most of the unwanted ions, including Ga, by using a narrow 1 mm opening window thus producing a purified beam of Cu ions for our measurements. In the production target, Ga is always more strongly produced relative to the Cu and Zn as the production cross-section increases with the Z on the low side of the lower fission peak. Furthermore, Cu and Zn have shorter half-lives which reduce the production because they take longer to get out of the target and ion source. Finally, Ga is much more easily ionized, making its ionization more efficient. The net result is the Ga isobar is several orders of magnitude stronger than the Cu isobar. We have already removed the Zn isobar utilizing the charge exchange cell while the high-resolution isobar separator is

www.manaraa.com

capable of removing the Ga ions providing the pure Cu beam which is injected into the tandem accelerator for acceleration or directly sent to the Low-energy Radioactive Ion Beam Spectroscopy Station (LeRIBSS).

3.1.7 Tandem Accelerator

The HRIBF Tandem accelerator is an electrostatics accelerator which can operate between 1–25 MV. This accelerator is located inside a 100-ft high and 33-ft diameter vessel. Sulfur hexafluoride (SF_6) at 7 atm is used as the insulating gas inside the vessel. The Tandem can be used to accelerate either stable or radioactive ions. The negative ion beams are bent into the vertical direction by a dipole magnet at the base. The ions are then accelerated toward the positive potential at the top of the Tandem. A 180^o magnet bends the beam back toward the ground. The beam then goes through a stripping foil which results in a distribution of positive charge states which is then accelerated away from the positive potential of the Tandem. The desired charge state and energy is selected by a second dipole magnet at the base of the tandem. These post-accelerated ion beams were delivered to the experimental station.

3.2 Detector End Stations

Experiments could be carried out in two different ways: either with accelerated beams using the Ranging-Out system, or non-accelerated beams using LeRIBSS. Ranging-Out was used for $^{76-77}$Cu experiments, while the measurements at LeRIBSS included ^{74,75,77}Cu.

www.manaraa.com

3.2.1 Discussion of Ranging Out mode vs. LeRIBSS

For the Ranging-Out system, the negatively charged ion beam from the high-resolution mass separator could be accelerated to 2-3 MeV/u by the HRIBF tandem accelerator. With the additional energy for the beam, it could be transmitted through a Micro-channel plate (MPC) detector and a six segmented mini ionization chamber (mini-IC) which is filled with Tetrafluoromethane (CF_4) gas at low pressure. The measurement of six ion energy loss signals in the mini-IC allowed us to identify the atomic number Z of individual mono-energetic isobars. Higher atomic number Z-ions lose more energy, i.e. those closer to stability and of less interest. It was, therefore, possible to purify the beam by increasing pressure in the mini-IC, thus ranging out higer -Z ions in the exit window of the mini-IC and allowing through only the beam component having the lowest atomic number [40]. Because the beam had lost most of its energy and had scattered significantly in the slowing process, the MTC deposition point needed to be placed immediately behind the exit window of the mini-IC as shown by position 1 in Fig. 3.4. This is known as the Ranging-Out (RO) mode. Alternatively, the mini-IC could be run at a lower pressure which allowed all the ions to pass through and be deposited on the MTC at the center of the CARDS array (position 2 in Fig. 3.4). The PT mode of the experiment has the advantage that it allowed us to identify each ion present in the beam. By knowing the exact amount of each ion deposited and measuring absolute γ-ray intensities, absolute branching ratios could be determined. A more detail explanation of this Ranging Out method is given in Refs. [40,114]. After removal of long-lived higher-Z isobars, very pure ion beams (with final rates of a few

www.manaraa.com

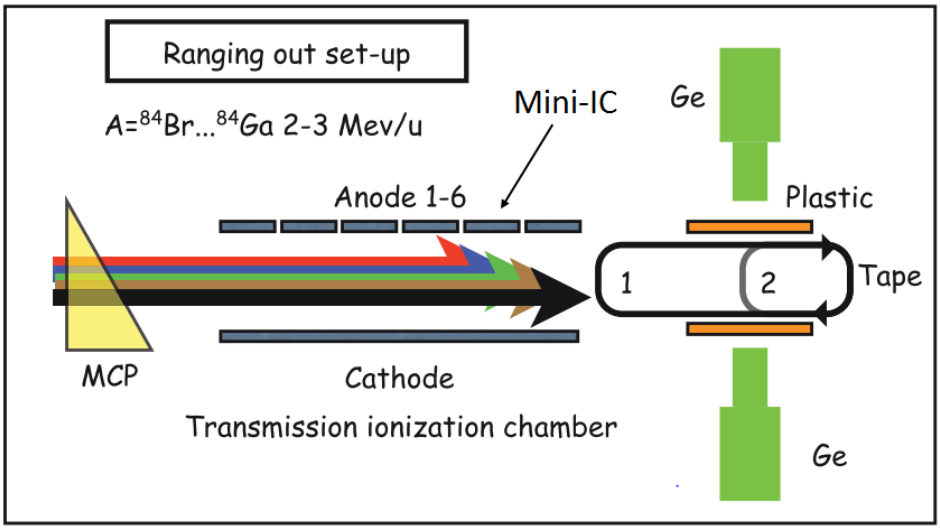

Figure 3.4: Schematic diagram of Ranging Out taken from Ref. [21].

hundred ions per second) were deposited onto a moving tape collector (MTC) in the detector set up.

For the LeRIBSS system, a pure ion beam from the high-resolution isobar separator was delivered to LeRIBSS and was deposited onto the MTC with a deposition point in the center of the detector set up. The advantage of LeRIBSS is there is no loss of beam intensity due to charge stripping in the tandem accelerator. The majority of the instrumention used for both end stations were the same as will be explain in the following section.

3.2.1.1 Moving Tape Collector

An isotope of interest was deposited on the Mylar tape which transports from implantation point to measurement point and away from the detector region in order to distinguish the γ rays emitted by nuclides with different half-lives. There are two modes of operation with the MTC.

www.manaraa.com

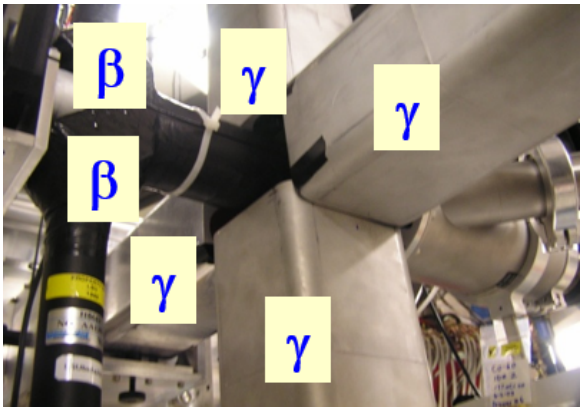

Figure 3.5: Four clover High-purity Germanium detectors set up along with two plastic β scintillators as used at LeRIBSS.

1. The move into place mode is where the beam is collected on the MTC and then periodically moved into the detector array. This was only used for part of the RO measurements when the pressure in the ion chamber was high (position 1 in Fig. 3.4). For both ^{76,77}Cu this mode was used. The MTC transport time to move the source into position was about 500 ms.

2. The take way mode is where the point of deposit is at the center of the detector array allowing observation of grow-in and decay time periods before the activity is moved away. All experiments used this mode at some point, and it is the only mode used at LeRIBSS. The MTC transport time for taking away the source was between 250 ms and as improvements were 500 ms made for later experiments.

www.manaraa.com

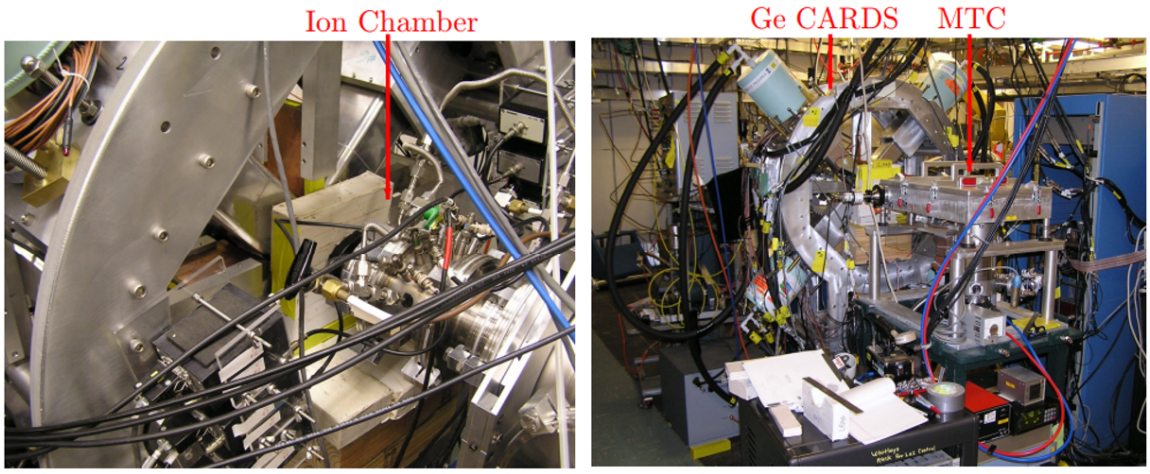

Figure 3.6: For the RO mode of the experiment, figure on the left shows the mini-IC while the figure on the right shows the MTC and HPGe detectors in CARDS set up.

3.2.1.2 CARDS Array

For either the RO or LeRIBSS locations, the same basic detector array was used. The detectors were housed in the Clarion Array for Radioactive Decay Spectroscopy (CARDS) framework and consisted of four HPGe clover γ-ray detectors and 2 plastic scintillator counters for detecting β decays. Each clover detector has four Germanium crystals. Therefore, we have 16 crystals and thereby 16 channels for γ-ray detection. The two β detectors are used to reduce the background by gating the γ-ray spectra. The detector efficiency of the HPGe depends on the energy of the γ rays. As wil be discussed in Chapter 4, the absolute photopeak efficiency of four clover detectors in LeRIBSS setup has a maximum efficiency of 31.0% at 100 keV and 6.2% at 1.33 MeV.

When discussing the detector in γ-ray spectroscopy, there are three types of efficiency which are considered based on the interaction in the detector. When a γ ray enters a detec-

www.manaraa.com

tor, it can go through a number of interactions including photoelectric, Compton and pair production, which each deposits energy in the detector. If all the γ-ray energy is deposited, then we observe a full energy peak. However, the γ ray can lose energy and scatter out of the detector which results in the Compton continuum. The absolute photopeak efficiency is the probability that if a γ ray is emitted that the full energy of the γ ray is deposited in the full energy peak. The total γ-ray efficiency refers to the probability that any signal is deposited in the detector and therefore includes the photopeak and Compton background. Making absolute measurements is not always easy but getting the relative photopeak efficiency is much easier. In determining the relative γ-ray intensities, it is sufficient to use the relative photopeak efficiency because the uncertainty is much smaller. Nevertheless, we need the absolute efficiency to correctly make the summing corrections as will be discussed later.

The two plastic β scintillators are made using BC404 [1] of 15 cm length and 5.12 cm diameter covering almost 4π solid angle around the 0.5 mm thin-aluminum beam pipe and connected to photomultiplier tube by a short light guide as shown in Fig. 3.6. Most of the β particles have energy more than 1 MeV so that they can pass through the aluminum pipe of thickness 0.5 mm to the plastic scintillators where they are detected. Because the β-decay energy is split between the β particle and the anti-neutrino, the detection efficiency of the β detectors is also energy dependent. However, β particles at lower energy or which enter the pipe at a small angle will be stopped in the pipe and not detected and this set up. The Q_β value of the decay determines the maximum β particle energy for feeding to an excited state and hence the β particles that could reach the β detectors. Although there is

www.manaraa.com

some variation for a particular decay, the main determining factor for a decay is Q_β. For example, we see the β efficiency close to 50% for the ^{74}Cu (Q_β = 9.75 MeV) whereas ^{74}Zn (Q_β = 2.29 MeV) has less than 10% efficiency. This knowledge helps to associate the γ rays with a decay and can even help in the placement of the γ rays in the decay scheme.

3.2.1.3 Data Acquisition System

A triggerless data acquisition system was used to record the energy and absolute time of each γ ray emitted during β decay based on a common clock which was synchronized across all modules. Triggerless data acquisition system used in our experiment benefits by avoiding the loss of valid data. We used the first generation DGF-4C modules for the RO experiments with a 40 MHz clock (25 ns time stamp) while for the LeRIBSS setup, DGF Pixie-16 modules were used with a 100 MHz clock (10 ns accuracy) [41, 42]. The scintillators were used to tag the β-decay events, while the HPGe detectors were used to measure the γ-ray energies. All the events were time tagged allowing the offline generation of γ-single spectra and $\gamma\gamma$ coincidence matrix both with or without a β gated. The signals from the Germanium clover detectors were also subject to the "add-back" procedure (summing of signals from each detector) to reduce background and increase photopeak efficiencies. However, the resulting add-back γ-ray singles spectrum showed significant degradation of the resolution as well as questions about the proper photopeak efficiency. Therefore the γ-ray singles spectra without add-back were used to determine the intensity of the γ rays. A time gate of 100 ns was applied to construct $\gamma\gamma$ and $\beta\gamma$ coincidences.

www.manaraa.com

CHAPTER IV

DATA ANALYSIS

The working principle of all nuclear radiation detectors follows similar characteristics: radiation enters the active volume of the detector, interacts with the atoms of the detector material, and releases a large number of the low-energy electrons from their atomic orbits. These electrons then get collected and form the voltage or current pulse. The amplitude of the current pulse corresponds to the energy of the nuclear radiation.

For radiation like α or β-particles, when they pass through the detector, electron-ion or electron-hole pairs are created. But, for radiation like X rays or γ rays, they do not directly ionize the detector medium. Hence, the detectors measure the secondary electrons arising from the interactions of the radiation with the detector material. The absorption of the γ ray energy occurs mainly through the photoelectric effect, Compton scattering or pair-production. If the total energy of a γ ray is absorbed in the detector, the signal contributes to the full energy peak, whereas if a γ ray is inelastically scattered out of the detector, then the signal contributes to the Compton background.

A low-energy γ ray with a few hundred keV energy transfers all of its energy to the orbital electrons of the detector, the electrons get ejected and the γ ray disappears. In this case, the energy of the ejected electrons is equal to the incident γ-ray energy less than elec-

www.manaraa.com

tron binding energy. The vacancy created in the electron shell because of the photoelectric emission is filled by electron arrangement with the liberation of binding energy either in the form of X-rays or Auger electrons. The photoelectric effect decreases sharply for γ-ray energies few hundred keV. For γ rays in the several hundred keV to MeV range, Compton scattering becomes the dominant mode of energy loss. In this process, the incident γ ray transfers a fraction of its energy to the outer shell electrons inside the detector and get scattered with less energy. The remaining lower energy photons may undergo multiple Compton scattering events or photoelectric interactions and deposits all their energy in the detector. When the energy of the incident γ ray is more than 1.022 MeV, i.e. total rest mass energy of an electron-positron pair, part of the original γ ray may disappear with the creation of an electron-positron pair in the process known as pair production. The positron subsequently annihilates with an orbital electron and produces two 511-keV γ rays which will be absorbed in the detector by the photoelectric effect or Compton scattering. These two photons can escape the detector without interactions or can partially or fully be absorbed. When both photons escape from the detector, they result in a separate peak in the spectrum whose energy is equal to 1022 keV less than the original γ-ray energy. This is called the double escape peak (DEP). If, instead, only one of the photons escapes, it results in a peak having energy 511 keV less than the original γ-ray peak. This is known as the singe escape peak (SEP). For the high energy γ rays, pair production phenomena more dominant than the photoelectric effect and Compton scattering. All these interactions cause the electrons to move in some way creating the electric current which can be

www.manaraa.com

amplified and measured to estimate the energy of the γ ray. The detailed explanation of the process is given in Ref. [60].

As explained in Chapter 3, we used four clover HPGe detectors, two β scintillator detectors, and data were collected in trigger-less data acquisition mode in order to avoid the loss of valid events. The digital electronics were coupled with the detectors to analyze the signals. A cryostat setup was used for the HPGe to avoid the thermal excitation in the detector active volume which would decrease the energy resolution. Each clover in a HPGe detector has four crystals. This multi-crystal structure has benefits of fast signal rise time and better energy resolutions. Each Ge clover crystal detector was independently biased by applying a high voltage. The detector signal was picked up by a charge sensitive pre-amplifier to convert the charge pulse into a voltage signal. These signals were directed to the DGF-4C modules in the RO experiment and to the Pixie-16 modules in the LeRIBSS measurements. The modules digitized the energy signal utilizing an ADC to convert the strength of the signal into a channel number adding a time stamp. A γ ray can Compton scatter into a neighboring crystal and be detected as two separate γ rays. To overcome this effect, an add-back technique was implemented in the RO mode of the experiment but wasn't used in LeRIBSS mode due to the resolution problems. In the add-back method, the full energy of the γ ray was reconstructed by by summing the energies deposited within the event time for each crystal in a clover detector thus reducing the background in the spectrum.

Each crystal in a clover detector has a different response to the γ rays, so that raw spectra vary from crystal to crystal. In order to obtain the single cumulative spectrum, we

www.manaraa.com

energy calibrated each crystal by selecting some reasonably pure, statistically strong γ-ray peaks which are well known and have already been cataloged in the NNDC database. An iterative process was followed to extend the preliminary energy calibration beyond the energies available for the NNDC by using single and double escape peaks. We have selected γ-ray peaks covering the entire energy range of the observed spectra for each mass chain studied. Energy calibration of all 16-crystals was performed using a reduced chi-square method. After the energy calibration, all the spectra from the different crystals lined up and a summed γ-ray singles spectrum could be obtained. Finally, we performed a scan of the data to generate a histogram files, to be discussed in more detail later, containing the various spectra and coincidence matrices to be analyzed.

The transition energy between two states of the nucleus has a unique signature. For an ideal detector, the full energy of the γ ray will be perfectly absorbed giving the extremely narrow peak (δ function) in the spectrum. But in practice, the decay spectrum would be the Gaussian-shaped peak which arises from the several possible events that may occur when the γ ray enters the detector and gets converted to signal. To determine the energy and intensity of the γ-rays detected, we have used the gf3 fitting program from the RadWare software packages [80]. The center of the fitted peak gives the energy whereas the area gives the intensity of the corresponding γ ray. Different factors like statistical fluctuation in number of charge pairs produced in the detector, incomplete charge collection, and noise associated with electronic devices can affect the shape of the γ-ray peaks. Therefore, the γ-ray peaks have both Gaussian and skewed Gaussian components. In addition, γ-ray peaks below about 200 keV can have a step function in the background. The shape of the γ ray

www.manaraa.com

can be modeled using several shape parameters, namely R, β, FWHM and the step-size. Fit parameters: R defines the height of the peaks for both Gaussian and skew Gaussian profile, β is the decay constant of the skew Gaussian profile, the step is the relative height of the smoothed step function, and FWHM represents the peak width (broadening of the peak) in the spectrum. For proper fitting of the γ-ray peaks, the shape parameters were calibrated through multiple iterations before being held fix during the final fitting step. Details on the shape parameters are given in the following paragraph.

The R and β parameters vary linearly with the channel number while FWHM varies quadratically as govern by the equations:

$$R = A + Bx, \tag{4.1}$$

$$\beta = C + Dx, \tag{4.2}$$

and

$$FWHM = \sqrt{(F^2 + G^2x + H^2x^2)}, \tag{4.3}$$

where, x is the channel numbers, and A, B, C, D, F, G and H are the coefficients of fit parameters. The step size has less contribution to the peak shape and is only important at low energy, so we first fixed the step size and varied other parameters in a cyclic fashion. We started by performing the gf3 fitting of some major peaks in the spectra (for the ^{74}Ga β decay, we fitted the 596-, 868-, 1064-, 2353- and 4255-keV γ-ray peaks), recorded the R values as a function of channel number and initialized the fitting parameters A and B in the gfinit.dat file (file used by gf3 software for proper fitting of γ-ray peaks). Next, we fixed the step size and R value, freed the other parameters, β and FWHM. We again performed

www.manaraa.com

the fitting of the same set of γ-ray peaks and record the β values as a function of channel number, and initialized the C and D parameters in gfinit.dat. In the third step, we fixed everything except FWHM, then fitted the same sets of peaks and determined the FWHM value as a function of channel number, used that information to initialize the values of F, G and H, and added the information to gfinit.dat. We repeated all the above steps several times until we obtained stable coefficients for the fit parameters.

Once the fit parameters were statistically established, we used gf3 to fit all possible γ-ray peaks seen in the γ-ray singles spectrum, with the result stored in a raw data file including peak centroids and areas. The raw data files were read by the MASTER program to generate the energy and intensity of the γ-ray peaks by taking into consideration the efficiency and energy calibration files. Different efficiency files were used for different projects detector configurations. Figure 4.1 shows the absolute photopeak efficiency curve used for our first project (^{74}Ga β decay). The Ge clover array has a maximum photopeak efficiency of 29% about 100 keV and falls to 5% at 1.33 MeV in LeRIBSS set up. In the RO set up, these values were 22% at 100 keV and 5% at 1.33 MeV. The γ-ray efficiency of the clover detectors were determined using the standard γ-ray sources including ^{57,60}Co, ^{88}Y, ^{109}Cd, ^{113}Sn, ^{133}Ba ^{137}Cs, ^{139}Ce, ^{152,154,155}Eu, ^{210}Po, ^{226}Ra and ^{241}Am.

During the analysis, we have used four different types of spectra: γ-ray singles, β-gated γ-ray singles ($\beta\gamma$), $\gamma\gamma$ coincidences and β-gated $\gamma\gamma$ coincidences spectra. For each β-decay event, if it doesn't directly feed to the ground state, it will populate an excited state based on the selection rule given in Table 2.1, and should emit a single γ ray or a cascades of γ rays which are in coincidence with the β event. Although, the β-gated

www.manaraa.com

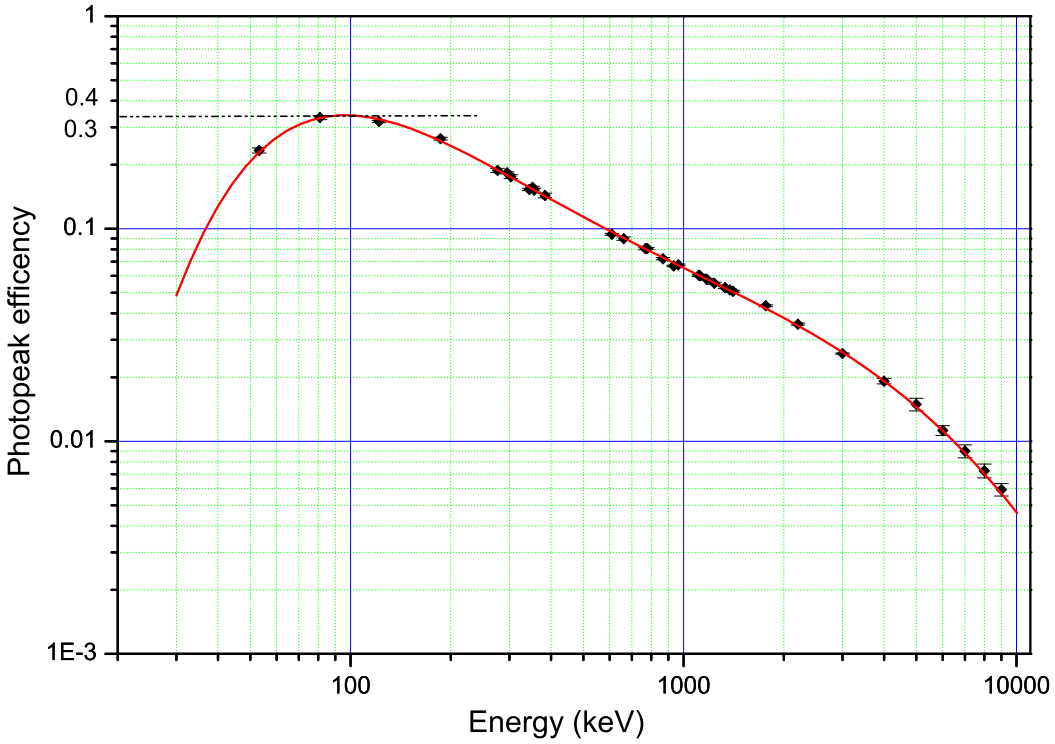

Figure 4.1: Example sum of four clover HPGe detector absolute photopeak efficiency curve measured for the CARDS setup at LeRIBSS.

spectra significantly decreases the γ-ray intensity compared to the γ-singles spectrum, it provides a strong advantage in reducing the large background and unwanted radiations during the analysis. The $\beta\gamma$ spectra allow for the assignment of γ ray to decays based on β detection efficiency. During the process of populating the high energy states, the emitted electrons may have very low kinetic energy, which will not be able to pass through the beam line wall to the scintillator detectors. This will result in the exclusion of the some of the low-intensity γ rays in the $\beta\gamma$ coincidence analysis. The γ rays detected by two detectors within a certain time window are used to generate the $\gamma\gamma$ coincidence spectra. These coincidence spectra were used to build the decay scheme connecting the cascades of

www.manaraa.com

γ rays. The coincidence information was also used to reconstruct the actual γ-ray intensity for unresolved doublets.

4.1 Decay Scheme Development

We made a general assumption that the strongest transition in the decay scheme should de-excite the low-lying states by decaying to either the ground or an isomeric state. As our collected γ-ray singles spectra have the γ rays associated with all daughter nuclei, we first needed to identified the γ rays associated with each member of the decay chain, though our interest here is the Ga isotopes. With a set of identified γ rays, we could begin the process of building a decay scheme. The primary method of determining the placement of the γ rays in the decay scheme was based on the coincidence information and construct the decay scheme based on the statically significant $\gamma\gamma$ coincidences.

4.1.1 Coincidence Gating Techniques

By setting a gate on the horizontal axis of the two dimensional $\gamma\gamma$ matrix, a spectrum of γ-rays coincident with the gating energy range was obtained. A peak gate is made to accept most of the events associated with a specific γ ray of interest along with the Compton background present in that region as well as possible overlapping γ rays. An associated Background gate (that includes Compton scattering events or unresolved γ rays) was taken in the same region of the spectrum and was subtracted from the Peak gated spectrum to obtain the $\gamma\gamma$ coincident information. In most cases, the coincidence gating process was complicated due to the overlap of the γ-ray peaks such that a single background gate was insufficient to remove the contamination from the adjacent γ rays. Figure 4.2 shows an

www.manaraa.com

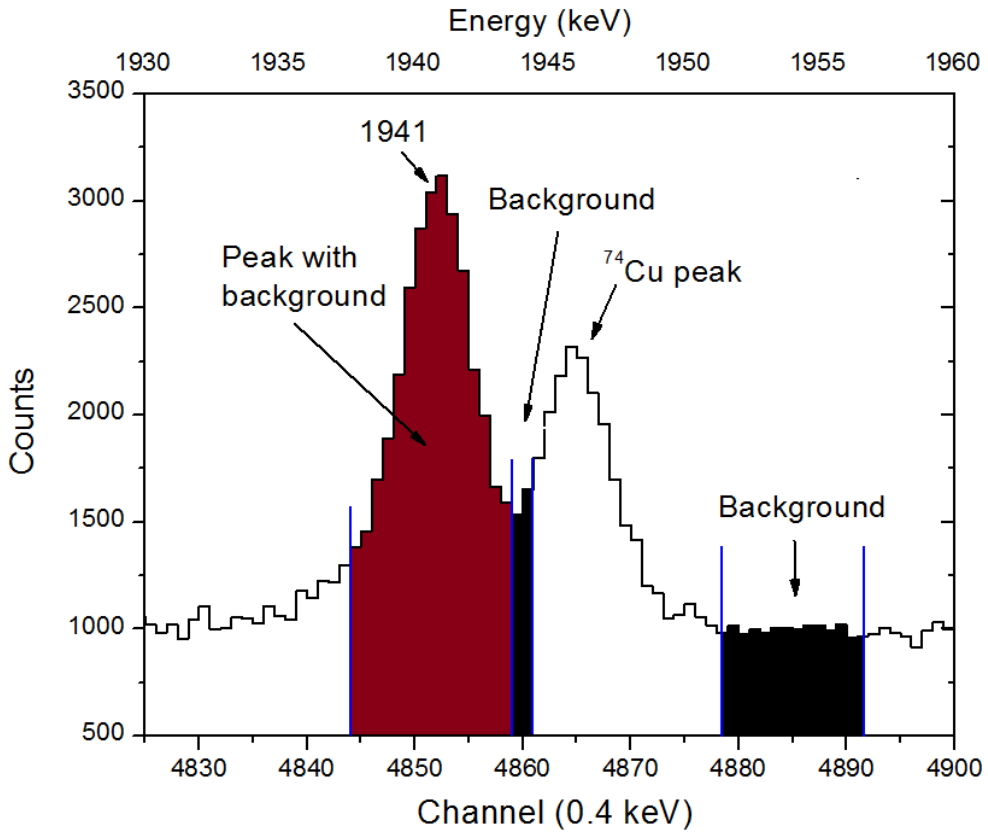

Figure 4.2: Figure showing the gates for the 1941 keV γ-ray peak which contains some little contribution from the near by peak. The red colored region represents the peak with background whereas the black colored regions represent background. The horizontal axis is scaled at 0.4 keV/channel in order to perform the precise gates. The true energy is displayed at the top of the plot.

example of the gating technique utilized for the 1941-keV γ-ray peak associated with ^{74}Ga β decay to obtain a clean $\gamma\gamma$-coincidence spectra. For this γ ray, the problem is overlap with the adjacent 1945-keV γ ray from ^{74}Cu β decay which extends into the regions of the 1941-keV γ-ray peak. For the 1941-keV γ-ray peak, we have chosen peak gate from

www.manaraa.com

channel numbers 4844 to 4460 while the background gate was the sum of channel number 4860 to 4862 and 4878 to 4882. Generally, we adjust the background gate several times so that the contribution of the overlapping γ rays can be completely subtracted out. Furthermore, background gates were sometimes scaled to improve the subtraction process. We have used the add-back $\gamma\gamma$ coincidence matrix for the for coincidence analysis but used the non add-back coincidence matrix for estimating the intensity purpose.

4.1.2 Statistically Significant Coincidences

In the past, most $\gamma\gamma$ coincidence analysis involved only a visual inspection of the background-subtraction coincidence spectrum to determine coincidences. However, in the simple qualitative visual inspection of the background subtracted spectra, it is not always clear which γ rays are in real coincidence or if an observed peak is just the residue from an incorrect background subtraction. Another important issue to address was how to justify the placement of a γ ray to new level if it was the only γ ray observed coming from the new levels, i.e. how do we have confidence in such a placement? To put a quantitative answer to this question, we have developed a more objective plan by determining the statistical significance factor (S) for each observed γ ray obtained from the projection of a $\gamma\gamma$ coincidence gate as described in the next paragraph.

Due to the low statistics and distorted peak profiles of the γ-ray peaks observed in the background subtracted spectrum, we have used the peak-gated and background-gated spectra for analysis purpose. Gaussian functions were fitted to any peak observed in the peak gate using the DAMM program with up to 15 peaks selected at a time. The positions

www.manaraa.com

of these peaks were fixed, and the same set of peaks was then fitted in the Background gate. The significance factor (S) was determined for each peak as the difference in the two areas (ΔA) divided by the total uncertainty (σ), where, σ_{A_P} and σ_{A_B} are the uncertainties in Peak area and the Background area. As a formula this is

$$S = \frac{\Delta A}{\sigma} = \frac{A_P - A_B}{\sqrt{\sigma_{A_P}^2 - \sigma_{A_B}^2}}. \tag{4.4}$$

If a peak was found to have S $\geq$ 2.00, i.e. 2σ above background, then the coincidence is considered to be possible, while if S $\geq$ 3.75 (probability of 99.98 %) it is considered a definite coincidence. This statistical significance factor provides the justification for the placement of γ rays to a new level as well as removes any evaluator bias from the analysis.

4.1.3 Resolving the Doublets

The relative intensity of the observed γ rays is calculated using the area obtained from the Gaussian fit of each peak in the γ-ray singles spectrum normalized to the area of the principal peak in the decay. Some of the detected γ rays can have nearly the same energy and appear as a single unresolved peak in spectra. These γ rays may either belong to different members of the decay chain or follow a different de-excitation path in the decay cascade even if they belong to a single β-decay parent. These unresolved γ rays which should be placed in different locations within a decay scheme are known as doublets. The doublets are so close in many cases that the $gf3$ fitting cannot separate the peaks even if we know they are present. Therefore we needed an alternative method to extract the energies and intensities for these close doublets. This is one of the main issues in the current NNDC

www.manaraa.com

database have. All the previous measurements multiply placed several γ rays without dividing the intensity, which causes incorrect feeding predictions to the energy levels.

After constructing the complete decay scheme, we can resolve the doublets by taking the $\gamma\gamma$ coincidence information into consideration. To resolve the possible γ-ray doublets and assign the proper intensity to each in the decay scheme, two methods have been developed as described in the following sections. To determine the energy of two members of the doublet, we have used the centroid of the γ-ray peaks seen in the coincidence gate. Most of the time, we have checked several γ-rays coincidence spectra in cascade and took a weighted average of their energies. To predict the uncertainty associated with their energy, we have used the gf3 fitting software. We fixed the height (that comes from the area of the doublets estimated form the methods explained below) and freed the position of the peak which gives the position and uncertainty associated to the γ-ray doublets.

4.1.3.1 Method-I

A simple decay scheme is shown in Fig. 4.3 in which γ rays γ_j and γ_k both feed into level L_1 which can be depopulated by several γ rays including γ_i. We will assume that the coincidence data suggest that γ_k is part of a doublet while γ_i and γ_k are well defined clean peaks. We need to derive a method to estimate the number of counts to correctly associate the γ_k. By setting a gate on the γ-ray peak γ_i, we can generate the coincidence spectra and estimate the coincidence counts of γ_j and γ_k with the γ_i. The expected number of counts for γ_k in the γ-ray singles spectrum (A(γ_k)) can be estimated by multiplying the ratio of

www.manaraa.com

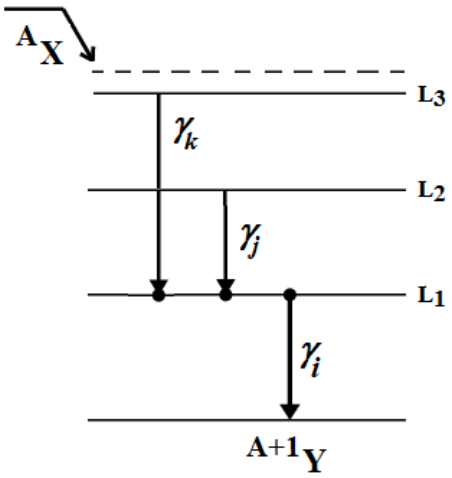

Figure 4.3: Sample decay scheme-I.

coincidence counts of γ_k and γ_j (A($\gamma_{i/k}$) and A($\gamma_{i/j}$), respectively) with the number of counts for γ_j obtained from the γ single spectrum (A(γ_j)), which is written as:

$$A(\gamma_k) = \frac{A(\gamma_{i/k})}{A(\gamma_{i/j})} A(\gamma_j). \tag{4.5}$$

This method is very useful for most of the scenarios where the intensity of a doublets needed to be divided.

4.1.3.2 Method-II

Consider the case shown in Fig. 4.4. In this decay scheme, the γ-rays γ_i, γ_j and γ_k are in a sequential cascade. Evidence from the coincidence gate set on γ_k suggest that it is an unresolved doublet, and we need to divide the intensity determined form the singles spectrum between two different placements. To extract the intensity to associate with γ_k for the indicted cascade, we first define the unknown total number of decays as N_0 for the parent, N_i as the number of γ_i detected in the γ-ray singles spectrum, ϵ_i is the absolute

www.manaraa.com

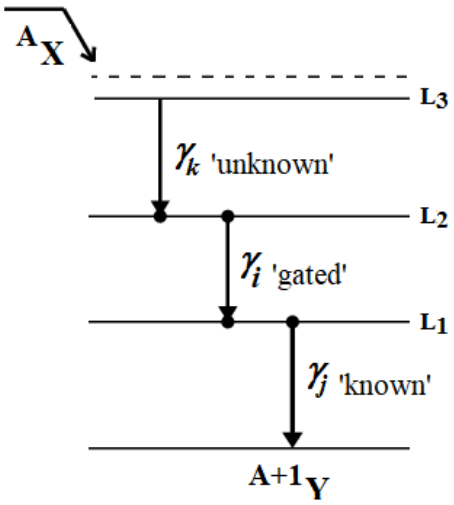

Figure 4.4: Sample decay scheme-II.

photopeak efficiency for γ_i, and B_i is the branching ratio, the percentage of the decays which produce the γ ray, for γ_i. The value of N_i is given its terms of the other parameters by:

$$N_i = N_0 \epsilon_i B_i. \tag{4.6}$$

Next we designate the number of γ_j detected in coincidence with a gate on γ_i, as $\gamma\gamma_{i/j}$. This value is determined from the number of detected events for γ_i (Eqn. 4.6), multiply by the probability that the γ_i will see γ_j, and then taking into account the detection efficiency for the γ_j (ϵ_j). The probability that γ_i will see γ_j is just the ratio of the intensity of γ_i (I_i) divided by the sum of the intensity for all γ rays observed to de-excite level L_1 (I_{L_1}). Combining this information we obtain;

$$\gamma\gamma_{i/j} = (N_0 \epsilon_i B_i)\epsilon_j \frac{I_i}{I_{L_1}}. \tag{4.7}$$

www.manaraa.com

In the same way, the number of detected γ_k in coincidences with a gate on γ_i, denoted as $\gamma\gamma_{i/k}$, is given by :

$$\gamma\gamma_{i/k} = (N_0\epsilon_i B_i)\epsilon_k \frac{I_i}{I_{L_2}} \frac{I_k}{I_i} = (N_0\epsilon_i B_i)\epsilon_k \frac{I_k}{I_{L_2}} \tag{4.8}$$

, where ϵ_k is the absolute photopeak efficiency for detection of γ_k, I_k is the relative intensity of γ_k, and I_{L_2} is the total summed intensity of all γ rays de-exciting the level L_2. From Equations 4.7 and 4.8, the ratio of the number of γ_k and γ_j in coincidence with γ_i is given by:

$$\frac{\gamma\gamma_{i/k}}{\gamma\gamma_{i/j}} = \frac{\epsilon_k}{\epsilon_j} \frac{I_{L_1}}{I_{L_2}} \frac{I_k}{I_j}. \tag{4.9}$$

The relative intensity of a γ rays can be written as some constant C which multiplies the ratio of the number of detected counts to absolute photopeak efficiency. Hence the ratio for the intensity of γ_k to γ_j is given by:

$$\frac{I_k}{I_j} = \frac{C\frac{N_k}{\epsilon_k}}{C\frac{N_j}{\epsilon_j}} = \frac{N_k}{N_j} \frac{\epsilon_j}{\epsilon_k}. \tag{4.10}$$

Then Equation 4.9 becomes:

$$\frac{\gamma\gamma_{i/k}}{\gamma\gamma_{i/j}} = \frac{I_{L_1}}{I_{L_2}} \frac{N_k}{N_j}, \tag{4.11}$$

$$\Rightarrow N_k = \frac{\gamma\gamma_{i/k}}{\gamma\gamma_{i/j}} \frac{I_{L_2}}{I_{L_1}} N_j. \tag{4.12}$$

This calculation gives us the γ-ray singles counts for γ_k in the decay scheme shown in Fig. 4.4. Similarly, we can calculate the γ-ray singles counts of the other complementary part of the doublet allowing proper splitting of the observed counts between the two γ rays.

www.manaraa.com

4.1.4 Level Energies and Feedings

After assigning the proper energies and intensities for the γ rays in the decay scheme, the MASTER program was used to calculate the least square fit level energies and the relative β-feeding intensity for all proposed energy levels. We assigned the strongest γ-ray transition intensity to be 100 and normalized the rest of the γ-rays intensity relative to this value. To convert the relative intensity to absolute intensity, we summed all the γ-rays intensity feeding the ground state. Then, ground state feeding was normalized to 100%. Furthermore, to get the exact feeding intensity summing correction was performed using MASTER program with considering few keV K_α energy for particular isotope of our interest. For the ground state, β-feeding could not be directly measured. Instead, we could make a reasonable estimate for the ground state feeding based on the ground state spin-parity assignments for the parent and daughter nuclei as determined in different measurements.

The Nuclear Structure and Decay Tool section of the NNDC data website was utilized to calculate the $\log(ft)$ value corresponding to each establish level. This tool takes the atomic number of parent nucleus, it's half-life, Q_β value, the energy values for the parent state and state being fed in the daughter nuclide with the absolute β-feeding intensity to generate the $\log(ft)$ value. A higher $\log(ft)$ value corresponds to a lower β-feeding intensity and vice versa. The $\log(ft)$ value ranges for different β-decay levels of forbiddeness are summarized in the Table 2.1.

www.manaraa.com

CHAPTER V

THE β DECAY OF ^{74}GA

5.1 Introduction

A detailed study of β-decay far from stability relies heavily on a good understanding of the daughter and grand-daughter nuclei decays in order to correctly assign weaker transitions to the decays. In this experiment, an attempt was made to perform a complete β-decay study of the $A = 74$ isobaric mass chain to obtain information on the structure of the daughter nuclei. A purified ^{74}Cu beam was used at the Holifield Radioactive Ion Beam Facility (HRIBF) of Oak Ridge National Lab (ORNL) to study the β-decay of the $A = 74$ decay chain using three High Purity Germanium (HPGe) clover detectors in the Low energy Radioactive Ion Beam Spectroscopy Station (LeRIBSS) set up. In this measurement, data on γ-ray emission following β decay including γ-ray singles and $\gamma\gamma$-coincidence spectra along with β-gated versions of the spectra, were obtained. The primary goal of this experiment was a precise measurement of the ^{74}Cu decay [110], but it also allowed for a detailed studied of all daughter nuclei, i.e. ^{74}Zn and ^{74}Ga. In the following sections are presented a discussion of the scientific motivation for the research, experimental details, and the results including the proposed decay scheme, β-feeding intensities, corresponding $\log(ft)$ values with tentative spin-parity assignments, and comparison with Nushellx theoretical calculations.

www.manaraa.com

5.2 Scientific Motivation

The evolution of the first excited states in a series of isotopes or isotones yields information about the gradual shape transition within these sequences nuclei. The experimentally observed lowering of the first 2^+ excited state in $^{70-76}$Ge even-even isotopes indicates the possible existence of spherical and deformed configurations with triaxiality [44, 104] in this region around the $N = 40$ subshell closure making ^{74}Ga an interesting physics case for a β-decay study. ^{74}Ga is an odd-odd nuclide with a ground state spin-parity of 3^- [68]. In the traditional shell model view of the β-decay process, one neutron in a $\nu 1g_{9/2}$ state converts into a proton in the $\pi 2p_{3/2}$ state resulting in stable even-even ^{74}Ge with a closed $\pi 2p_{3/2}$ orbital. The schematic diagram of this process is shown in Fig. 5.1.

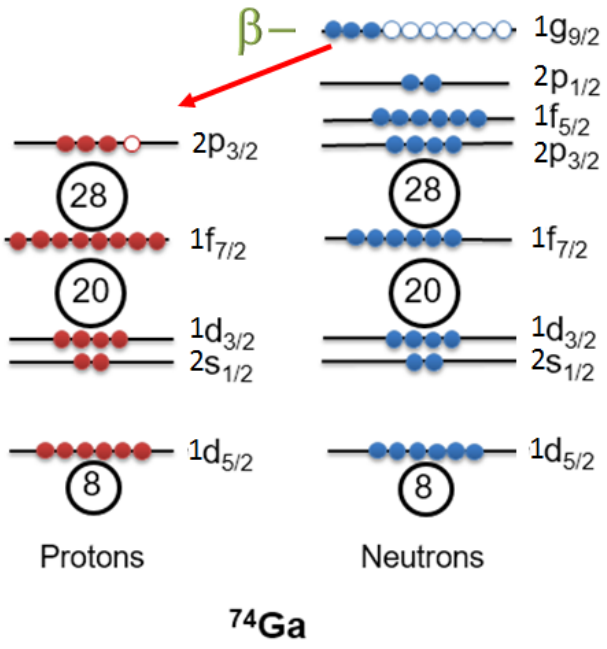

Figure 5.1: Shell model view of ^{74}Ga nuclei.

www.manaraa.com

The structure information of ^{74}Ge from the β decay of ^{74}Ge comes from previous two measurements by Camp *et al.* [24] and Taylor *et al.* [106] which are stored on the ENSDF of NNDC database. Both of the studies produced ^{74}Ga from (n, p) reaction using the ^{74}Ge powder target which was 95.8% and 94.48% pure in Camp *et al.* and Taylor *et al.* measurement, respectively. The two previous β-decay measurements of ^{74}Ga performed by Camp *et al.* and Taylor *et al.* [24, 106] lack a consistent description of ^{74}Ge. Although the two experiments agreed on the observed γ rays, the placement of these transitions into a decay scheme disagreed significantly. This leads to numerous double placements and erroneous levels being assigned within the ENSDF database. The level scheme below 2.6 MeV is agreement between the two measurements. However, above 2.6 MeV the decay scheme is fraught with inconsistencies. Of the 113 γ rays listed in the two papers, placement of only 59 are in agreement between the two studies. For the remaining 54 γ rays for which the placements are not in agreement, 11 are doubly placed so that there are actually only 102 γ rays assigned to the decay. The decay scheme proposed by Camp *et al.* [24] was developed from data obtained with a small single Ge(Li) detector (size 25 cm^3 whose relative efficiency was 3.8 %) allowing only use of energy sums and difference, and the γ-ray intensity balances. The later measurement by Taylor *et al.* Taylor *et al.* was slightly improved (used Ge(Li) detector of size 125 cm^3 with relative efficiency 9.5 %), but still didn't have $\gamma\gamma$ coincidence data. Due to the incorrect and double placements, the established levels and β-feeding patterns are not correctly determined. In general, we can say that the current β-decay data for ^{74}Ga is incomplete. This fact motivated us to

www.manaraa.com

revisit ^{74}Ga β decay with higher statistics data and the best technology/techniques currently available.

5.3 Experimental Technique

A proton beam with an energy of 54 MeV and average intensity of 10-12 μA was produced from the Oak Ridge Isochronous Cyclotron (ORIC) and impinged on a uranium carbide (UC_x) target of thickness 6 g/cm^2. The fission products were thermalized and accelerated to an energy of about 100 keV, subsequently ionized in a hot plasma ion source and extracted as positive ions. Isobaric separation of mass A = 74 was achieved using the low-resolution mass separator (M/ΔM = 600) [21]. For this experiment, the charge exchange cell was not used resulting in a smaller beam spot size and less beam dispersion which results in a higher effective resolution for the isobar separator ((M/ΔM = 10,000). A purified ^{74}Cu beam was then directed to the Low–energy Radioactive Ion Beam Spectroscopy Station (LeRIBSS) [5] and deposited onto a moving tape collector (MTC) in the center of detector set up which consisted of three HPGe clover γ-ray detectors with collective efficiency 3.5$\%$ at 1.33 MeV and 2 plastic scintillation counters with an efficiency of about 50$\%$.

The MTC allowed for moving the accumulated source away from the detector region in order to distinguish the γ rays emitted by nuclides with different half-lives: ^{74}Cu - 1.63(5) s, ^{74}Zn - 95.6(12) s and ^{74}Ga - 487(7) s. The large difference in the half-lives for this mass chain made it easy to distinguish them as the source strength built up. During the course of experiment, four runs were performed. The first run which lasted 309 s was used to identify

www.manaraa.com

A = 74 mass chain, and observed the excessive amount of ^{74}Zn and ^{74}Ga was not in the beam. The MTC was then moved to remove the some observed residual contamination from previous experiment. For the rest of the three runs, we identified no need of MTC as no member of the decay chain dominates the γ-ray spectra. The second and third run were performed for 3133 s and 2863 s, respectively which showed 606-keV γ ray from ^{74}Cu have the similar height as of the 596 γ rays from the ^{74}Ga, whose daughter ^{74}Ge is a stable nuclei. The final run was performed for 1810 s which showed a 50$\%$ increase in the height of 596-keV γ ray to the 606-keV γ ray indicating the slight drift in the beam tune. Altogether, total run time for this experiment was 8115 s. Only data from three clover HPGe detectors were used in analysis of the experiment after it was determined that the fourth HPGe detector was unusable due to radiation damage from previous measurements. The detectors were coupled with a triggerless data acquisition system using DGF-pixie-16 modules which recorded the energy and absolute time for each γ ray or β particle detected using a 100 MHz clock (10 ns accuracy) synchronized across all modules [41, 42]. The time gates of 100 ns were applied in order to construct $\gamma\gamma$ and $\beta\gamma$ coincidences and detect isomeric transitions following the β decay [73]. This allowed the offline analysis of the data to established $\gamma\gamma$ coincidences.

The efficiency calibration of the detector set up was performed using the standard γ ray sources of ^{57,60}Co, ^{88}Y, ^{109}Cd, ^{113}Sn, ^{137}Cs, ^{139}Ce, ^{210}Po, ^{226}Ra and ^{241}Am for an energy range 32 keV to 1836 keV. Then result were compared with the efficiency values determined from previous experiments [52,54] which used the calibrated sources of ^{133}Ba, ^{152,154,155}Eu, ^{137}Cs, ^{60}Co and ^{226}Ra for an energy range 53 keV to 2204 keV, where the

www.manaraa.com

one defective detector was removed from our current measurement. The results from both efficiency measurement were in agreement and combined data was used for our efficiency calibration purpose [110]. Energy calibration was extended up to 5 MeV by comparing the behaviour of the similar systems available in literature [66, 84, 92].

First round of energy calibration was done using the clean and strong γ-rays peaks between 89 keV to 3232 keV which are already known from different measurement. Then the calibration was extend to higher energy range up to 4289 keV by using the SEP and DEP peaks as explained in Chapter 4.

5.4 Experimental Results

Figure 5.2 shows the γ-ray singles spectrum for the $A = 74$ isobar chain. The energy spectrum was generated by summing over all 12 Germanium crystals and for all data runs at a resolution of 0.4 keV/channel covering the energy range from 20 keV to 5200 keV. We applied the Gaussian function fit for all potential γ-ray peaks seen in the spectrum using the RadWare program gf3 to determine the centroids and areas. This information was fed into the program MASTER along with energy and efficiency calibrations information to obtain energy and relative intensities. We have used the coincidence data as a primary source of information for assigning the γ ray to a particular element. For weak γ rays, we have utilized the β detection efficiency to identified them even they do not show any coincidence information. We identified a total of 109 γ rays associated with ^{74}Ga β decay (see Table 5.1) of which 595.85-keV γ ray was found to be the strongest and all other γ-ray intensities were normalized to this γ ray.

www.manaraa.com

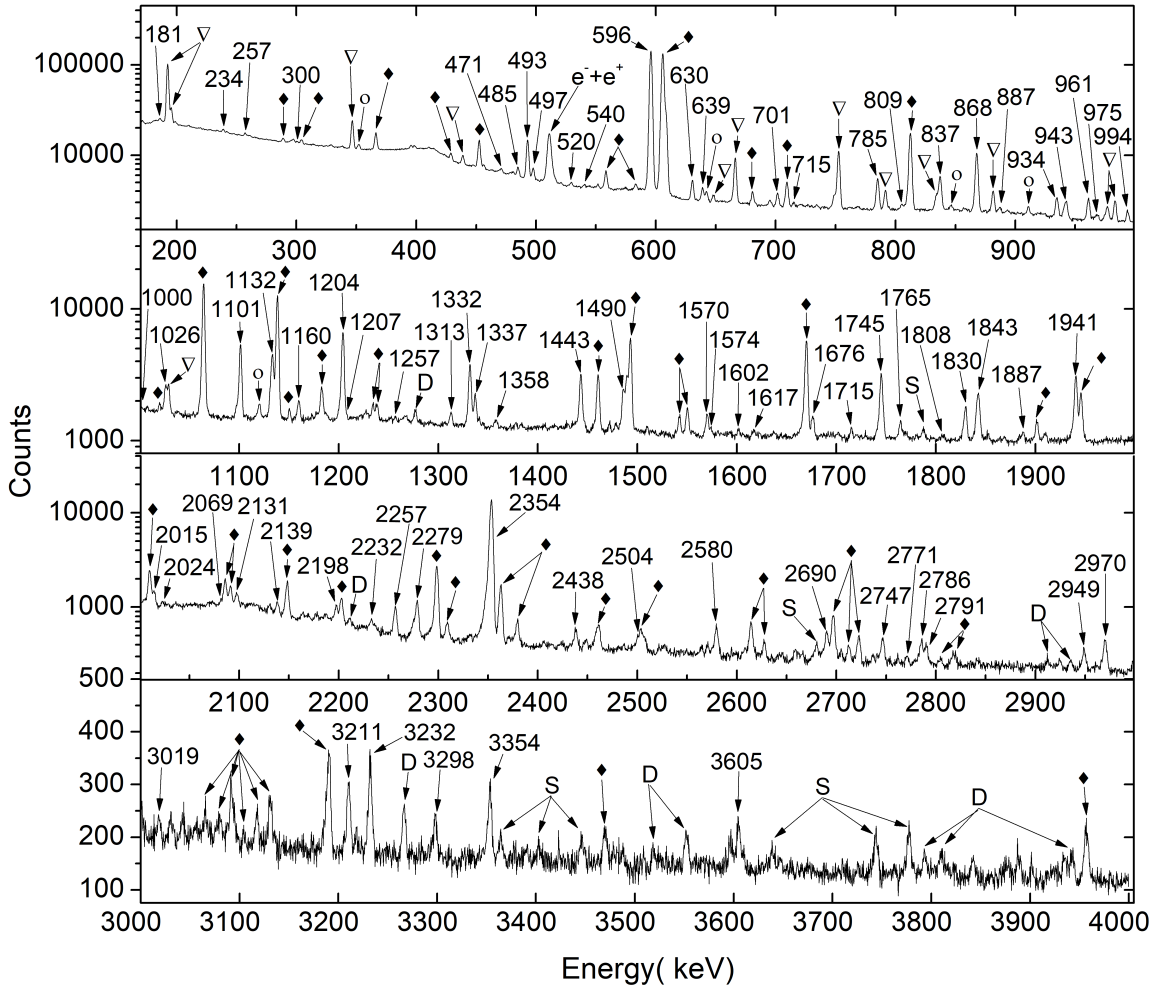

Figure 5.2: Summed γ-ray singles spectrum for all four data runs obtained at LeRIBSS from a purified ^{74}Cu beam in the energy range from 175 keV to 4 MeV. The γ-ray peaks associated with ^{74}Ga decay are marked with their energy. The other two members of the decay chain are indicated as ^{74}Cu: ♦ (solid diamond) and ^{74}Zn: ▽ (lower triangle). Single and double escape peak are denoted as S and D, respectively, and background by ○ (empty circle). The energy range focuses on the γ rays associated with ^{74}Ga. Prominent γ rays from ^{74}Zn and ^{74}Cu are presented above 175 keV and below 4 MeV, respectively.

www.manaraa.com

Table 5.1: Intensity and coincidence information of γ rays associated to ^{74}Ga β decay (probable coincidences are indicated with parentheses).

Energy	Intensity	Placement	$\gamma\gamma$-Coincidences
180.83(15)[e]	0.19(2)		(2353)
233.90(15)	0.16(2)	1697.16	(596), (608), 868
259.39(13)[b,c]	0.11(3)	2949.37	(2690)
300.43(10)	0.29(3)	3175.42	(2279)
463.3(3)[e]	0.09(3)		(1890)
468.68(28)[a]	0.15(3)	2165.22	(1101)
471.04(10)[b]	0.41(3)	3140.43	(596), (868), (1206), 2073
484.8(14)[b,c]	0.06(3)	1967.1	596, 887
484.98(9)[a,c]	0.89(3)	3175.42	2690
492.920(13)	5.62(4)	1697.16	596, 608, (999), 1132, 1178, 1204, (1252), 1337, 1443, 1479, (1574), 1781, (1807), 2000, (2023), 2131, 2198, 2504
497.54(3)	1.10(3)	3034.02	596, (1204), 1332, 1941
503.4(5)[b,c]	0.06(3)	1967.1	(868)
520.37(24)	0.25(4)	3696.4	(639)
540.39(15)[b]	0.21(3)	3140.43	2004
544.48(23)[b]	0.14(3)	3080.95	(1332)
551.48(12)[b]	0.26(3)	2248.64	(596), (1101)
595.848(11)	100.00(12)	595.84	(469), 471, 485, 493, 498, 541, 544, 551, 604, 608, 639, 702, 715, 785, (809), 837, 868, 887, 943, 961, 969, 975, 994, (999), 1025, 1101, 1132, 1160, (1178), 1183, 1205, (1313), 1332, 1338, 1358, 1443, (1472), 1480, 1490, 1570, (1574), (1602), 1677, 1745, 1830, 1843, 1888, 1941, 2014, (2067), (2073), 2098, 2139,(2233), 2257, 2279, 2354, 2438, 2504, 2580, (2737), 2747, 2786, 2791, 2970, (3032), 3211, 3233, 3298, 3354, 3605, 3763
603.99(5)	3.65(20)	3140.43	596, (608), (1204), 1331, 1941
608.442(12)	18.14(8)	1204.25	493, 596, (604), (785), (868), 943, 961, 994, 1332, 1338, 1443, 1490, 1745, 1830, 2139
638.93(4)	0.89(3)	3175.42	521, 596, 1332, 1941
701.54(4)	0.86(3)	2165.22	596, 868, (975), (1313), (1338), (1556)
715.06(12)	0.26(2)	2197.97	596, 887, 943
734.28(21)	0.15(2)	2197.97	868, 943
784.27(11)[b,c]	1.11(33)	3478.14	(596), (1204), 1490
809.24(19)[b]	0.29(4)	3478.14	(596), 1205

Continued on next page

www.manaraa.com

Table 5.1 – continued from previous page

Energy	Intensity	Placement	$\gamma\gamma$-Coincidences
836.1(8)[a,c]	0.30(11)	3034.02	994, (2197)
867.832(15)	8.73(5)	1463.68	234, 471, (504), 596, 702, (734), (786), 961, (975), (1101), (1132), 1206, 1313, (1338), 1472, (1510), (1556), 1570, (1617), 1677, (1715), (1808), 2015, (2036), 2233, 2257, (2487), 2737, (2771)
887.04(10)	0.36(3)	1482.89	485, 596, 715, 943, 1207
942.58(7)	1.22(6)	3140.43	596, (608), (715), (735), (887), 994, (1204), 1602, 2198
960.87(8)[a,c]	1.39(3)	2165.22	596, 608, (975), 1204, 1313, 1338, (1556)
961.07(8)[c]	0.28(5)	2424.74	596, 868, (943)
967.1(5)[a,c]	0.27(6)	3503.26	(596), 1941
974.75(29)	0.23(4)	3140.43	702, (868), (961)
993.82(5)	0.77(3)	2197.97	596, (608), 837, 943, 1204, (1443)
999.2(3)[b,c]	0.35(8)	2696.37	(493), (596), 1024
1023.8(9)[b,c]	0.12(6)	3720.48	(596), 999, (1204)
1101.307(20)	5.38(4)	1697.16	(468), (551), 596, (868), 1132, (1178), (1252), 1337, 1443, (1479), (1574), 2000, (2130), 2198, 2504
1131.64(14)[b]	0.92(12)	2828.8	493, (596), 1101, (1204)
1159.88(5)	0.87(3)	3696.4	596, (1204), 1332, 1941
1177.79(18)[b]	0.26(3)	2874.88	493, (1101), (1204)
1183.89(4)	0.34(14)	3720.48	(596), 1941
1201.1(3)[a]	0.24(5)	3894.48	1490, 1941
1204.210(22)	8.04(9)	1204.25	493, (498), (785), (868), (943), 961, 994, (1132), (1159), (1313), 1332, (1338), 1443, 1490, 1745, 1830, 1888, 2139, 2504
1205.2(5)[a,c]	0.39(6)	2669.25	(471), (485), (868)
1252.1(4)[a]	0.13(4)	2949.37	493, (1101), (1204)
1256.9(3)[e]	0.17(3)		(596), (1204)
1312.88(9)	0.60(3)	3478.14	(596), 702, (868), 961, 1204
1332.28(12)[c]	1.45(13)	2536.51	498, (545), 596, (604), 608, 639, 1160, 1204, (1358)
1336.68(11)[c]	1.33(13)	3034.02	493, 596, 608, 1101, 1204
1337.5(4)[a,c]	0.43(8)	3503.26	596, 608, (702), 961
1358.04(15)	0.34(3)	3894.48	(596),(1204), (1332), 1941
1443.31(3)	3.84(6)	3140.43	493, 596, 608, (994), 1101, 1201, 1204, (1698)
1471.96(15)[b]	0.36(4)	2935.63	(762), (785), 868

Continued on next page

www.manaraa.com

Table 5.1 – continued from previous page

Energy	Intensity	Placement	$\gamma\gamma$-Coincidences
1478.43(19)	0.28(4)	3175.42	493, 596, 1101, (1204)
1489.39(4)	2.95(6)	2693.64	596, (608), 785, (1201), 1204
1509.86(25)	0.22(3)	2973.54	596, 869, 1205
1555.73(29)[a]	0.19(3)	3720.48	(702), (868), (961)
1570.24(7)	1.03(4)	3034.02	596, 868
1574.18(18)[a]	0.34(3)	3271.34	(493), (596), (1102)
1601.90(18)	0.31(3)	2197.97	(596), (638), 943, (1204)
1616.7(9)[b,c]	0.17(5)	3080.95	868
1676.34(7)	1.05(4)	3140.43	596, 868
1745.10(5)	4.84(16)	2949.37	596, 608, (972), 1204
1780.7(7)[a]	0.09(4)	3478.14	(493)
1806.1(6)[c,d]	0.19(5)	3271.34	(868)
1806.9(6)[c,d]	0.27(13)	3503.26	(493)
1829.76(5)	2.21(5)	3034.02	596, 609, 1204
1852.03(24)[e]	0.36(4)		
1887.79(17)[a]	0.46(4)	3092.01	(596), 608, 1204
1940.71(4)	5.39(6)	2536.51	(470), 498, 596, 604, 639, 969, 1160, 1183, 1202, 1358
1970.87(73)[e]	0.10(4)		
1999.78(19)	0.44(4)	3696.4	493,(596), (608), 1101
2004.17(26)[b]	0.34(4)	2600.03	540, (967)
2014.55(8)	1.35(5)	3478.14	596, 868
2023.18(25)	0.33(4)	3720.48	493, 596
2036.4(4)	0.21(4)	4201.04	(702), 868
2069.1(5)[e]	0.19(5)		
2073.26(29)[b]	0.31(5)	2669.25	471, (596)
2097.68(9)	1.10(6)	2693.64	(452), 596, (785)
2130.3(14)[c]	0.16(8)	3827.2	(493), 1101
2138.45(10)	0.89(5)	3342.71	(596), (608), 1204
2197.5(7)[c]	0.33(6)	3894.48	(493), (1101)
2198.0(4)[c]	0.60(5)	2197.97	(837), 943
2231.2(15)[c,e]	0.16(4)		
2257.06(6)	1.71(4)	3720.48	596, 868
2278.99(6)[b]	2.28(5)	2874.88	(301), 596
2353.51(5)	45.49(13)	2949.37	180, 596
2438.33(11)	0.78(4)	3034.02	(596)
2486.5(4)	0.15(3)	3949.66	(595), (868)
2503.75(17)	0.82(5)	4201.04	493, (596), 1101, 1204
2579.50(15)	1.05(10)	3175.42	596

Continued on next page

www.manaraa.com

Table 5.1 – continued from previous page

Energy	Intensity	Placement	$\gamma\gamma$-Coincidences
2617.3(5)[e]	0.2(1)		(596)
2690.35(10)[b]	1.05(4)	2690.31	259, 485
2736.9(5)	0.15(3)	4201.04	(596), (868)
2746.89(11)	0.92(4)	3342.71	596
2771.2(3)[b]	0.22(3)	4234.98	(596), 868
2785.64(13)	0.75(4)	3381.47	596
2790.55(14)	0.67(4)	3386.39	
2949.23(15)	0.61(3)	2949.37	596
2970.38(12)	1.13(4)	3566.22	596
3031.0(4)	0.16(3)	4234.98	(596)
3091.95(24)	0.51(5)	3092.01	
3210.89(16)	0.74(4)	3806.73	596
3231.3(5)[c]	0.54(8)	3827.2	596
3298.39(21)	0.46(3)	3894.48	596
3353.75(17)	0.84(4)	3949.66	596
3487.6(5)[e]	0.16(3)		
3605.33(23)	0.51(4)	4201.04	596
3639.5(3)[b]	0.26(3)	4234.98	(596)
3763.2(5)[d]	0.14(4)	4359.05	596

[a] Newly observed γ ray.
[b] γ ray with different placement.
[c] γ ray energy and intensity determined from $\gamma\gamma$ coincident data.
[d] Previously observed γ ray in β-decay measurement [24, 106] but has not assigned to decay scheme.
[e] Unplaced γ ray.

5.4.1 Development of Decay Scheme

We set a coincidence gate on each γ-ray peak in the spectrum and generated the coincidence spectrum as explained in Chapter 4. Care was taken to set the background gate to remove all contamination. A visual inspection was made to identified possible coincidences. For the identified peaks, the statistical significance factor was determined. This

www.manaraa.com

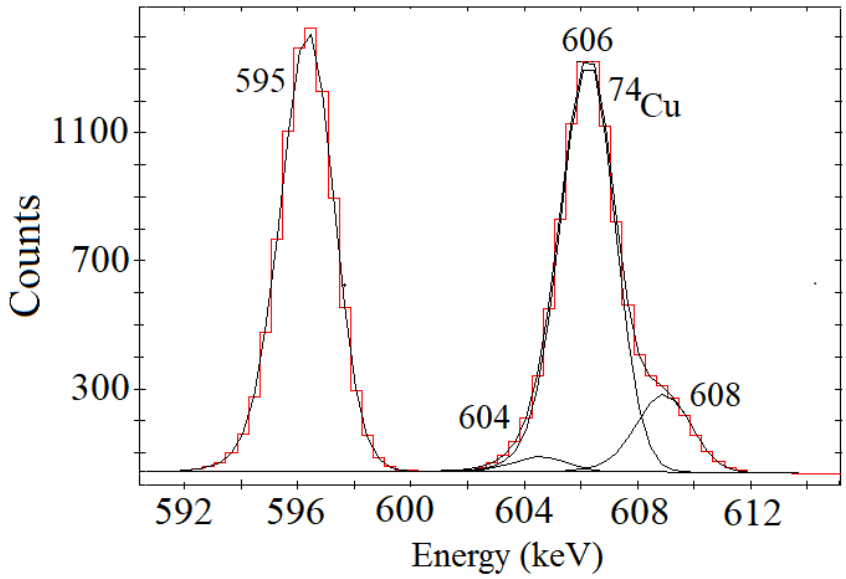

Figure 5.3: Portion of the γ-ray singles spectrum showing the gf3 fit of the primary γ rays from ^{74}Ga and ^{74}Cu, 596 and 606 keV, respectively. Also, observed are the weaker 604- and 608-keV γ rays from ^{74}Ga decay which could be separated in the fit from the much stronger 606-keV γ ray.

yields the $\gamma\gamma$ coincidence information in Table 5.1. If indicated by the coincidence data, additional γ rays were added to the list of assigned γ rays.

We placed the 596-keV γ ray as feeding the ground state and began constructing the decay scheme with 596-keV level based on the coincidences information. The preliminary decay scheme was developed based on the definite coincidences. Finally, we filled in the decay scheme with weaker transitions where the coincidence information is not as strong and attempted to place all the observed γ rays in the decay scheme.

All the γ rays assigned to the structure of ^{74}Ge are listed in the Table 5.1. The decay scheme proposed in Fig. 5.4 and 5.5 was constructed on the basis of observed statistically

www.manaraa.com

significant $\gamma\gamma$ coincidences measurements. Figure 5.3 shows a zoomed in portion of the γ-ray singles spectrum showing the peaks at 596, 604, 606 and 608 keV along with the Gaussian function fit obtained using gf3. Compound γ-ray peaks were isolated to predict their corresponding energy and intensity.

5.4.2 Placement of 471-keV γ ray: An Example of Fixing the Database

A 471-keV γ ray with a relative intensity of 0.42(5)% was reported for the decay of ^{74}Ga by Taylor *et al.* [106], but was not observed in the earlier experiment by Camp *et al.* [24]. Taylor *et al.* [106] placed this transition as de-exciting the level at 3950 keV and feeding the level at 3478 keV (Fig. 5.8 a). For this placement, the strongest $\gamma\gamma$ coincidence would be with the 2014-keV γ ray. By setting a gate on the 471-keV γ peak, the spectrum of coincident γ rays shown in Fig. 5.6 was obtained. However, visual inspection alone can't determine if all the observed peaks in the spectrum are real coincidences or if they are just the residue from incorrect background subtraction. To determine the real coincidences, the statistical significant factor (S) explained in Chapter 4 was determined for each coincidence peak in the spectrum. The information from this analysis is listed in Table 5.2 while Fig.5.7 shows the analysis for four identified coincidences.

As evident in Fig. 5.7 and Table 5.2, we do not see any evidence for a 2014-keV γ ray in coincidence with 471-keV γ ray. Instead, as shown in the Fig. 5.6 and Fig. 5.7, we observed the 471-keV γ ray to be in statistically significant coincidence with four transitions of energy 596, 868, 1205 and 2074 keV. These observations firmly establish this γ ray as de-exciting the level at 3140 keV and feeding the 2669-keV level where the

www.manaraa.com

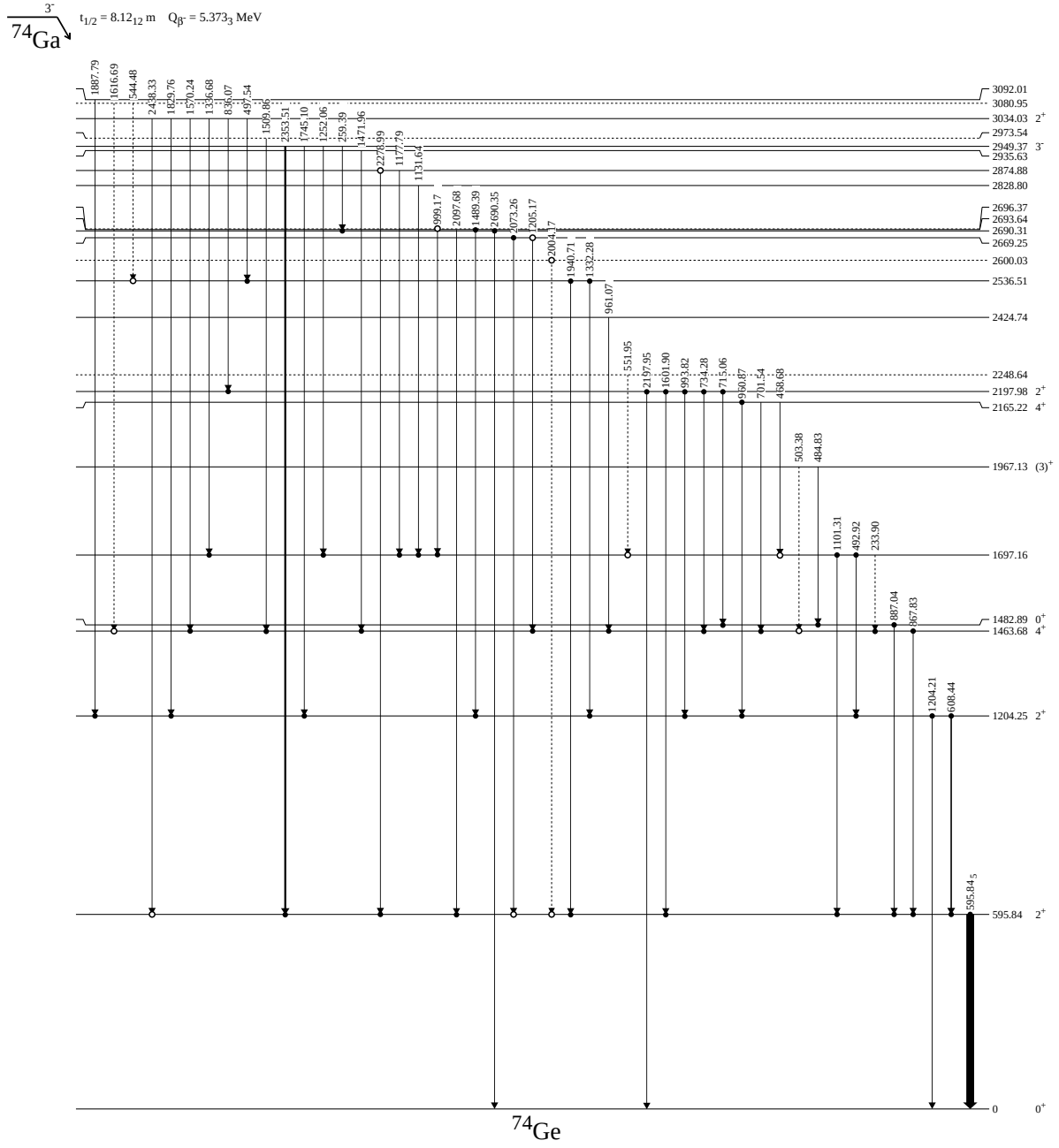

Figure 5.4: Part (a) of the proposed decay scheme for ^{74}Ga to excited states in ^{74}Ge showing low energy transitions.

www.manaraa.com

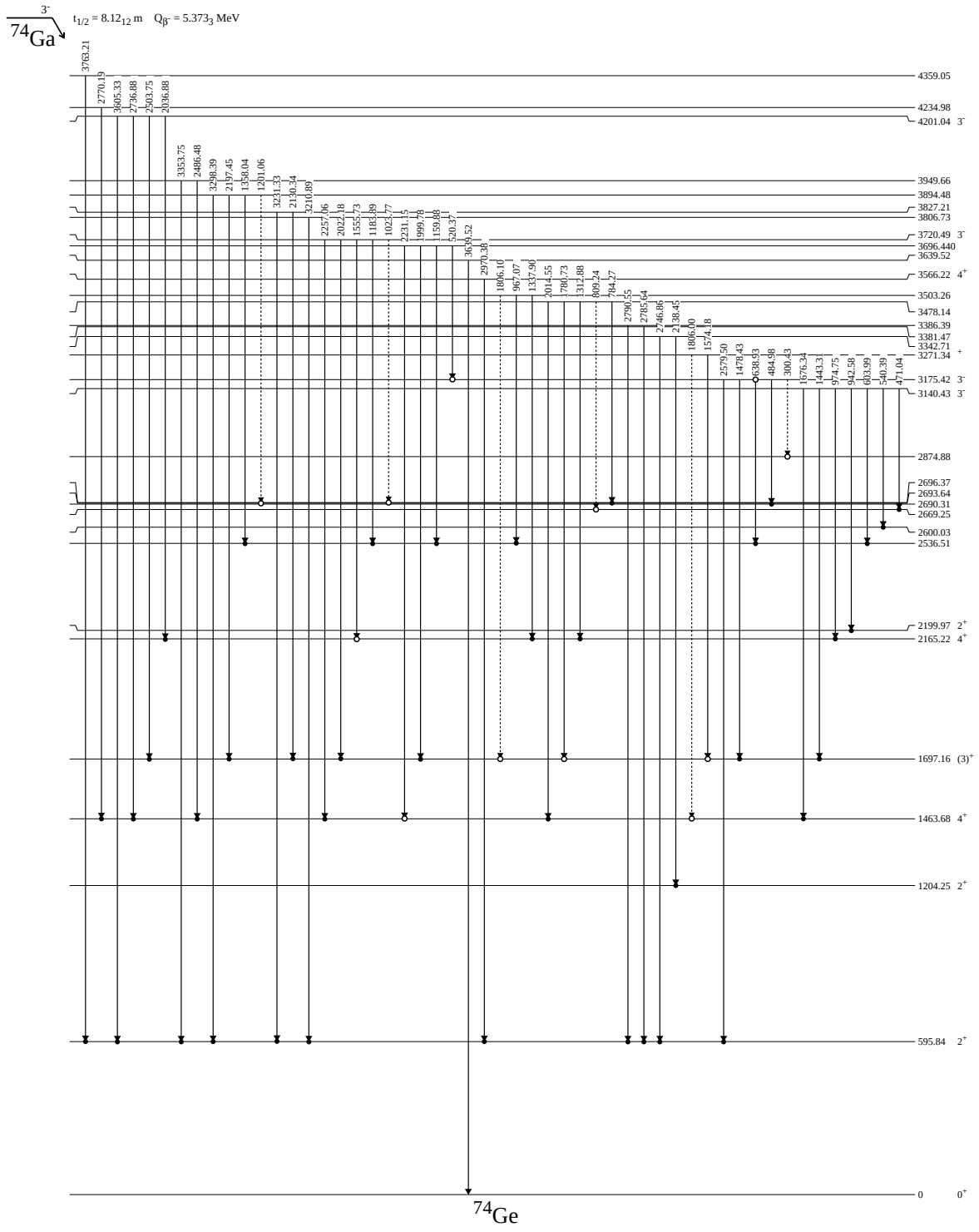

Figure 5.5: Part (b) of the proposed decay scheme for ^{74}Ga to excited states in ^{74}Ge showing high energy transitions.

www.manaraa.com

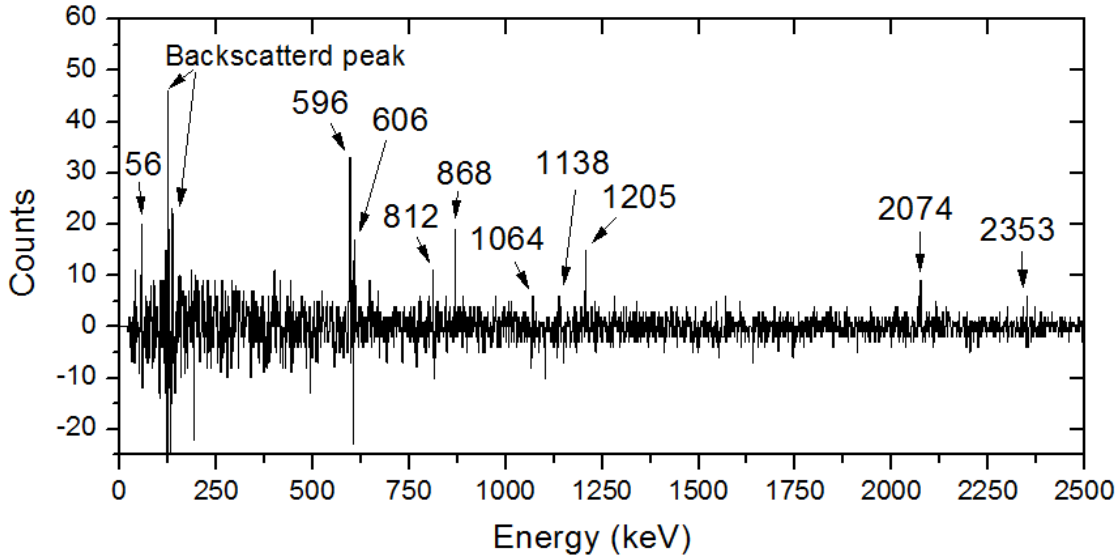

Figure 5.6: Background-subtracted $\gamma\gamma$ coincidence spectra obtained for a coincidence gate set on the 471 keV γ-ray peak. Energy of all possible coincidence peaks are indicated.

strongest de-exciting γ ray is at 2073 keV. This is further supported by the observations of the 471-keV γ ray in definite coincidence with the 2073-keV gate as shown in Fig. 5.8.

Table 5.2: γ rays in coincidence with the 471-keV γ ray

Energy	Peak area(error)	Background area(error)	S-value	Comments
56.8	81(18)	74(20)	0.3	No
141.6	97(18)	116(23)	-0.6	No
596.0	431(29)	316(24)	3.0	May be
606.2	425(29)	414(27)	0.3	No
812.2	83(11)	73(10)	0.7	No
868.0	95(11)	62(9)	2.3	May be
1064.2	82(9)	100(10)	-1.3	No
1493.0	30(5)	28(6)	0.3	No
1138.2	82(9)	57(9)	2.0	May be**
1205.4	57(8)	30(7)	2.7	May be
2073.8	29(5)	7(1)	3.9	Yes
2354.1	52(7)	41(6)	1.2	No

** Removed from the fact it is not seen in mutual coincidences

www.manaraa.com

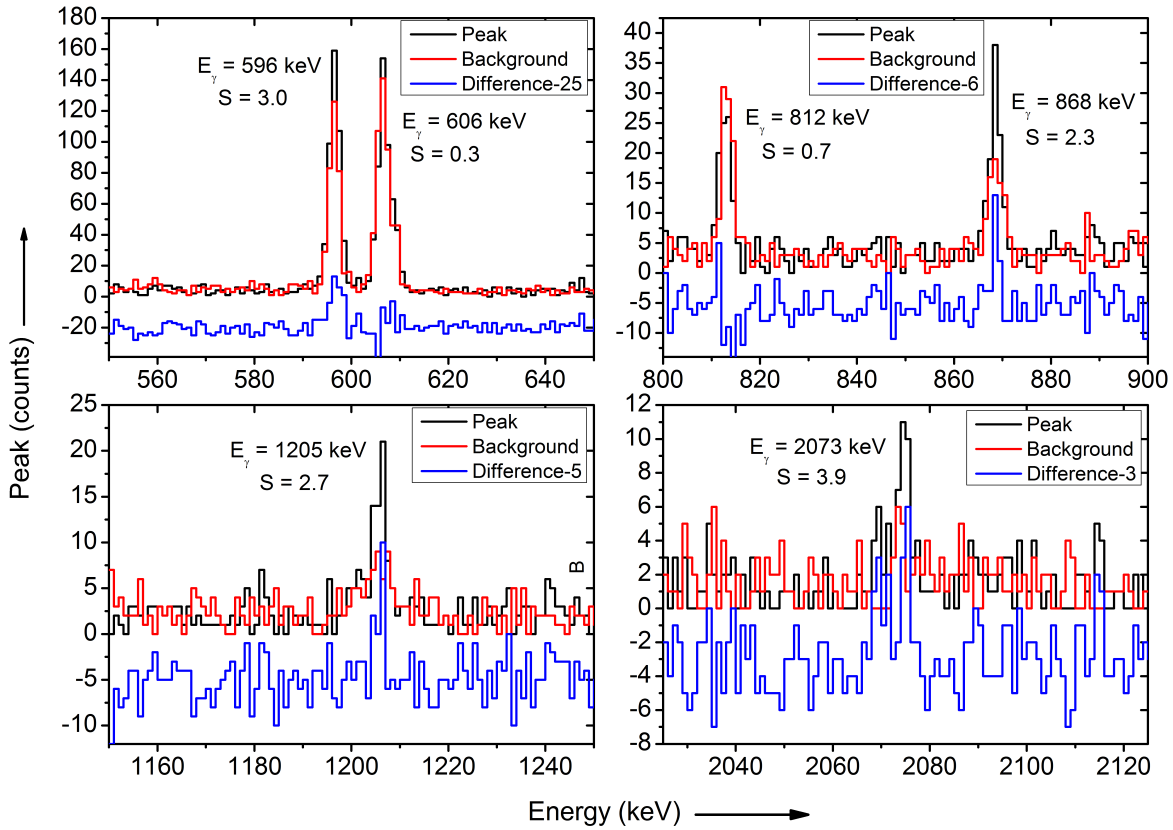

Figure 5.7: Selected region of coincidence spectra for gated 471 keV γ-ray peak showing peak (black), background (red) and difference (blue) spectra. Each γ-ray peaks are marked with energy and calculated statistical significant factor (S).

This is just one example of many within the previously published decay schemes where incorrect placements and double placements were corrected.

5.4.3 ^{74}Ga Decay Scheme

Following the procedure explained above, we have generated the coincidence file for all possible peaks seen associated with ^{74}Ga β decay and have developed a proposed decay scheme. The proposed decay scheme contains 43 excited states into which 101 γ-rays

www.manaraa.com

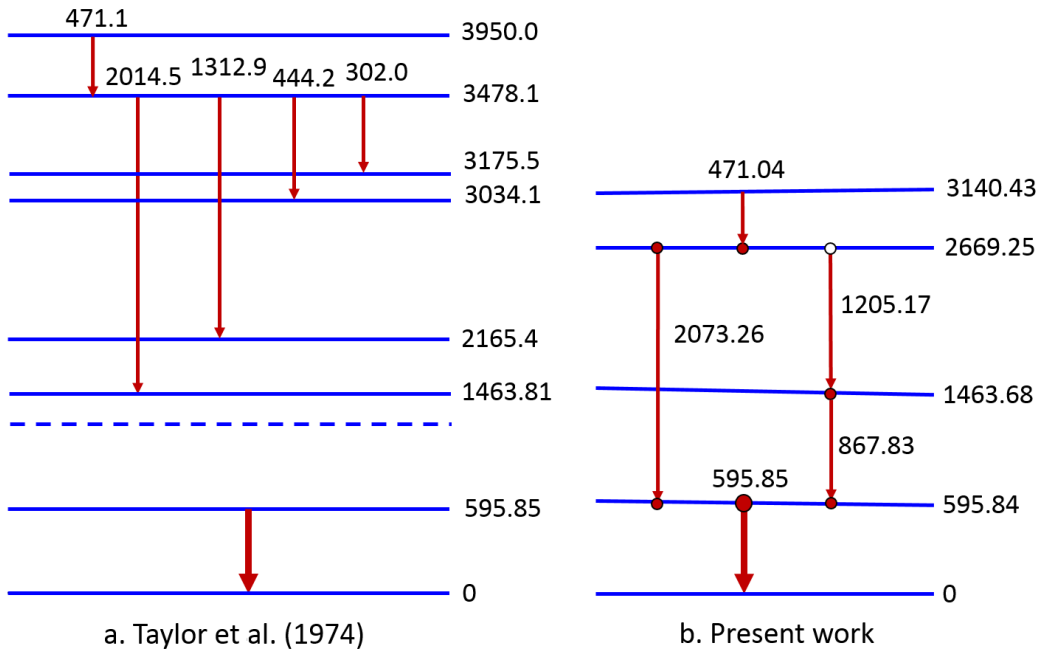

Figure 5.8: Decay scheme showing the correct placement of 471-keV γ-ray transition. Fig. a represents part of the decay scheme showing the placement of 471-keV γ ray by Taylor *et al.* [106] while the Fig. b is its corrected placement from current statistically significant $\gamma\gamma$ coincidence analysis.

transition have been placed. The total number of γ rays observed here is about 15% more than listed in the NNDC database [6], with the highest excited state at 4359 keV. Up to 2.6 MeV, our proposed decay scheme is in good agreement with the previous measurements by Camp *et al.* and Taylor *et al* [24, 106]. However, above 2.6MeV we have adjusted the placement of several γ rays. The 21 γ rays for which we have a different placement from the two previous studies are indicated by footnote *b* in Table 5.1. Thirteen γ rays which were reported in one or both of the previous studies were not observed. The γ-ray energies are 444, 653, 1631, 2110, 2617, 2625, 2997, 3044, 3274, 3627, 3717, 3895 and

www.manaraa.com

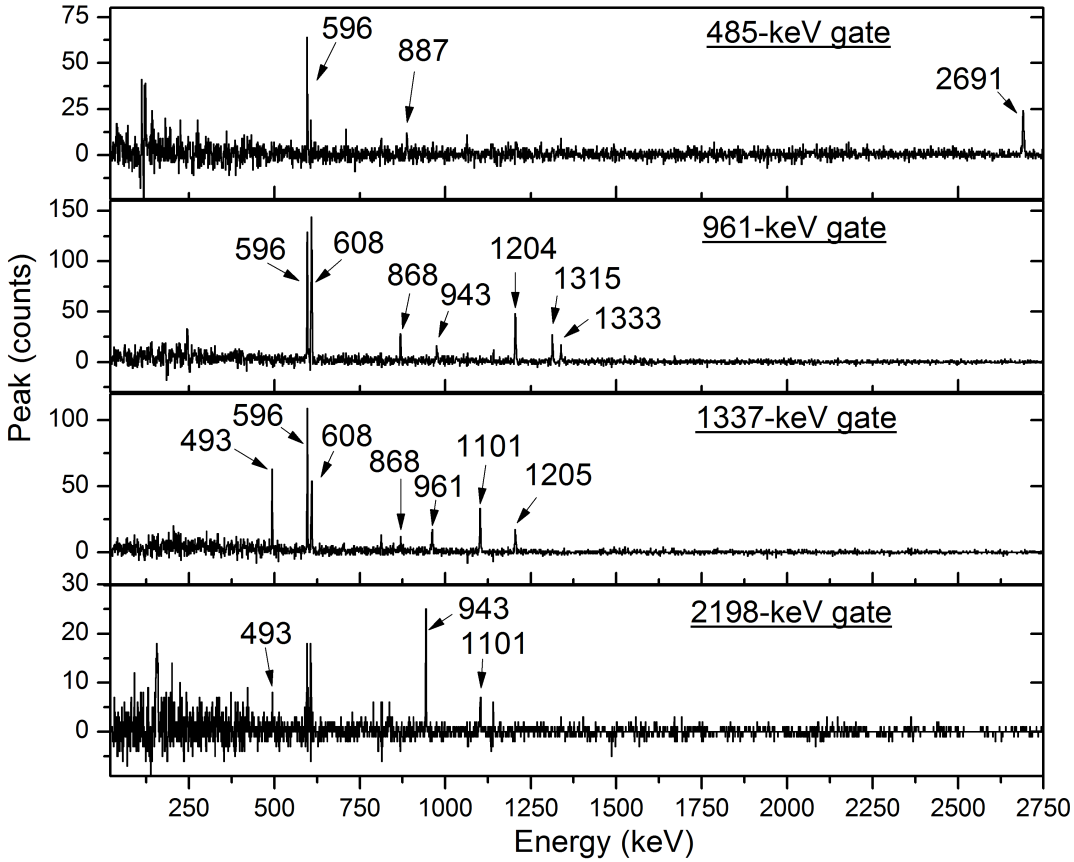

Figure 5.9: Background-subtracted $\gamma\gamma$ coincidence spectra for coincidence gates set on 485-, 961-, 1337- and 2198-keV peaks.

3992 keV. These γ ray cannot be removed from the database, but we have no evidence for their placement.

We have proposed 15 new energy levels in β decay out of which 8 energy levels were observed and cataloged in the NNDC database by other types of measurements [6]. Three totally new energy levels are proposed by multiple coincidence relationships, the other four levels are placed based on a single coincident γ ray. We have less confidence in the later two levels and represent them by a dotted line in the decay scheme. We identified 23

www.manaraa.com

new γ rays associated with this decay scheme which are designated by footnote a in Table 5.1. Furthermore, we resolved five γ-ray doublets of energy 485, 961, 1337, 1807 and 2198 keV where both γ ray belongs to ^{74}Ga β decay and assigned the proper intensity to each. The background subtracted $\gamma\gamma$ coincidence spectra for γ-ray peaks 485, 961, 1337 and 2198 keV are shown in Fig. 5.9 showing the coincident γ-ray peaks which indicate they are doublets. For example, the top most spectra of Fig. 5.9 shows 887- and 2691-keV γ rays are not in coincidence, but must be parallel to each other in the decay scheme. We identified additional γ-rays doublets which belong to ^{74}Ga as well as another member of decay elements of the decay chain. These include γ rays of energy 785, 837, 999 and 2031 keV belong to ^{74}Zn, and 967 keV which belongs to ^{74}Cu and determined the intensity associated with each decay. Furthermore, we observed that 1464-keV γ ray in the spectrum which we identify as a sum peak from the 596- and 867-keV coincident γ rays. Below is the description of the new levels proposed form this work:

5.4.3.1 Description of New Levels From the Present Study

Our coincidence analysis supports the existence of 15 energy levels which are not reported in the previous two studies [24, 106]. Details on the new levels are discussed in the following paragraphs.

An energy level at 1967.1 keV is proposed by placing the two newly identified γ rays of energies 484.83 keV feeding the level at 1482.89 keV and 503.38 keV feeding the level at 1463.68 keV. We observed that the 484.83-keV γ ray is in definite coincidences with the

www.manaraa.com

887-keV γ ray while the 503.38-keV γ ray is in probable coincidences with the 868-keV γ ray leading to their placements as de-exciting the new level at 1967.1 keV.

A level at 2248.64 keV is proposed by placing a single γ-ray transition of energy 551.48 keV. In the 551.48-keV coincidence gate, the 551.48-keV γ ray is observed in probable coincidences with the 596- and 1101-keV γ rays but none of the γ rays de-exciting the 3342.97-keV level reported by Taylor *et al.* [106]. The 551-keV γ ray is observed in both the 596- (definite) and 1101-keV (probable) coincidence gates. Since the 2248.64-keV level is proposed based on a single transition with probable coincidences, we marked it with a dotted line in the decay scheme.

An energy level at 2424.74 keV is proposed by the placement of a 961.07-keV γ ray feeding the 1463.68-keV level. The 961.07-keV γ ray is observed in definite coincidence with the 596- and 868-keV γ rays leading its placement feeding the 1464-keV level. We have represented the 2424.74-keV level by a solid line because the placement of 961-keV γ ray is based on definite coincidences in both directions.

An energy level at 2600.03 keV is proposed by placing the 2004.17-keV γ ray feeding the at 595.84-keV level. The 2004.17-keV γ ray is observed in definite coincidences with the 540.39-keV γ ray but not any of the γ rays de-exciting the 4201.1-keV level reported by Taylor *et al.* [106]. Furthermore, the 540.39-keV γ ray is observed feeding the 2600.03-keV level with definite coincidences with 2004.17-keV (but not the any γ rays de-exciting the level 3715.5 keV as reported by Taylor *et al.* [106]). Hence, our data support that there is a level at 2600.03 keV.

www.manaraa.com

An energy level at 2669.25 keV is proposed form this work by placing two γ rays of energies 2073.26 keV feeding the 595.84-keV level and 1205.17 keV feeding the 1463.68-keV level. We observed a 2073.26-keV γ ray in definite coincidence with 471-keV γ ray and not any of the γ rays de-exciting the level at 3950.0 keV Ref. [106], leading its placement de-exciting the level at 2669.25 keV. Furthermore, a 1205.17-keV γ ray is observed in definite coincidences with 867.83-keV γ ray leading its placements to the level at 2669.25 keV. Consequently, our data suggest that there is a level at 2669.25 keV.

An energy level at 2690.31 keV is proposed by placing a γ ray of energy 2690.35 keV feeding the ground state. In this work, we observed a 2690.35-keV γ ray which is in definite coincidence with 259.39 keV and 484.98-keV γ rays but not any of the γ rays de-exciting the 1204.25-keV level as reported by Taylor *et al.* [106]. Hence, our data support the existence of the level at 2690.32 keV.

An energy level at 2828.80 keV is proposed by placing the 1131.64-keV γ ray feeding the 1697.16-keV level. We observe a 1131.64-keV γ ray which is in definite coincidences with 492.92- and 1101.31-keV γ rays but not any of the γ ray de-exciting the 3566.77-keV level as reported by Camp *et al.* [24].

An energy level at 2874.88 keV is proposed by the placement of two γ rays of energies 1177.79 keV feeding the 1697.16-keV level and 2278.99 keV feeding the 595.84-keV level. We observed a 1177.79-keV γ ray in definite coincidences with 492.92-keV γ ray but not any of the γ rays de-exciting the 2165.27-keV level as reported by Camp *et al.* and Taylor *et al.* [24, 106]. Furthermore, an observed 2278.99-keV γ ray shows a definite coincidence with 596-keV γ ray but not any of the γ rays de-exciting the 3976.1-keV level

www.manaraa.com

reported by both Ref. [24, 106]. Consequently, our data support that there is a level at 2874.88 keV.

An energy level at 2935.63 keV is proposed by placing a single γ ray of energy 1471.96 keV feeding the 1463.68-keV level. We observed a 1471.96-keV γ ray which is in definite coincidences with 867.83-keV γ ray but not any of the γ rays de-exciting the level 3140.45 keV leading its placement to the 2935.63-keV level.

An energy level at 3092.01 keV is proposed by placing the γ ray of energy 1887.79 keV feeding the 1204.25-keV level. In this work, we observed a 1887.79-keV γ ray which is in definite coincidence with 1204- and 608-keV γ rays leading its placement to the 3092.01-keV level.

An energy level at 3381.47 keV is proposed by placing the γ ray of energy 2785.64-keV feeding the 595.84-keV level. We observed a 2785.64-keV γ ray which is in definite coincidence with 595.85-keV γ ray leading its placement to the 3381.47-keV level. This level is in agreement with NNDC evaluators (n, γ) study [6].

Similarly, an energy level at 3386.39 keV is proposed by placing the γ ray of energy 2790.55 keV feeding the 595.84-keV level. We observed that 2790.55-keV γ ray is in definite coincidences with 595.85-keV γ ray but not any of the γ rays de-exciting the 1204.25-keV level as reported by Taylor *et al.* [106], leading its placement to the 3386.39-keV level.

An energy level at 3503.26 keV is firmly proposed by placing the γ rays of energies 1806.10 keV feeding the 1463.68-keV level, 1337.47 keV feeding the 2165.22 keV level and 697.07 keV feeding the 2536.51-keV level. The 1806.10-keV γ ray was reported by

www.manaraa.com

both previous measurements [24, 106] but hasn't placed them in the decay scheme. We observed a 1806.10-keV γ ray in probable coincidences with 868-keV γ ray leading its placement to the 3503.26-keV level. Furthermore, a 1337.47-keV γ ray is observed in definite coincidences with 961.07-keV γ ray leading its placement to the 3503.26-keV level. Besides that, a 967.07-keV γ ray is observed in definite coincidences with 1940.71-keV γ rays leading its placement to the 3503.26-keV level. Consequently, our data suggest that there is a level at 3503.26 keV.

Finally, the level at 4359.05 keV is proposed by placing the γ ray of energy 3763.21 keV feeding the 595.84-keV level. A 3762.6-keV γ ray was observed from both previous measurements [24, 106] but has not placed in the decay scheme. We observed a 3763.21-keV γ ray which is in definite coincidences with 596-keV γ ray leading its placement to the level at 4359.05 keV.

Additionally, we identified the 10 more γ rays associated with the ^{74}Ga decay but could not place them in the decay scheme whose intensity and coincidence information are listed in Table 5.1 with footnotes e. The total summed intensity of the unplaced γ ray is observed to be 1.80(15) relative to the intensity of the 595.84-keV γ ray.

5.4.3.2 Description of Previously Reported Levels Which are not Observed in the Current Study

Our results do not support the existence of 10 energy levels reported in the previous two studies [24, 106]. Details of those levels which are refuted by our results are discussed in the following paragraphs.

www.manaraa.com

An energy level at 2821.6 keV was proposed by Camp *et al.* [24] by the placement of γ rays with energies 1617.2 keV feeding the 1204.25-keV level and 1357.19 keV feeding the 1463.72-keV level. In the present work, we observe a 1616.7-keV γ ray which is in definite coincidence with the 868-keV γ ray and not with either the 608- or 1204-keV γ rays de-exciting the 1204.25-keV level. Therefore, we placed the 1617-keV γ ray as de-exciting the level 3081-keV level. Furthermore, an observed 1358.04-keV γ ray is not observed to be in coincidence with any γ rays depopulating the 1463.72-keV level but is in definite coincidence with the 1941-keV γ ray which supports it's placement as de-exciting the 3894.48-keV level. Consequently, our data suggest that there is no evidence for 2821.6-keV level.

Taylor *et al.* [106] proposed a 3211.9-keV level by the placement of γ rays of energies 2616.6 keV (I_γ = 0.19(8)) feeding the 595.85-keV level and 3211.4 keV (I_γ = 0.70(8)) feeding the ground state [106]. Camp *et al.* [24] also observed both γ rays (2616.8 keV, I_γ = 0.26(2) and 3211.10 keV (I_γ = 0.81(2)), did not placed 2626.68-keV γ ray in the decay scheme while placed 3211.10-keV γ ray de-exciting the level at 3807.0 keV [24]. In our study, we observed a 2617.3-keV γ ray in the ungated singles spectrum but is not evident in the β-gated spectrum. This γ ray is also observed not evident in the 596-keV coincidence gate where an upper limit on the relative intensity 0.12 can be set. Hence, we observe no conclusive evidence for this γ ray, and certainly nor for the proposed placement. An observed 3210.89-keV γ ray (I_γ = 0.74(4)) shows a definite coincidence with the 596-keV γ ray and is placed de-exciting the 3806-keV level which agreed with the Camp *et al.* [24] placement. Hence, our data does not support the existence of 3211.9-keV level.

www.manaraa.com

An energy level at 3716.8 keV was proposed with the placement of γ rays with energies of 540.8 keV feeding the 3175.75-keV level and 3717.1 keV feeding the ground state by Taylor *et al.* [106]. In our present work, we observed a 540.39-keV γ ray which is in definite coincidence with the 2004-keV γ ray and not with either the 1331.1-keV or the 1940.63-keV γ rays which de-exciting the 2356.54-keV level. Our result, therefore, indicates this γ ray placement as de-exciting the 3716.8-keV level. Furthermore, Taylor *et al.* reported a very weak γ ray of energy 3717.1 keV and intensity 0.03 directly feeding the ground state. A γ ray of this intensity is below the detection limit for our system, so we can make no claims about its existences. Hence, we observe no evidence for a 3716.8-keV level.

A level at 3976.1 keV was proposed by the placement of γ rays with energies of 2771.8 keV feeding the 1204-keV level and 2279.05 keV feeding the 1697.19-keV level in both previous studies [24, 106]. In the present work, we observe a 2271.8-keV γ ray which is in definite coincidence with the 868-keV γ ray and not the 608-keV γ ray as would be expected it the γ ray fed the 1204-keV level. Instead, we place the γ ray as de-exciting a level at 4234.98 keV. Furthermore, an observed 2278.99-keV γ ray shows only a definite coincidence with the 596-keV γ ray with no observed coincidences with the 492- and 1101-keV γ rays de-exciting the 1697-keV level. Therefore, this γ ray is placed as de-exciting a level at 2874.88 keV. Consequently, our data suggest that there is no level at 3976.1 keV.

A level at 3995.1 keV was proposed by placing γ rays with energies 2790.38 keV feeding the 1204.25-keV level and 3992.4 keV feeding directly to the ground state by the Taylor *et al.* [106]. In the present work, we observed a 2790.55-keV γ ray which shows

www.manaraa.com

no evidence for any coincidences with γ rays de-exciting the 1204.25-keV level. Instead, it shows the 596-keV γ ray in definite coincidences. Therefore, we placed this γ ray as de-exciting the 3386.39-keV level. Finally, we did not observe the 3992.4-keV γ ray in our spectra, but it is also below our detection limit. Thus, our data suggest that there is no level at 2995.1 keV.

A 4223.8-keV energy level was proposed by placing γ rays of energies 3018.8 keV (I_γ = 0.07(1)) feeding the 1204.25-keV level and 3626.7 keV (I_γ = 0.036(5)) feeding the 595.85-keV level in Taylor *et al.* [106]. In our present work, we observed a 3018.75-keV γ ray with intensity 0.16(3) which has been assigned to ^{74}Cu β decay based on β detection efficiency and cannot be the same γ ray observed previously. There is no evidence in the 3019-keV coincidence gate for coincidences with the 608- and 1204-keV γ rays, nor is the 3019-keV γ ray is observed in the 596-, 608-, or 1204-keV coincidence gates. We could not observe the 3628.0-keV γ ray of energy in our spectrum because it is below our detection limit. Hence, our data provide no evidence to support a level at 4223.8 keV.

An energy level at 4367.3 keV was proposed by placing the γ rays of energies 1024.3 keV (I_γ = 0.15(3)) feeding the 3342.97-keV level and 1417.6 keV (I_γ = 0.12(11)) feeding the 2949.52-keV level in Camp *et al.* [106]. In the present work, we observed a 1023.8-keV γ ray (I_γ = 0.12(6)) which is in definite coincidences with the 999-keV γ ray and not the 1177.99-, 2138.45- or 2746.89-keV γ rays which de-exciting the level at 3342.97-keV leading us to place this γ ray as feeding the 2696.37-keV level (This disagrees with both proposed placements for this γ ray reported at the NNDC). We observe a 1417.4-keV γ ray (I_γ = 0.11(4)) in our spectra. But the β detection efficiency suggest this γ ray is from ^{74}Cu

www.manaraa.com

and not the one reported previously. Coincidence gates on 1417 keV and 2354 keV show no evidence for a component of the 1417-keV peak matching the proposed placement. Hence, our data suggest no evidence to support a level at 4267.3 keV.

A level at 4477.6-keV was proposed by placing five γ rays of energies 999.9 keV (I_γ = 0.28) feeding the 3478.12-keV level, 1134.5 keV (I_γ = 0.42(4)) feeding the 3342.97-keV level, 1337.18 keV (I_γ = 1.75(4)) feeding the 3140.45-keV level, 1443.38 keV (I_γ = 4.0(8)) feeding the 3034.17-keV level, and 3273.40 keV (I_γ = 0.04(1)) feeding the 1204.25-keV level in Camp *et al.* [106]. In the present work, we observed a 999.17-keV γ ray (I_γ = 0.35(8)) which is in definite coincidence with the 1023.77-keV γ ray. Therefore, this γ ray is placed de-exciting the level at 2696.37 keV (The placement of 999-keV γ ray has corrected to level 2696.37 keV from 3950.0 keV proposed by Taylor *et al*). We do not observed a 1134.0-keV γ ray in our spectrum. Furthermore, we observed a 1443.31-keV γ ray (I_γ = 3.84(6)) in definite coincidences with the 493-keV and 1101-keV as well as all transitions below these γ rays indicating it feeds into the 1697-keV level. We observe no evidence of this γ ray being a doublet. We do not observe a 3274-keV γ ray in our spectrum because it is below our detection limit. Hence, our data suggests that there is no level at 4477.62 keV.

A level at 4611.6-keV was proposed by the placement of γ rays of energies 1471.7 keV feeding the 3140.45-keV level and 2074.14 keV feeding the 2536.54-keV level in Taylor *et al.* [106]. From this study, we observed a 1471.96-keV γ ray (I_γ = 0.36(4)) which is in definite coincidences with the 868-keV γ ray and not with any γ rays de-exciting 3140.45-keV level, leading its placement feeding the 1464-keV level. Furthermore, a 2073.26-

www.manaraa.com

keV γ ray (I_γ = 0.31(5)) was observed which is in definite coincidence with the 471-keV γ ray with no observed coincidences with the γ rays de-exciting the 2536.54-keV level. Therefore, the 2073.26-keV γ ray is placed de-exciting the level at 2669.25 keV. Hence, our data do not support the existence of level at 4611.6 keV.

Finally, an energy level at 4698.3 keV was proposed by placing γ rays of energies 1131.52 keV feeding the 3566.77-keV level and 2004.6 keV feeding the 2693.68-keV level in the Camp *et al.* [24]. In the present work, we observed a 1131.64-keV γ ray (I_γ = 0.92(12)) which is in definite coincidences with 493-and 1101-keV γ rays but not any of the γ rays de-exciting the level at 3566.77 keV, leading to its placement as feeding the 1697-keV level. Furthermore, we observed a 2004.17-keV γ ray (I_γ = 0.34(4)) is in definite coincidence with the 540-keV and not any γ rays de-exciting the level at 2693.68 keV nor any other γ ray de-exciting the 3140-keV levels. Since the γ ray cannot feed the 3140-keV level, it must lie below the 540-keV γ ray and is placed de-exciting a level at 2600 keV. Consequently, our data do not support the existence of level at 4698.3 keV.

5.5 β-Feeding, $\log(ft)$ Value and Spin-Parity Assignment

As we do not know the exact number of β decays leading to the observed γ rays, we initially assign that strongest γ-ray peak of energy 596 keV in the spectrum to have a relative intensity of 100% and the intensity of all other γ rays associated with ^{74}Ga decay were determined relative to the intensity of the 595.84-keV γ ray. These are the experimental values given in the Table 5.1. Determination of absolute γ-ray intensities therefore

www.manaraa.com

will only require determination of a normalization constant specifying the absolute feeding through the 596-keV γ ray.

After constructing the decay scheme, we have calculated the β-feeding intensity for each level by subtracting the summed γ-rays intensity feeding in the level form the summed γ-rays intensity feeding out from that level. We did this relative β-feeding calculations using the MASTER program. Then the summing correction was performed with k-alpha X-ray energy 9.86 keV [3].

We observed five γ rays feeding the ground state with a summed relative intensity of 111.07(18). We can assume no ground state feeding of the spin/parity consideration of the parent (^{74}Ga) and daughter nuclei (^{74}Ge) nuclei. So, the only 11.07% of the ground state feeding comes from the transitions other than the 596-keV γ ray. The summed intensity sets the normalization factor for the principle 596-keV γ ray to be 90.45(17)%. The absolute β-feeding intensity for each proposed levels are listed in Table 5.3.

Lower limit $\log(ft)$ values for the energy levels in ^{74}Ge, fed in the β decay of ^{74}Ga as shown in Table. 5.3, were calculated as explained in Chapter 4 using the NNDC webiste [7]. We have used the $Q_{\beta^-} = 5372.8$ keV taken from AME2012 [112] for this calculation. We did not measure the half-life of ^{74}Ga β decay, but used accepted value from the NNDC database. Estimated $\log(ft)$ lower limits and accepted spin-parity assignments taken from the NNDC for the proposed energy levels are listed in the Table 5.3.

www.manaraa.com

Table 5.3: Feeding intensities (I_{β^-}), $\log(ft)$ lower limits and assigned spin-parity values for ^{74}Ga β decay. The β-feeding values are given per 100 decays.

Energy Level	$\mathbf{I}_{\beta^-}$	$\log(ft)$	**Spin-parity**
0.00	-	-	0^+
595.84(1)	2.88(47)	8.18	2^+
1204.25(1)	4.07(27)	7.77	2^+
1463.68(2)	0.36(16)	8.70	4^+
1482.89(8)	0.05(5)	9.50	0^+
1697.16(2)	0.53(29)	8.40	
1967.1(5)†	0.11(4)	8.95	$(3)^+$
2165.22(4)	0.70(13)	8.04	$(3, 4)^+$
2197.97(4)	0.48(14)	8.18	2^+
2248.64(12)†	0.25(3)	8.43	
2424.74(8)†	0.27(5)	8.29	
2536.51(3)°	0	>10.65	
2600.03(13)‡	0.12(5)	8.53	$(1, 2, 3)^+$
2669.25(9)‡,°	0	>10.00	
2690.31(6)‡	0.05(5)	8.85	
2693.64(4)	2.45(34)	7.15	$(3, 4^+)$
2696.37(29)‡	0.22(10)	8.20	$(2)^+$
2828.80(14)‡	0.91(12)	7.49	(4^+)
2874.88(5)†	2.05(6)	7.10	
2935.63(15)‡	0.34(4)	7.84	
2949.37(4)	45.41(20)	5.70	3^-
2973.54(25)	0.21(3)	8.02	(3)
3034.03(3)	6.29(18)	6.50	$(3, 4^+)$
3080.95(22)	0.30(5)	7.78	(3^+)
3092.01(14)‡	0.85(6)	7.32	$1(^+)$
3140.43(3)	10.34(22)	6.20	3^-
3175.42(4)	2.86(11)	6.73	3^-
3271.34(18)	0.34(3)	7.57	(2^+)
3342.71(8)	1.64(6)	6.82	$(3^-, 4^+)$
3381.47(14)‡	0.67(3)	7.18	3^-
3386.39(14)†	0.59(3)	7.23	
3478.14(5)	3.38(33)	6.38	$(2, 3)^+$
3503.26(28)†	0.97(16)	6.9	
3566.22(12)	1.01(3)	6.83	$(2^+, 3, 4^+)$
3639.52(33)	0.22(3)	7.41	
3696.40(6)	1.52(7)	6.52	(3, 4)
3720.49(4)	2.61(16)	6.26	$(3, 4^+)$

Continued on next page

www.manaraa.com

Table 5.3 – continued from previous page

Energy Level	$\mathbf{I}_{\beta^-}$	log (ft)	**Spin-parity from NNDC**
3806.73(16)	0.66(3)	6.76	3^-
3827.2(5)	0.64(11)	6.75	1^- to 4^+
3894.48(12)	1.29(9)	6.37	(2, 3, 4^+)
3949.66(16)	0.89(5)	6.46	(2^+, 3, 4^+)
4201.04(13)	1.62(8)	5.87	2^+
4234.98(25)	0.37(4)	6.46	(3, 4^+)
4359.05(52)†	0.12(4)	6.76	

°Feeding to this level was consistent with zero.
†Newly proposed energy level for β decay.
‡Newly proposed energy level for β decay which agreed with other studies [99].

Figure 5.10 shows the I_{β^-} feeding profile for all three β-decay experiments. In the present work, low direct β-feeding to the first excited state at 596 keV (2.88 %) is observed in disagreement with the previous two measurements (Camp: 4.81% and Taylor: 15.11%) [24, 106]. The observed β-feeding intensity to the 1204-keV level is around 4.07% which is much greater than reported in previous work (Camp: 0.92%, Taylor: 0.0%). The reason behind this discrepancy is Taylor *et al.* placed the 1971-, 2562-, 2691-, 2771-, 2791-, 3019- and 3030-keV γ rays feeding the 1204-keV level, but our coincidence data clearly do not support these placements and instead placed them feeding into different states. Almost zero β-feeding is observed to the 1483-, 2536- and 2669-keV levels which are less than reported by the previous works [24,106]. The present work observed comparable β-feeding intensity for the 2949-keV level (Camp: 50.61%, Taylor: 45.87% and present: 45.41%). For the 3140-keV level, the β-feeding intensity has increased Camp (3.33%) to Taylor (7.29%) to the present (10.34%). Camp *et al.* proposed level at 3140 keV by placing the four γ rays (604.22, 942.45, 974.90 and 1676.62 keV) de-exciting the level with one γ ray

www.manaraa.com

(809.8 keV) feeding in. Later, Taylor *et al.* proposed the same level with one additional 1443.4 keV γ rays de-exciting the level. In our measurement, we confirmed the level at 3140 keV with two more γ rays (471.04 and 540.39 keV) in addition to Taylor *et al*. Furthermore, we have adjusted the placement of 809-keV γ ray feeding the level at 3478.14 keV. Hence due to the placement of two addition γ rays and corrected placement of γ ray has increased the observed higher β feeding intensity at 3140 keV level. In general, we can say there is higher feeding in the energy range from 2000 to 3000 keV whereas less feeding to the lower-energy states compared to the previous two experiments [24,106]. This clearly shows the shifting of β-feeding to the higher levels from the correct understanding of the γ-ray cascades and coincidences.

5.5.1 Nushellx Calculation and Spin-Parity Assignments

We have calculated the level structure of ^{74}Ge using Nushellx [23] with the $JUN45$ effective interaction within the $JJ44$ model space which has been proposed for use in the fp- and $g_{9/2}$ orbitals for both protons and neutrons. We have performed the calculations for spins up to 5 for both positive and negative parity states, determining the first 30 states for each spin/parity. Figure 5.11 shows the result we obtained. The 2^+ and 4^+ states clearly show that the results from the theoretical calculation are slightly stretched up by about 100 keV in comparison to the experimental results which indicates the need of some deformation factor in our theoretical model.

In our proposed decay scheme, β-feeding to the 596-keV energy level is reduced (2.88%) in comparison to the values of 15.11% by Camp *et al.* followed 4.81% by Tay-

www.manaraa.com

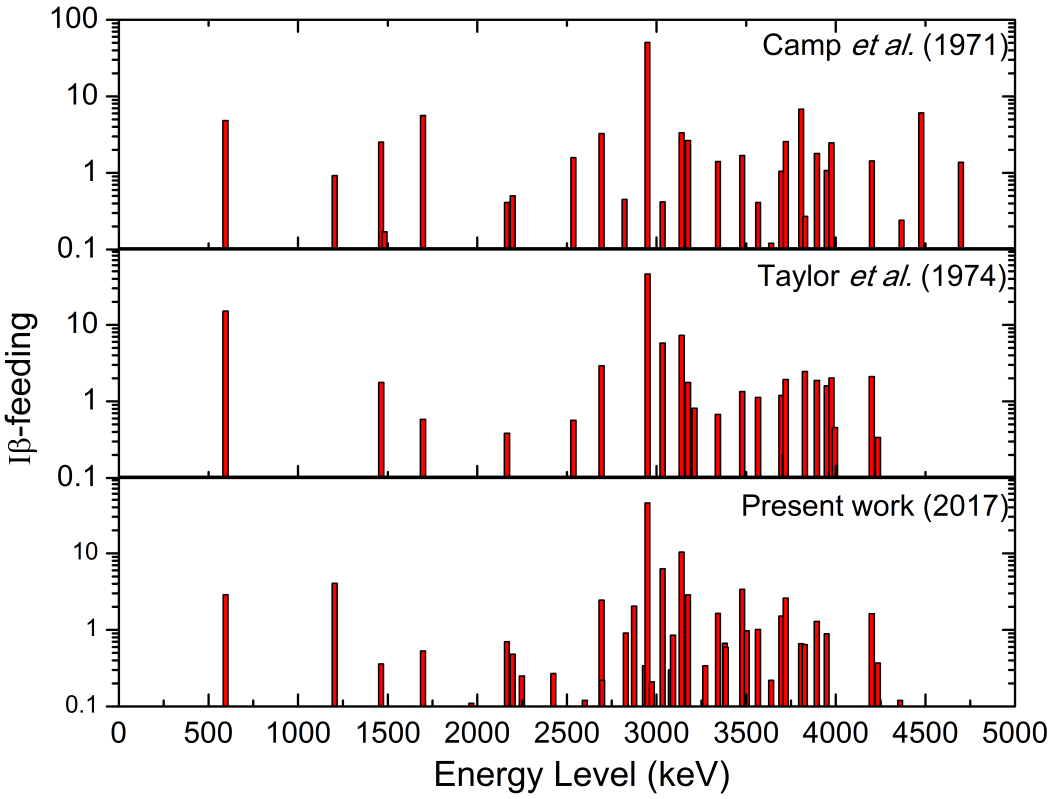

Figure 5.10: I_{β^-} feeding profile for ^{74}Ga β decay: comparison from each experiments.

lor *et al*. Our observed diminishing β-feeding indicates that there is low direct feeding to the 596-keV level from ^{74}Ga. The spin-parity assignment to the 596-keV level in ^{74}Ge us known to be 2^+ [6] as expected for an even-even nucleus. The β transition from parent to daughter nuclei for this scenario is 3^- to 2^+, which is a first forbidden. Therefore, our lower-limit $\log(ft)$ value for the 596-keV level should be between 6.0 to 8.0 (Ref. Table 2.1). The observed value from this present work is 8.18 which is nearly conclusive.

For the 1204.5-keV level, it connects to both the 0^+ (ground state) and 2^+ (595.85 keV) state. So, it's spin/parity should be 2_1^+ as agreed with all other measurements [6]. This is

www.manaraa.com

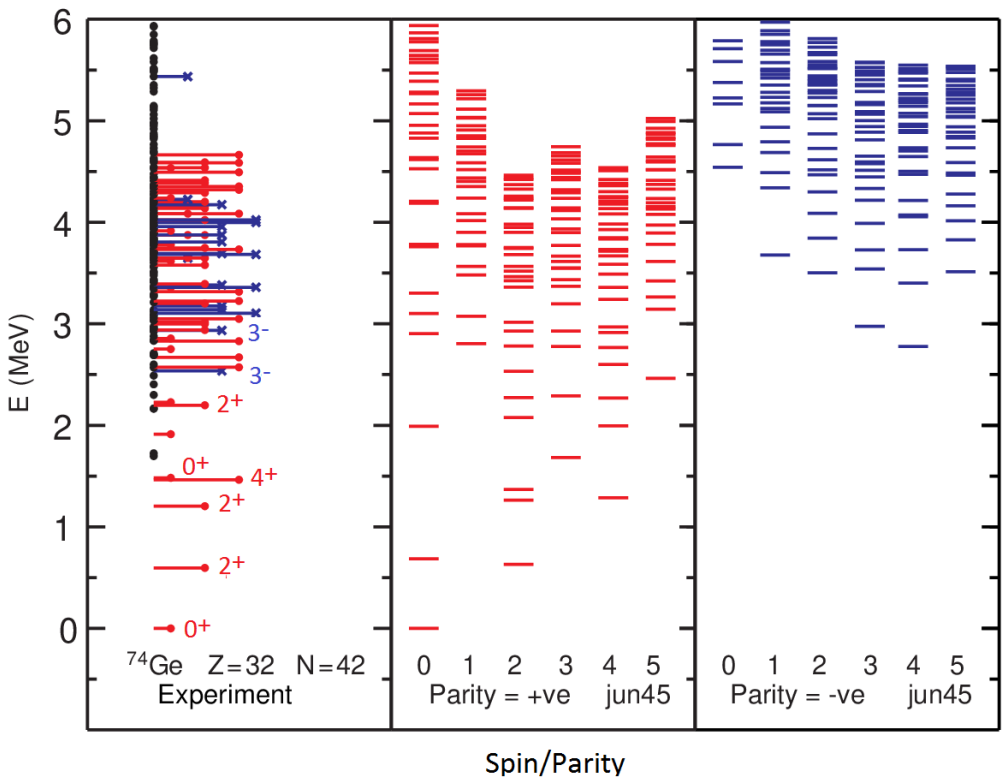

Figure 5.11: Nushellx prediction of structure of ^{74}Ge.

also a first forbidden transition where our calculated $\log(ft)$ lower-limit of 7.77 is in good agreement with expectations.

The 1463.68-keV level has a well-established spin/parity assignment of 4^+. There is no direct ground state transition from this level and it connects only to the 2_1^+ state at a lower excitation energy. This is also a first forbidden transition where the lower-limit $\log(ft)$ value is 8.70- is high but consistent if there is a poor wave function overlap.

For the 1482.89-keV level, our calculated $\log(ft)$ lower-limit of 9.50 is consistent with a first-forbidden unique transition ($J = \pm 2$).

www.manaraa.com

For the level at 1482.89 keV, our calculated $\log(ft)$ value comes to 8.7 leading to the first unique transition ($J = \pm 2$), which is not conclsive from previous 0^+ assignment [6].

The 1697.16-keV level has a calculated lower limit of $\log(ft)$ value 8.40. As this level has γ-ray transitions connecting the 2_1^+, 2_2^+ and 4_1^+ levels suggesting spins from 2 to 4. Our calculated lower-limit of $\log(ft)$ value of 8.40 is consistent with a first forbidden and too high for an allowed decay. Hence, our results are consistent with the NNDC spin-parity value.

For the newly established energy level at 1967.1-keV, our calculated lower limit of $\log(ft)$ is 8.95. The level decays by two γ-ray transitions connecting to the level 0_2^+ and 4_1^+. Therefore, we predict it's spin-parity to be $(2)^+$. Nushellx result shows three 2^+ states below 2 MeV, which supports our assignment.

The energy level at 2165.22 keV has γ-ray transitions connecting to the 2_2^+, $(3_1)^+$ and 4_1^+ states but not to any ground 0^+ state, and is assigned spin-parity 4^+ by Taylor *et al*. Our calculated $\log(ft)$ value lower-limit comes out to be 8.04, which is in agreement with the Taylor *et al*. Our Nushellx result indicate the 4_2^+ state lies below the 3_2^+ state which further supports a 4^+ assignment.

The 2197.97-keV level is assigned 2^+ by multiple experiments. Our $\log(ft)$ value (8.18) for this level is consistent with this spin/parity assignment.

For the 2536.50-keV level, spin-parity assigned by both Camp *et al.* and Taylor *et al.* is 3^-. We observed almost zero feeding to this level which gives the large $\log(ft)$ value (>10.65) suggesting the second forbidden transition with change of spin $\Delta J = \pm 2$ but no change of parity from the 3^- ground states of ^{74}Ga. Hence, our calculated $\log(ft)$ value is

www.manaraa.com

not in agreement with this 3^- assignemnt and $\log(ft)$ values reported previously (Camp: 7.52, Taylor: 7.99) [24, 106].

The level at 2949 keV is observed to have large β-feeding value. The calculated $\log(ft)$ value for this level is 5.70 indicating allowed transition and have assigned its spin/parity to be 3^-. This is the first low energy negative states confirmed experimentally from our experiment which is in agreement with Nushellx result shown if Fig 5.11.

5.6 Discussion and Conclusion

In this measurement, we have been able to identify 109 γ rays associated with ^{74}Ga β decay, placed 99 of them in a proposed decay scheme with 44 levels based on statistically significant $\gamma\gamma$ coincidences. This work has modified the placement of 20 γ rays confirmed the placements of 67 γ rays and 27 energy levels proposed in the previous two β-decay measurements. Besides that, the present study confirms several additional levels proposed by the NNDC evaluators based on (n, γ) measurements. Altogether, this work has confirmed the placement of 87 γ rays reported in the previous two β-decay measurements. We have added 15 new levels to the decay scheme of which 9 are in agreement with other types of measurements [99]. We do not observe 15 γ rays reported in the previous studies and finally removed 10 possibly erroneous levels based on modified placements of γ rays as well as un-observed γ rays. Furthermore, we identified 22 new γ rays that belong to this decay of which 12 γ rays were successfully placed in the decay scheme. With the better understanding of the $\gamma\gamma$ and $\beta\gamma$ coincidence information, we have established a more comprehensive decay scheme for ^{74}Ga nuclei. The feeding intensities and $\log(ft)$ values

www.manaraa.com

were determined for each proposed level and compared with the previous measurements. Furthermore, shell model-calculations are used for comparison to the observed levels.

www.manaraa.com

CHAPTER VI

THE β DECAY OF ^{75}GA

6.1 Scientific Motivation

The study of β-decay spectroscopy for exotic nuclide provides important information on the nuclear structure and fundamental nuclear astrophysics. Despite previous spectroscopy efforts, there are substantial gaps in our knowledge of decay properties of neutron-rich nuclei. Detailed β-decay studies of nuclides in the region around $Z = 28$ and $N = 28 - 50$, i.e. nuclides in $pf_{5/2}g_{9/2}$ shell which exhibit interesting behaviors like structure variation and shell evolution [22, 56], are important in understanding the evolution of nuclear structure.

In the traditional shell model view of ^{75}Ga, the 31^{st} proton should be in a $\pi 2p_{3/2}$ orbitals suggesting the ground state spin-parity $J^{\pi} = 3/2^{-}$. This prediction was confirmed in a deep inelastic reaction experiment by Stefanescu *et al.* [102]. The β-decay study of ^{75}Ga is also important as it lies near the $\pi 2p_{3/2} - \pi 1f_{5/2}$ orbital crossing point. Evolution of the $9/2^{+}$, $7/2^{+}$ and $5/2^{-}$ states relative to the $1/2^{-}$ states in the Ge isotopes with each additional neutron pair added in the $\nu 1g_{9/2}$ states adds special interest to this study. The evolution of states in the Ge nuclei are consistent with the theoretical calculations which consider the monopole component of the residual nucleon-nucleon interaction [78].

www.manaraa.com

The β-decay data currently available for ^{75}Ga in the National Nuclear Database Center (NNDC) database comes from a study performed in 1973 by Chacko *et al.* [26]. The ^{75}Ga was produced from the (γ, p) reaction of ^{76}Ge powder which was 73.89% pure, and had used two Ge(Li) detectors (19 cc and 60 cc) for low and high-energy part of γ-ray spectrum studies. They observed 37 γ rays associated with this decay and constructed the decay scheme up to a 2664-keV level, placing 31 γ rays. The Q_{β^-} value of ^{75}Ga is 3.392 MeV, which suggest that there might be some higher-lying energy levels missing. In this high resolution and higher efficiency investigation of ^{75}Ga, we expect to extend the existing decay scheme, filling gaps as well as extending the scheme. Also, from the understanding of the recent work on ^{74}Ga β decay, we assume that we will correct the placement of the some of the γ rays and energy levels by use of the statistically significant $\gamma\gamma$ coincidence technique.

6.2 Experimental Details

Mass A = 75 isobars were produced by proton-induced fission of a uranium carbide target (UC_x) at the HRIBF of ORNL. Isobaric separation was achieved using the low-resolution mass separator (M/ΔM = 600). After passing the beam through a charge exchange cell, ^{75}Zn ions were removed from the beam by passing it through the high-resolution mass separator (M/ΔM = 10,000) which also easily separated the ^{75}Ga components of the beam and provided an essentially pure beam of ^{75}Cu ions. These ions were then passed to the Low–energy Radioactive Ion Beam Spectroscopy Station (LeRIBSS) [5] and were deposited onto a moving tape collector (MTC) in the center of the detector set up, which

www.manaraa.com

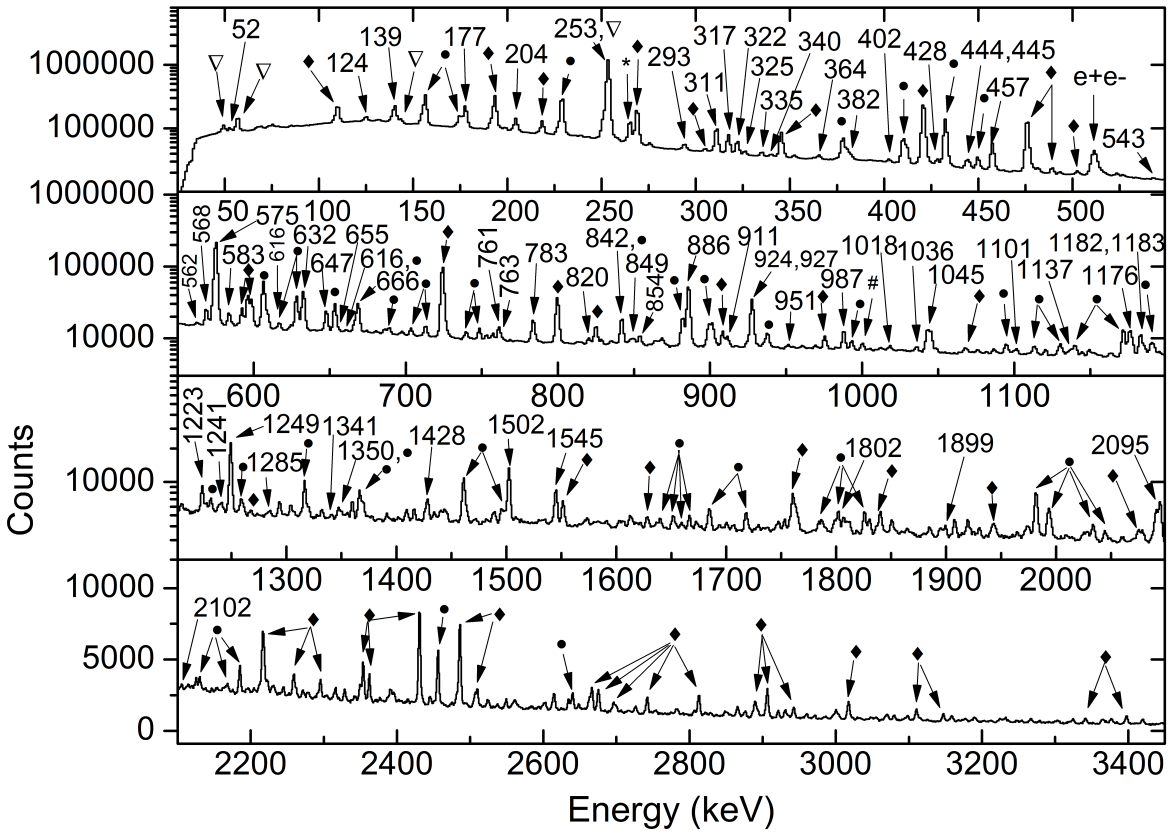

Figure 6.1: Saturation spectrum obtained in the LeRIBSS data run with a purified ^{75}Cu beam in the energy range 25 keV to 3.45 MeV. The γ-ray peaks associated with ^{75}Ga decay are marked with their energy. Prominent γ rays from other members of the decay chain are indicated by symbols. ^{75}Cu: ♦ (solid diamond), ^{75}Zn: • (bullet), ^{74}Cu: # (hash), ^{74}Zn: ▽ (open down-triangle). The room background is denoted by $*$ (asterisk). The energy range focuses on the γ rays associated with ^{75}Ga.

consisted of four HPGe clovers γ-ray detectors and two plastic scintillation counters. The clover array has a measured absolute photopeak efficiency of 29% at about 100 keV and 5% at 1.33 MeV.

www.manaraa.com

Due to the location of LeRIBSS just past the high-resolution mass separator and not using a post-accelerated beam, the beam intensity obtained was of a factor of 10 more than previous experiments [116, 117], achieving 2,000 ions/s. The MTC allowed for moving the accumulated source away from the detector region in order to distinguish the γ rays emitted by different nuclides with different half-lives: ^{75}Cu (1.22 s), ^{75}Zn (10.2 s), and ^{75}Ga (123 s) [6]. A timing cycle for the MTC of 5 s growth with 7 s delay was used to maximize the observation of ^{75}Cu [54]. For most of the experiment, while a saturation spectrum was also obtained. The later spectrum is the focus of this research. Data were collected using a trigger-less digital data acquisition system which recorded the energy and absolute time when each γ ray was detected [41, 42]. This allowed offline analysis of the data to establish $\gamma\gamma$ coincidences. The total experimental run time was around three hours including building the saturation spectrum. The primary goal of the experiment was a precise measurement of the ^{75}Cu decay [54], but it also allowed for detailed studies for the decays of ^{75}Zn and ^{75}Ga. Detail of the decay scheme for ^{75}Ga is presented in the following sections.

6.3 Experimental Results

A representative γ-ray singles spectrum including all members of the $A = 75$ decay chain starting from ^{75}Cu is shown in Figure 6.1. Efficiency calibration of the detector set up was done offline with the standard γ-ray sources ^{133}Ba, ^{152,154,155}Eu, ^{137}Cs, ^{60}Co and ^{226}Ra. After energy matching of all the raw spectra, energy calibration of the summed single spectrum was performed. The Gaussian function fit using the gf3 software was

www.manaraa.com

performed to obtain centroids and areas for all the γ-ray peaks. From the analysis of the data, we identified 78 γ rays associated with ^{75}Ga β decay. The initial γ-ray intensities were normalized with respect to the 253-keV γ ray which is the strongest transition in the ^{75}Ga β decay. After building the decay scheme, as described later, coincidence summing correction were made to obtain the final relative intensities. Table 6.1 contains the energy, intensity and $\gamma\gamma$ coincidences information for the γ rays assigned to the ^{75}Ga β decay. Using this infromation, decay shceme was constructed. The proposed decay scheme for ^{75}Ga from this work is shown in Fig. 6.2, which contains 30 energy levels into which 72 γ rays have been placed. We have extended the decay scheme up to 2765 keV from the 2664 keV proposed from previous measurement by Chacko *et al* [26]. Of the levels proposed by Chacko *et al.*, we agree with the placement of 12 levels but do not see evidence for the levels at 584.1, 1222.5 and 2664.4 keV as will be discussed later. We also confirmed some of the previously proposed states observed in other types of experiment by placing previously unobserved γ rays de-exciting those levels. Details on the decay scheme are presented in the following section.

www.manaraa.com

Table 6.1: Energy, intensity, placement and coincidence information for γ rays associated with ^{75}Ga β decay (probable coincidences are indicated with parentheses).

Energy	Intensity	Placement	$\gamma\gamma$-Coincidences
52.23(2)[‡]	1.31(8)	192.63	124
118.62(16)[‡]	0.21(3)	1359.47	666
124.31(8)[b]	1.87(3)	317.29	(335), 568, 583, (820), (924), (1018), 1183
139.45(8)	8.12(3)	140.03	
177.03(8)	11.42(4)	317.29	335, 365, 445, 568, 583, 820, 924, (951), 1036, 1183, 1285
203.81(7)	5.10(3)	457.21	253, 444, 783, 1045, (1341), 1544
253.08(7)	100.00(15)	253	204, (311), 322, 340, 444, (616), 632, 647, 783, 884, 927, 988, 1043, 1045, 1101, 1176, 1249, 1350, 1545, (1802), 1899, 2105
310.64(7)	7.90(3)	885.6	253, 322, 575, 616
316.95(7)	4.95(3)	317.29	(365), 568, 583, 820, (849), 924, 1183, 1285, (1899)
321.68(7)	3.16(3)	574.58	253, 311, 562, 854, 927, 1182, 1223
325.72(8)[a]	0.72(3)	900.57	(340), 575
334.62(8)[a]	0.68(3)	652.08	(124), 177, 317, 589, 849, 951
339.96(10)[a,‡]	0.30(3)	1101.48	(444), 761
340.16(10)[a,‡]	0.19(3)	1240.85	(326), (583), 647
365.02(8)[a]	0.77(3)	1501.79	(177), (457), (562), (575), (680), 820, 884, 1137
382.28(8)[a]	0.94(4)	839.19	457, 661, (763), 927
401.3(5)	0.13(5)	1240.85	382, (457)
443.53(7)[b,‡]	0.55(4)	900.57	204, 253, (340), 457
444.68(7)[‡]	0.28(5)	761.52	177, 543, 656, 917, 1018, 1036
457.12(6)	6.21(3)	457.21	365, 382, 444, (661), (680), 783, 1045, 1341, 1544
542.77(21)[a]	0.15(2)	1304.3	445
562.38(13)[†]	0.20(2)	1136.95	(322), (365), 575
568.39(6)	2.26(3)	885.6	124, 177, 317, (616)
574.78(6)	40.96(13)	574.58	311, 326, 562, (616), 666, 842, 854, 927, 1223, 1426
583.32(6)[b]	2.07(3)	900.57	(124), 177, 317, (340), 661
589.1(5)[c,‡]	0.6(2)		335
616.44(7)[a]	0.85(3)	1501.79	311, (575), 632, 886
632.29(6)	8.27(4)	885.6	253, 616 , 1802
647.45(6)[b]	2.96(3)	900.57	253, 340, 1101
655.57(28)[a]	0.14(3)	1416.18	445

Continued on next page

www.manaraa.com

Table 6.1 – Continued from previous page

Energy	Intensity	Placement	$\gamma\gamma$-Coincidences
660.58(21)[a]	0.16(3)	1500.00	(382), (457), (583)
666.14(7)[†]	1.37(4)	1240.85	119, 575
680.15(18)[†]	0.19(3)	1136.95	(365), 457
761.01(6)	1.48(3)	761.52	340, 1036
763.00(6)	0.10(1)	1602.64	(382)
783.43(7)[‡]	1.37(5)	1240.85	204, 253, 457
820.14(9)[†]	0.46(3)	1136.95	(124), 177, 317, 365
841.69(6)[†,‡]	0.16(2)	1416.18	575
849.42(8)[a]	0.72(3)	1501.79	(177), (317), 335
853.7(7)[a]	0.87(3)	1428.44	575
863.44(12)[c,‡]	0.47(3)		
883.87(5)[†,‡]	0.14(3)	1136.95	(253), (365)
885.87(5)[‡]	14.48(6)	885.6	616, 911
911.19(6)	0.19(4)	1797.62	886
917.30(37)[a]	0.09(3)	1678.83	(445)
924.23(12)[†]	0.46(3)	1240.85	(124), 177, (317)
927.25(5)	9.46(5)	1501.79	253, 322, (382), 575
951.06(17)[a]	0.21(3)	1602.64	(124), 177, 335
987.65(6)	2.17(4)	1240.85	253
1012.2(5)[c]	0.15(3)		(1176)
1017.98(10)[a,‡]	0.13(3)	1918.54	124, 445
1035.55(10)[a]	0.40(3)	1797.62	177, 445, 761, 1176
1042.32(2)[c]	2.58(4)		253
1044.95(6)	2.36(4)	1501.79	204, 253, 457
1086.29(14)[c]	0.49(6)		(1350)
1101.13(11)[a,‡]	0.08(2)	2001.84	(647), (761)
1136.52(20)[†]	0.60(5)	1136.95	365
1175.59(7)	3.22(10)	1428.44	253, 1012, 1037
1181.82(6)[c,‡]	0.15(1)	1756.35	322
1183.32(6)[a,‡]	4.1(10)	1500.00	124, 177, 317
1223.18(6)	1.83(4)	1797.62	(253), 322, 575
1241.03(13)	0.49(4)	1240.85	
1249.07(5)	8.37(5)	1501.79	253
1284.73(17)[†]	0.30(3)	1602.64	(177), (317)
1298.33(21)[a]	0.21(3)	1756.35	204
1340.81(18)[a]	0.26(3)	1797.62	(204), (457)
1349.85(25)	0.42(4)	1602.64	253, 1086
1415.93(8)[†]	0.80(4)	1416.18	
1426.09(16)[b]	0.05(6)	2001.84	575

Continued on next page

www.manaraa.com

Table 6.1 – Continued from previous page

Energy	Intensity	Placement	$\gamma\gamma$-Coincidences
1487.19(26)[c,‡]	0.42(7)		
1502.26(6)	5.43(5)	1501.79	
1544.09(6)[†,‡]	0.18(4)	2001.84	204, 253, 457
1545.19(6)[‡]	1.26(12)	1797.62	253
1798.53(12)	0.71(5)	1797.62	
1801.93(8)[a,‡]	0.18(2)	2687.53	(253), 632
1899.18(14)	0.69(5)	2152.2	253
2102.5(9)[c]	0.08(4)		
2105.6(3)[a]	0.27(4)	2358.59	253

[a] Newly observed γ ray.
[†] Newly observed γ ray which is observed in at least one other measurement [6, 47, 55, 71].
[b] γ ray with different placment than Chacko et al. [26].
[‡] γ ray energy and intensity determined from $\gamma\gamma$ coincident data.
[c] Unplaced γ ray.

6.3.1 Development of Decay Scheme

The strongest γ ray associated with the ^{75}Ga β decay is observed to be of energy 253 keV. There is a known γ ray from ^{75}Zn β decay of energy 252.9 keV. Hence, the 253-keV γ-ray peak observed in our singles spectrum was a compound peak from ^{75}Ga and ^{75}Zn β decay thus requiring determination of the contaminant component. We have used the relative intensity in the single spectrum of 409.78-keV ($I_\gamma = 35(4)$) and 432.29-keV ($I_\gamma = 100(3)$) γ rays to determine the intensity of the 253.9-keV ($I_\gamma = 7(2)$) γ ray associated with ^{75}Zn decay [6] which is shown in Figure 6.3. This intensity 1.5(3)% of the total intensity for the 253-keV γ ray observed in our γ-ray singles spectrum. Also, we set a coincidence gate on the 178-keV level from ^{75}Zn decay [6, 32], and used the coincidence information for γ rays of energies 428 keV and 253 keV to estimate the intensity of the

www.manaraa.com

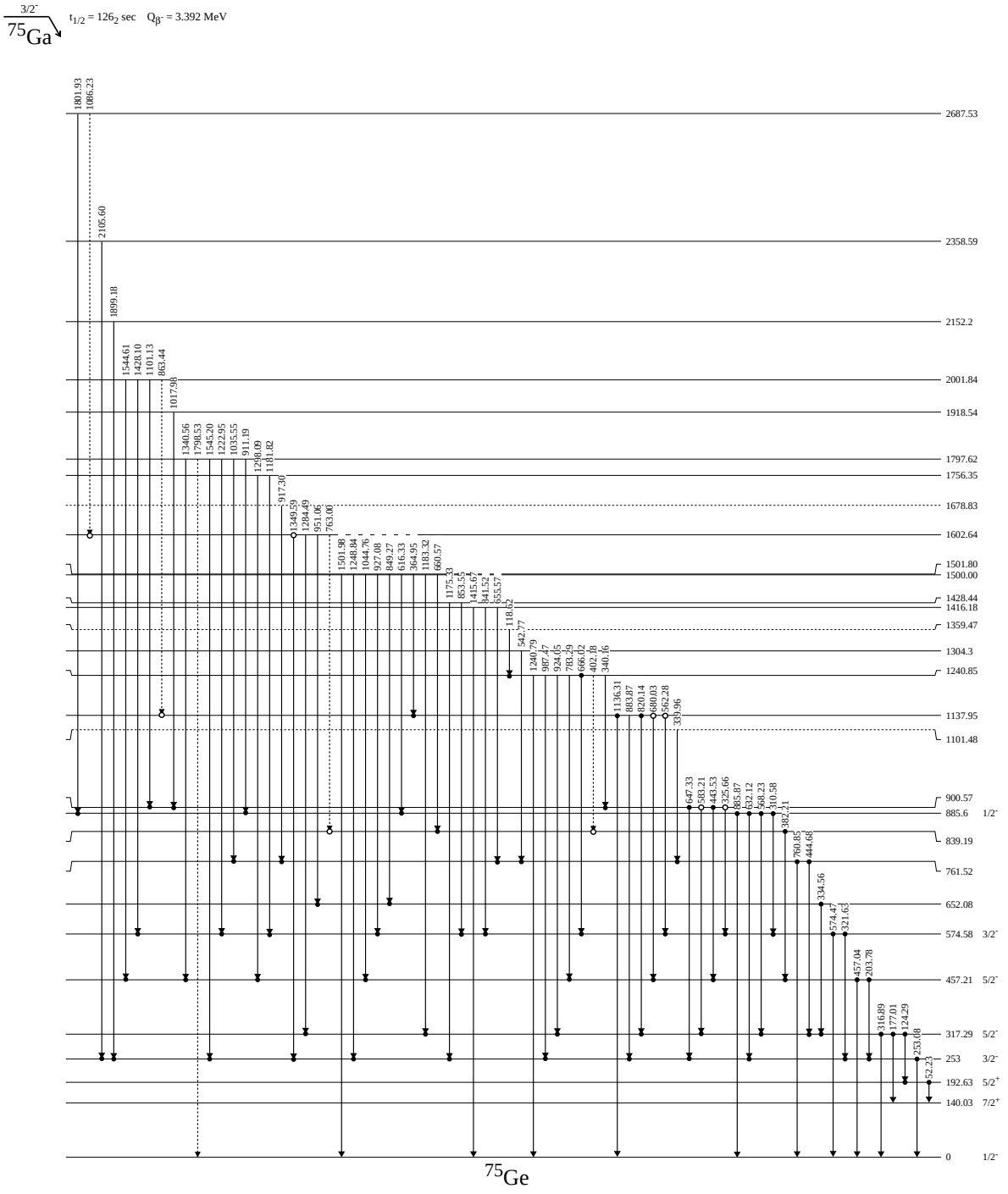

Figure 6.2: Proposed decay scheme for ^{75}Ga to excited states in ^{75}Ge.

www.manaraa.com

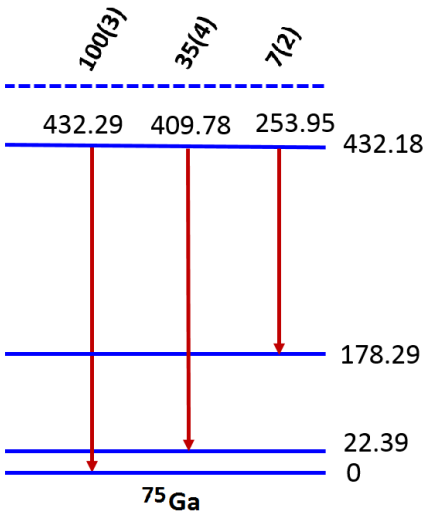

Figure 6.3: Part of level scheme for ^{75}Ga from Kestorm *et al* [32].

253-keV γ ray as explained in Chapter 4. From both techniques, we obtained very similar results and take the weighted average to assign the areas of the 253.9-keV γ ray associated with ^{75}Zn decay. Then we subtracted this value to determine the area of the 253.08-keV γ ray associated with ^{75}Ga decay. We normalized the intensities for the rest of the γ rays based on the corrected area.

First, we established the 253-keV level by placing the 253-keV γ ray feeding the ground state. We observed a strong γ ray of energy 575 keV which is not is coincidences with principle γ ray of energy 253 keV. Hence, we established the levels at 575 keV by placing the 575-keV γ ray feeding the ground state. Similarly, we established the energy levels at 317, 761 and 886 and 1502 keV by placing the corresponding γ rays as they are not in coincidence with either the 253-keV or 575-keV γ rays. Then placed the 322-keV γ ray to 575-keV level, 311-keV and 632-keV γ ray to 886-keV level, and 616-keV, 927-keV and 1249-keV γ rays to 1502-keV level. Then, we observed the three γ rays of energies

www.manaraa.com

124, 177 and 317 keV. These γ rays do not see each other in coincidences as well as with other γ rays already placed in the decay scheme including 253 keV and 574 keV. Then we proposed a level at 317 keV by placing the 317-keV γ ray. Furthermore, we placed the other two γ rays of energy 177 keV and 124 de-exciting the level at 317 keV which feeds in the energy levels at 140 keV and 193 keV. The levels at 140 keV and 193 keV are well established isomeric states from several previous studies [6]. So, we do not expect to observe direct feeding of the γ rays connecting the ground state. But in our γ-singles spectrum, we observed γ rays of energies 52 keV and 139 keV. To estimate the proper intensities of them, we used the internal conversion coefficient reported in the NNDC [6] database. Our data also support the existence of 139- and 193-keV isomeric states. We placed rest of the γ rays observed from our measurements connecting levels based on the coincidence information and construct the decay scheme which is shown in Fig. 6.2.

The energy levels we observed at 140 keV, 253 keV, 317 keV, 457 keV, 575 keV, 762 keV, 885 keV, 1241 keV, 1427 keV and 1502 keV are in agreement with those proposed by Chacko *et al*. Our coincidence data reveled that, in addition to the 988-keV and 1241-keV γ rays reported by Chacko *et al.*, four more γ rays of energies 340 keV, 401 keV, 666 keV, and 924 keV de-excite the level at 1341 keV. Another 854-keV γ ray is observed de-exciting the level 1428 keV along with the 1176-keV γ ray reported by Chacko *et al*. Furthermore, the γ rays of energies 365, 616 keV and 849 keV were placed de-exciting the level at 1502 keV along with 927-keV, 1043-keV, 1249-keV, and 1502-keV γ rays reported by Ref. [26]. Also, the γ ray of energies 911 keV, 1037 keV and 1341 keV de-excite

www.manaraa.com

the level at 1798 keV in additon to 124-keV, 1544-keV and 1799-keV γ rays reported by Chacko *et al.* [26].

From this measurement, a new energy level at 652 keV is firmly proposed by placing the γ ray of energy 335 keV feeding the 317-keV level. We observed a 335-keV γ ray which is in definite coincidences with the γ rays of energies 177 and 317 keV leading to its placement as de-exciting the 652-keV level. Furthermore, it shows two more γ rays of energies 849 and 951 keV in definite coincidences which feeds-in the level as shown in Fig. 6.2. The level at 652 keV was also reported by previous (p, d) reaction of Ge nuclei measurements [38, 90, 96]. Hence, our data suggest that there a level at 652 keV.

A level at 839 keV is proposed by placing a γ ray of energy 382 keV feeding the level at 457 keV. We observed that the 382-keV γ ray is in definite coincidences with 457-keV γ ray leading it's placement as de-exciting the 839-keV level. Furthermore, 382-keV γ ray shows definite coincidences with γ rays of energies 401 keV and 661 keV which feeds in the level 839 keV suggesting that there is a level at 839 keV.

A level at 901 keV is firmly proposed based on four γ-ray transitions of energies 326-, 444-, 583- and 647-keV feeding the levels at 575, 457, 317 and 253 keV respectively. In this work, we observed a 326-keV γ ray which is in definite coincidence with the 575-keV γ ray leading its placement de-exciting the level at 901 keV. Another 444-keV γ ray was observed in definite coincidences with 457- and 253-keV γ rays leading its placement as de-exciting the level at 900.57 keV. Furthermore, a 583-keV γ ray was observed which is in definite coincidence with 177- and 317-keV γ rays and placed as de-exciting the level at 901 keV. Besides that, a 647-keV γ ray was observed in definite coincidences with

www.manaraa.com

253- and 340-keV γ rays and placed it de-exciting the level at 901 keV. Consequently, our data support that there is level at 901 keV. Moreover, this proposed level at 901 keV is in agreement with previous studies from (n, γ) reactions [47, 55, 71].

A level at 1101 keV is tentatively proposed by placing a γ ray of energy 340-keV feeding the 762-keV level. A 340-keV γ ray was observed in definite coincidences with 761-keV γ ray leading its placement as de-exciting the level at 1101 keV. This level is represented by a dashed line in decay scheme as it was proposed based on a single γ-ray transition with weak intensity resolved from the 340-keV γ-ray doublets.

A level at 1304 keV is proposed by the placement of γ ray of energy 543 keV feeding the 761.52-keV level. We observed a 542.68-keV γ ray which is in definite coincidence with 445-keV γ ray leading its placement as de-exciting the level at 1304 keV. The energy level at 1304 keV is represented by a solid line in the decay scheme (even it was proposed by a single γ-ray transition) because the placement of 445-keV γ ray is based on definite coincidences in both directions.

A level at 1416 keV is firmly proposed by the placement of three γ rays of energies 656, 842, and 1416 keV feeding the levels at 762 keV, 575 keV and ground state respectively. In the present work, a 656-keV γ ray is observed in definite coincidence with 445-keV γ ray leading its placement as de-exciting the level at 1416 keV. Furthermore, an observed 842-keV γ ray shows a definite coincidence with 575-keV γ ray leading its placement as de-exciting the level at 1416 keV. Besides that, a 1416-keV γ ray was observed which shows no coincidences with any γ rays and tentatively placed it as de-exciting the level at

www.manaraa.com

1416 keV. Our proposed level at 1416 keV is in agreement with previous studies by (n, γ) and (p, d) reactions [47, 71].

A level at 1500 keV is proposed by placing the two γ rays of energies 661 keV feeding the level at 839 keV and 1183 keV feeding 317 keV. We observed a 660-keV γ ray in probable coincidences with 380-keV γ and placed it de-exciting the level at 1500 keV. In addition, 1183-keV γ ray is observed in definite coincidences with 124-, 177- and 317-keV γ rays leading its placement to the 1500 keV. Hence our data suggest that there is a level at 1500 keV.

A level at 1603 keV is firmly proposed by placing four γ rays of energies 763, 951, 1285 and 1350 keV feeding the levels at 839, 652, 317 and 253 keV respectively. We observed a 951-keV γ ray which is in definite coincidence with 334- and 177-keV γ rays leading it's placement as de-exciting the level at 1603 keV. Besides that, a 1285-keV γ ray was observed which shows definite coincidences with 177-and 317-keV γ rays leading its placement as de-exciting at 1603-keV level. Furthermore, a 1350-keV γ ray was observed which shows the definite coincidences with 253-keV γ ray and placed it as de-exciting the level at 1603 keV. Also, γ-ray of energy 763 keV shows probable coincidence with 382-keV γ ray and tentatively placed it de-exciting the level at 1603 keV. Consequently, our data strongly suggests that there is a level at 1603 keV, which is in agreement with previous ^{76}Ge(p, d), (d, t) and (^{3}He, α) studies [38, 90, 96].

A level at 1679 keV is proposed by placing the γ ray of energy 917 keV feeding the level at 762 keV. We observed a 917-keV γ ray which shows a definite coincidence with 445-keV γ ray leading it's placement as de-exciting the level at 1679 keV. The level at

www.manaraa.com

1679 keV is represented by a dashed line in the decay scheme as it is established with a single γ-ray transition.

A level at 1756 keV is proposed by placing two γ rays of energies 1182 keV feeding the level at 575 keV and 1298 keV feeding the level at 457 keV. We observed a 1182-keV γ ray which is in definite coincidences with 322-keV γ ray leading to its placement as de-exciting the level at 1756 keV. Furthermore, a 1298-keV γ ray was observed which shows definite coincidence with 204-keV γ ray leading it's placement as de-exciting the level at 1756 keV. Consequently, our that suggest that there is a level at 1756 keV.

A level at 1919 keV is proposed by placing the γ ray of energy 1018 keV feeding the level at 901 keV. In this work, a 1018-keV γ ray is observed which shows definite coincidence with 445- and 124-keV γ rays leading its placement as de-exciting the level at 1919 keV. This level is also represented by a dashed line in the decay scheme.

A level at 2002 keV is proposed by the placement of γ rays of energies 1101, 1428 and 1544 keV feeding the levels at 901, 575 and 457 keV respectively. In this work, a 1101-keV γ ray was observed which shows probable coincidence with 647-keV γ ray and have tentatively placed it as-exiting the level at 2002 keV. A 1428-keV γ ray was observed in definite coincidence with 575-keV γ ray leading its placement de-exciting the level at 2002 keV. Besides that, a 1544-keV γ ray was observed in definite coincidence with 253-keV γ ray and placed it as de-exciting the level at 2002 keV. Consequently, our data firmly suggest that there is a level at 2002 keV.

www.manaraa.com

A level at 2152 keV is proposed by placing the 1899-keV γ ray feeding the 253-keV level. We observed a 1899-keV γ ray in definite coincidences with 253-keV γ ray leading it's placement as de-exciting the level at 2152 keV.

A level at 2359 keV is proposed by placing the γ ray of energy 2106 keV feeding the level at 253 keV. We observed a 2106-keV γ ray which is in definite coincidence with 253-keV γ ray leading its placement as de-exciting the level at 2359 keV. This level at 2359 keV is represented by a solid line because the placement of 253-keV γ ray is based on definite coincidences in both directions.

Finally, a level at 2688 keV is proposed by placing the γ ray of energy 1803 keV feeding the level at 886 keV. We observed a 1802-keV γ ray in definite coincidences with 632-keV γ ray leading its placement as de-exciting the level at 2688 keV. Thus, our data suggest that there is a level at 2688 keV.

Our analysis supports the placements of the most of the γ rays and energy levels reported in the previous β-decay study [26]. However, a γ ray of energy 124 keV was placed de-exciting the level at 885 keV by Chacko *et al*. For this placement to be correct, the 124-keV γ ray should see γ rays of energies 444 and 761 keV in coincidence. Our result does not support this fact since neither γ ray is observed in the 124-keV coincidence gate, nor is the 124-keV γ ray observed in the gates set on the 444- and 761-keV γ rays. Rather the 124-keV γ ray is observed in definite coincidences with the 1183-keV γ ray which is also in coincidences with 317- and 177-keV γ rays. Therefore, we placed the 124-keV γ ray as de-exciting the 317-keV level and populating an isomeric state at 193 keV, which is in agreement with previous ^{74}Ge(n, γ) study [6].

www.manaraa.com

Chacko *et al.* observed several γ rays which we did not observe and were likely due to contamination in their experiment. In the Chacko *et al.* experiment, ^{75}Ga was produced from the (γ, p) reaction on ^{76}Ge which was only 73.89% pure. Other Ge isotopes present in the targe sample were ^{74}Ge (10.08%), ^{73}Ge (1.69%), ^{72}Ge (6.65%) and ^{70}Ge (7.69%) [26]. We assume that the purity of our beam removes any of the possible contaminants present in the previous experiment. Consequently, we are able to remove a total of six γ rays. A 279-keV γ ray was reported by Chacko *et al.* with intensity 2.9(6) [26]. Our γ-ray singles spectrum does not show any evidence for this γ-ray peak. Furthermore, we removed five other γ rays reported in previous β-decay study: γ ray of energy 1239.5 keV is identified associated with ^{69}Ga, γ rays 1358.8, 1796.4, and 2089.7 keV are identified associated with ^{75}Zn of the same decay chain whereas γ ray of energy 1745.6 keV is identified associated with ^{74}Ga decay.

We do not see any evidences for four energy levels at 584.1, 1222.5, 2103.7 and 2664.4 keV reported by Chacko *et al*. The energy level at 584.1 keV was proposed by two γ rays of energies 444.8 and 584.1 keV. In the present work, we observed the 443.53-keV γ ray in definite coincidences with γ rays of energies 203 keV, 253 keV and 457 keV indicating it feeds the 457.21-keV level. Furthermore, a 583.32-keV γ ray was observed is in definite coincidences with 177- and 317-keV γ rays indicting it feeds the level at 317 keV. Therefore, both γ rays were placed de-exciting the level at 900.57 keV. The 1222.5-keV level was proposed based on γ rays of energy 648 and 1222 keV de-exciting the level. In the present work, 647-keV γ ray is assigned to a level 901 keV as it sees definite coincidences with 253-keV γ ray and does not see the evidence for 1223-keV doublets.

www.manaraa.com

So, we removed the level at 1223 keV. The energy level at 2103.7 keV is proposed based on a single γ-ray transition which feeds the ground state. Chacko *et al.* reported the γ-ray of energy 2103.7 keV with intensity 0.20(5). In our measurement, we do not observe any γ ray having energy 2103.7 keV, and removed this level. The energy level at 2664.4 keV was proposed with a single γ ray of energy 2089.7 keV but we identified it belongs to ^{75}Cu. In addition, we have adjusted the placement of 1427.0-keV γ ray to the level at 2002.50 keV as it sees definite mutual coincidences with 575-keV γ ray.

In the Chacko *et al.* study, they reported the observation of γ rays of energies 1182, 1358 and 1745 keV but were unable to place them in the decay scheme [26]. The 574.7-keV γ ray from the Chacko *et al.* was a compound peak as it contains the component of 573.4-keV γ ray peak form ^{69}Ga β decay. Our data is free from that contamination. The relative intensity of 574.67-keV γ ray in our spectrum is 40.96% which is slightly higher than Chacko *et al.* estimates 31.6%. We proposed that the 1182-keV γ ray is a doublet where the two γ rays have been placed with confidence as de-exciting the level at 1502 and 1756 keV respectively. We observed some γ rays which have been associated with the $A = 74$ decay chain and was no surprise as a ^{75}Cu has 3.5(6)% [83] chance of βn decay to the ^{74}Zn - ^{74}Ga - ^{74}Ge decay chain. Our coincidence data shows evidence for some of the γ rays which we assigned to ^{75}Ga as being also associated with the other members of the same decay chain suggesting unresolved doublets. From knowledge of the $\gamma\gamma$ coincidence areas in the cascade and their corresponding ratio, we have calculated the proper γ-ray intensity to assign each γ-ray in the unresolved doublets. Here, γ rays of energies 783, 841, 864, 1017, 1101, 1488 and 1802 keV are also associated with either ^{75}Cu or ^{74}Zn

www.manaraa.com

decay. Besides that, in our measurement, five γ rays of energies 340, 444, 885, 1182 and 1544 keV appeared as doublets and we have divided the proper intensity to them applying the methods explained in Chapter 4.

We observed a γ ray of energy 52.23 keV as a compound peak associated with the ^{74}Zn and ^{75}Ga decay. The previous experiment by Ishikawa *et al.* [55] reported the 52-keV γ ray in coincidences with 124-, 392- and 481-keV γ rays and proposed its placement as de-exciting the anomalous $5/2^+$ state of at 193 keV, connecting to the isomeric state at 140 keV with spin-parity $7/2^+$. We not only observed 52-keV γ ray in coincidences with 124-keV γ ray but also agree with placing it de-exciting the level at 193 keV. Since the 52 keV γ ray is a weak γ ray feeding the isomeric state, we used the conversion electron coefficient of 4.2(10) from Ishikawa *et al.* [55] to estimate the total relative transition intensity for the 52-keV γ ray as 5.2(24).

We also observed seven γ rays associated to the ^{75}Ga β decay but do not have enough confidence to place them in the decay which is listed in the Table 6.1 with c footnote. The total summed intensity of unplaced γ rays is around 1.80(15) relative to 253-keV γ ray.

www.manaraa.com

Table 6.2: Feeding intensities (I_{β^-}), $\log(ft)$ and assigned spin-parity value for ^{75}Ga β decay. The β-feeding values are given per 100 decays.

Energy Level	$\mathbf{I}_{\beta^-}$	$\log(ft)$	**Spin-parity from NNDC**
0.00	90(20)	5.45	$1/2^-$
140.03(5)	0.07(1)	8.50	$7/2^+$
192.63(7)†	2.0(10)	7.00	$5/2^+$
253.00(3)	2.70(1)	6.82	$3/2^-$
317.29(3)	0.32(4)	7.71	$5/2^-$
457.21(3)	0.22(1)	7.79	$5/2^-$
574.58(3)	0.85(1)	7.12	$3/2^-$
652.08(6)$^{\dagger,\circ}$	0	>10.00	
761.52(4)$^{\circ}$	0	>10.00	
839.19(6)$^{\ddagger,\circ}$	0.01	>10.00	
885.6(3)	1.34	6.78(1)	$1/2^-$
900.57(4)†	0.25	7.43	
1101.48(11)$^{\ddagger,\circ}$	0.01	8.56	
1136.95(4)†	0.03	8.10	
1240.85(4)	0.27	7.12(1)	
1304.30(21)$^{\ddagger,\circ}$	0.01	>9.00	
1359.47(17)$^{\dagger,\circ}$	0.01	>9.00	
1416.18(5)†	0.05	7.74	
1428.44(5)	0.17	7.15	
1500.00(3)‡	0.18(4)	7.07	
1501.80(3)	1.21(4)	6.24	
1602.64(11)†	0.04	7.63	
1678.83(37)$^{\ddagger,\circ}$	0	>9.00	
1756.35(6)$^{\dagger,\circ}$	0.02	7.89	
1797.62(4)	0.20(1)	6.73	
1918.55(10)$^{\ddagger,\circ}$	0.01	9.00	
2001.84(5)†	0.07	>7.00	
2152.20(14)†	0.03	7.70	
2358.59(29)$^{\dagger,\circ}$	0.01	7.24	
2687.53(8)$^{\ddagger,\circ}$	0.01	>7.00	

‡ Newly proposed energy level.

† Newly proposed energy level which agreed with at least one other studies [6, 47, 55, 71].

$^{\circ}$ Intensity balance consistent with zero.

www.manaraa.com

6.3.2 Estimation of Absolute Branching Ratio

After constructing the detailed level scheme of ^{75}Ge, we have attempted to calculate the relative β-feeding intensity for each level using the MASTER program. Calculation of normalization factor for the 253-keV γ ray was complicated due to the presence of isomeric states at energy 140 and 192 keV. Furthermore, we cannot directly measure the absolute normalization factor for 253-keV γ ray as we do not know the exact amount of ^{75}Ga which decayed.

Hence, in estimating the normalization constant, we will make some assumptions. First, we will assume that we have observed all the γ rays from the decay. Second, we will assume there is no direct feeding to the ground state, 140- or 193-keV levels as shown in Fig. 6.4 (a). However, this assumption is not completely true as there should be direct feeding to the ground state which is governed by allowed transitions from the parent nuclei ($3/2^-$ to $1/2^-$ [6]). Our assumptions impose the upper absolute limit on the normalization factor which is going to overestimate the β-feeding intensity to the levels. Then, we summed all the γ-rays intensities feeding the levels at 192, 140 and the ground state, which is represented by white arrows in the Figure 6.4 (a).

Then we took the spin-parity consideration for those states to estimate the β-feeding. The ground state of the parent nuclei ^{75}Ga has spin-parity of $3/2^-$ from its unpaired proton being in the $2\pi p_{3/2}$ state which decays to ^{75}Ge through β decay. The ground state of ^{75}Ge has a confirmed $1/2^-$ spin-parity [6] which create the scenario of allowed transition from $3/2^-$ to $1/2^-$ suggesting it should have a low $\log(ft)$ value. We have estimated the un-observed ground-state β-feeding by considering a $\log(ft)$ value of 5.45(10) for the

www.manaraa.com

allowed transition [62] giving an estimated 90(20)% direct β-feeding to the ground state which is shown in Fig. 6.4(b). Similarly, we can assume a $\log(ft)$ value of 8.5(1) for the first isomeric state at 140 keV as it is first forbidden unique transition from a $3/2^-$ to $3/2^+$ state. The estimated direct β-feeding is less than 1%, so we will assume 0%-feeding. For the second isomeric state at 193 keV, the spin-parity assigned from other studies is $5/2^+$, hence is a first forbidden transition from a $3/2^-$ to a $5/2^+$ state. Therefore, we assume that the $\log(ft)$ value for this states is 6.5(2) which gives the β feeding of 2(1)%.

Based on the assumed feedings, the rest of the β-feeding which is around 8% comes from the higher lying states inducing 253-keV state. Then the absolute branching ratio for 253-keV γ ray is estimated to be around 4.34%. The β-feeding intensity ($I_{\beta-}$) for all levels were normalized based on the above estimation to get the absolute β-feeding value which is listed in the Table 6.2.

6.3.3 Log(ft) Value and Spin-Parity Assignment

Lower limits $\log(ft)$ value for the energy levels in ^{75}Ge fed in the β decay of ^{75}Ga as shown in Table. 6.2 were calculated as explained in previus Chapter 4 using the NNDC webiste [7]. We have used the well accepted Q_{β^-} = 3392.4(24) keV [112] and half-life ($T_{1/2}$) = 126(2) s [6] taken from AME2012 [112] for this calculation. The estimated $\log(ft)$ lower limits and possible spin-parity assignments for the established energy levels are listed in the Table 6.2.

As seen in the low-energy level systematic of the $N = 43$ isotones shown in Fig. 6.5, we have assigned the spin-parity of ^{75}Ge ground state to be $1/2^-$. The ^{75}Ge ground state

www.manaraa.com

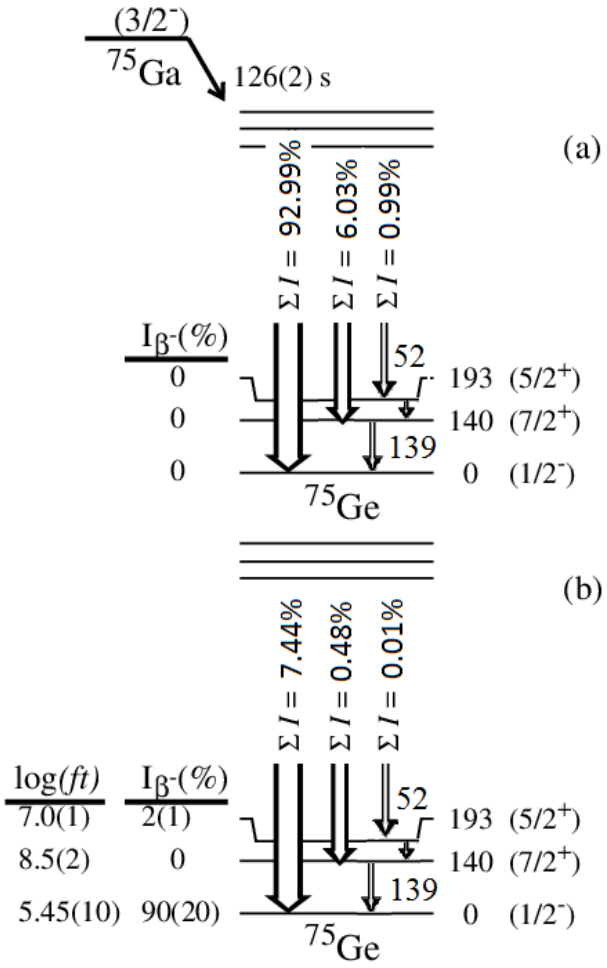

Figure 6.4: Different scenarios of β decay of ^{75}Ga (a and b) to levels in ^{75}Ge used to determine the absolute brancing ratio of the 253-keV γ-ray transtion. The sum relative γ-ray intensities to corresponding levels are represented by white arrows and absolute β intensities are shown on the left next to the energy levels. (See text for details.)

must come from a $(\nu 1g_{9/2})^4 \otimes (\nu 2p_{1/2})^1$, where the stronger pairing force for the $\nu 1g_{9/2}$ orbital puts the odd neutron in the $\nu 2p_{1/2}$ orbital. The strong pairing is behind all the deformation observed in this region. Our calculated $\log(ft)$ values are not conclusive for any of the states to confirm the previously assigned spin-parity values. The theoretical

www.manaraa.com

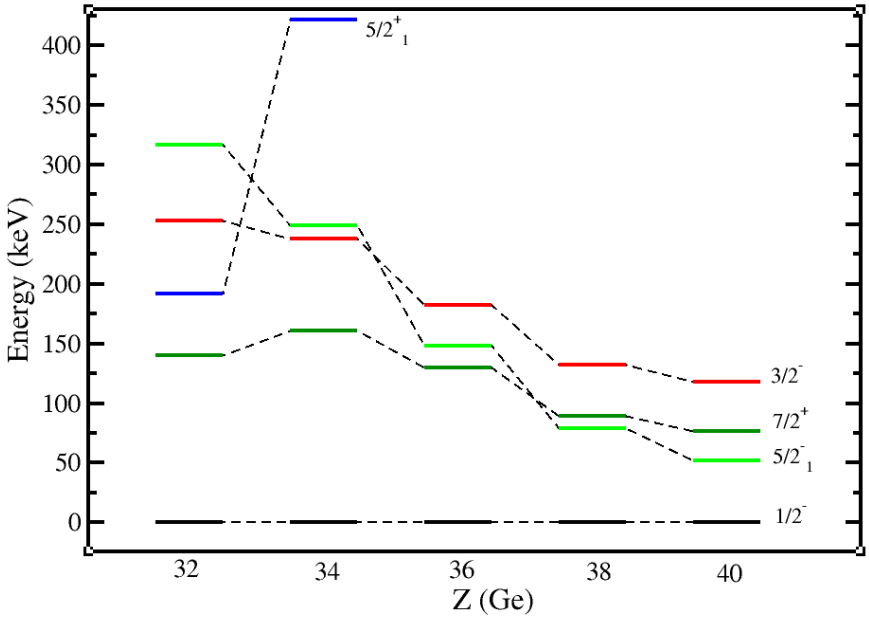

Figure 6.5: Low energy level systematics of $N = 43$ isotones [6, 20, 70, 76, 98, 100].

prediction of spin-parity and states using Nushellx@MSU [23] using $JUN45$ effective interaction and $JJ44$ model space is shown in Fig. 6.6. This calculation predict the ground state to be $7/2^+$ from a $(\nu 1g_{9/2})^3$ configuration. Other energy levels are slightly stretched up than we observed in our proposed decay scheme. Hence, the Nushellx prediction is failing to describe the observed structure of ^{75}Ge nuclei.

6.4 Discussion and Conclusion

Having a very pure ^{75}Cu beam, $\gamma\gamma$ coincidence data from a high efficiency/high resolution HPGe clover detector array, and better data analysis techniques, we have been able to identify 78 γ rays associated with ^{75}Ga β decay, placed 71 of them and constructed the decay scheme with 30 energy levels occupying up to 2.7 MeV. The total number of γ

www.manaraa.com

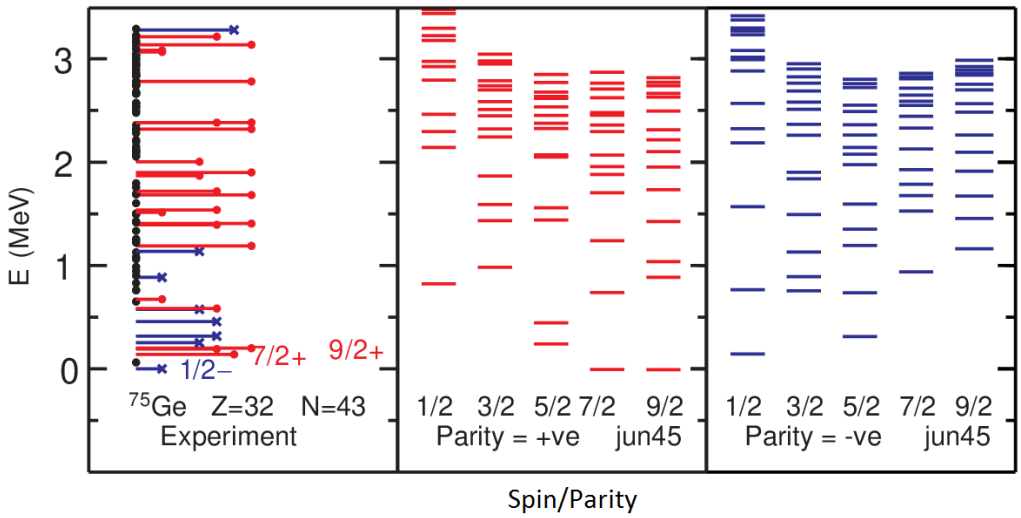

Figure 6.6: Nushellx prediction for structure of ^{75}Ge.

rays observed in this measurement is twice as many as reported by the previous β-decay study [26]. Out of the 30 energy levels proposed from this work, 18 were not included in the previous β-decay study. Of these 18, 11 are in agreement with levels observed in other studies [76]. The remaining seven levels are totally new. We have also corrected the placements of five γ rays and do not observe the evidence for four levels proposed in the previous β-decay measurement. Hence the present work has extracted more detail structure information of ^{75}Ge and better understanding of level systematics.

www.manaraa.com

CHAPTER VII

THE β DECAY OF ^{76}GA

7.1 Introduction

The ^{76}Ge nuclei is a possible candidate for neutrinoless double-β decay ($0\nu\beta\beta$) which violates the conservation of total lepton number, as well as a candidate element for measuring the neutrino mass [19]. Understanding the nature of the neutrino is important as it is supposed to be Majorana particle, i.e neutrinos are their own antiparticles. During the double-β decay, two neutrinos emitted will annihilate one another and disappear, which violates the conservation of lepton number as opposed by Dirac equation, hence will explore physics beyond the standard model [33]. ^{76}Ge is the only candidate nuclide with reported half-life for double-β-decay study [59] and has a large international focus like MAJORANA [10] and GERDA [14]. The MAJORANA and GERDA are the international collaborative efforts to search for neutrinoless double-β decay in ^{76}Ge. Furthermore, ^{76}Ge exhibits interesting structural features such as shape co-existence [49] and tri-axial deformation at low excitation energy [108] which makes this nuclide important for structure studies. Several studies including a β decay [25], charged particle scattering [82, 93], neutron scattering [28, 31, 75, 86], transfer reactions [74, 85], Coulomb excitation [46, 64] and total absorption spectroscopy [30] have been carried out to understand the structure of ^{76}Ge nuclei. The low-lying level structure systematics for even-even Ge isotopes from

www.manaraa.com

mass number A = 70 to 80, as shown in Fig. 1.2, indicates that there is enhanced proton-neutron interactions for ^{76}Ge as evident by the lowering of the first excited state relative to the other even-even Ge isotopes. Our research on other nearby nuclides suggested that the current data available for ^{76}Ge in NNDC may lack some details. Hence, this present work of detailed β-decay study of ^{76}Ga will help to understand the evolution of singles particle states for medium-mass even-even Ge nuclei with the addition of neutron pairs, as well as will provides necessary knowledge for Majorana particle detection.

The information on the β decay of ^{76}Ga available at the National Nuclear Data Center (NNDC) comes from Camp *et al.* in 1971 [25]. They utilized the ^{76}Ge(n, p)^{76}Ga reaction to produce the ^{76}Ga nuclei. Two sources of GeO_2 was used having 73.9% and 95.2% ^{76}Ge and the β-decay measurement was performed using the small Ge(Li) detector of size 38 cm^3. They observed a total of 107 γ rays associated to ^{76}Ga decay, placed 97 of them and proposed a decay scheme up to 6.1 MeV containing 41 energy levels. Out of the 97 γ rays, 35 γ rays were only tentatively placed which generated uncertainty in the existence of on 16 energy levels in the proposed decay scheme. The main problem Camp *et al.* had was they did not have coincidence data and had to establish the decay scheme based on γ-ray energy sums and differences along with consideration of the relative γ-ray intensities. With data obtained in an experiment to measure the β-delayed neutron emission from ^{76}Cu [116] using a four-detector clover array, we assumed we would have sufficient data on ^{76}Ga β decay to confirm or correct the placement of all reported γ rays, thus providing an improved decay scheme with a better understanding for the structure of ^{76}Ge.

www.manaraa.com

7.2 Experimental Technique

A 54-MeV proton beam with an intensity of 10-15 μA was used to bombarded a Uranium carbide (UC_x) target inside a hot plasma ion source at HRIBF of ORNL. Mass $A = 76$ isobaric separation was achieved using the low-resolution mass separator (M/ΔM = 600). After passing the beam through a charge exchange cell, ^{76}Zn ions from the beam were removed by passing it through the the high-resolution separator (M/ΔM = 10,000) which separated the ^{76}Cu and ^{76}Ga components of the beam providing an essentially pure beam of ^{76}Cu ions.

These negatively charged ions were accelerated to 2-3 MeV/u by the HRIBF tandem accelerator and then sent to a shielded room containing the detector setup. The beam was transmitted through a micro-channel plate (MCP) detector and six segmented mini ionization chamber (mini-IC) [40] which is filed with CF_4 gas at 100 to 200 torrs pressure. The measurement of six ion energy loss signals in the mini-IC allowed identification of the atomic number Z of individual mono-energetic isobars. Higher atomic number (Z) ions lose more energy in the mini-IC and can be made to range out (stop) by adjusting the gas pressure in the mini-IC, the so-called "Ranging Out"method [40]. Thus beam purification was done by increasing the gas pressure in mini-IC to stop all isobars except the one having the lowest atomic number. By using the mini-IC, we could distinguish the different ions present on the beam based on their energy loss and could determine the absolute branching ratio (BR) for a decay since we were able to count the individual beam particles. A more detail explanation of the RO method is given in Refs. [40, 114]. After removal of long-lived higher-Z isobars, very pure ^{76}Cu ion beam was deposited onto a

www.manaraa.com

moving tape collector (MTC) in the detector set up. Two modes of operation were used during the experiment. If the gas pressure was high ∼200 torrs, we would do ranging out. In this mode, the MTC was placed just behind the mini-IC and the source was moved into the array. If the pressure was low ∼100 torrs, then we were in the "Pass Through"mode with the MTC collection point in the center of the array. As the only component of the beam was the Cu, the timing cycle was designed to maximize the detection rates for γ rays from the Zn daughters thus enhancing the study of short-lived Cu isotopes [116]. The detector array which consisted of four HPGe clovers γ-ray detectors and two plastic scintillation counters. The full clover array has a measured peak efficiency of 29% at about 100 keV and 5% at 1.33 MeV. The rate of ^{76}Cu ($T_{1/2}$ = 0.64s [63]) beam for this particular experiment was about 160-320 ions/s. Data were collected using a triggerless digital data acquisition system which recorded the energy and absolute time (25 ns accuracy) [41, 42] when each γ ray was detected. This allowed offline analysis of the data to establish $\gamma\gamma$ coincidences. This experiment was initially intended to measure ^{76}Cu β-delayed neutron emission only [116] but it allowed for the analysis of all daughter and grand-daughter (^{76}Zn [94] and ^{76}Ga respectively) β decay free of cost.

7.3 Experimental Results

After the experiment, We have performed the efficiency and energy calibration of the raw spectra from 16 HPGe crystals, summed them to generate the γ singles, $\beta\gamma$ and $\gamma\gamma$ coincidence spectra similarly as explained in previous projects. A representative γ-ray singles spectrum obtained from our measurement for all $A = 76$ decay chain starting from

www.manaraa.com

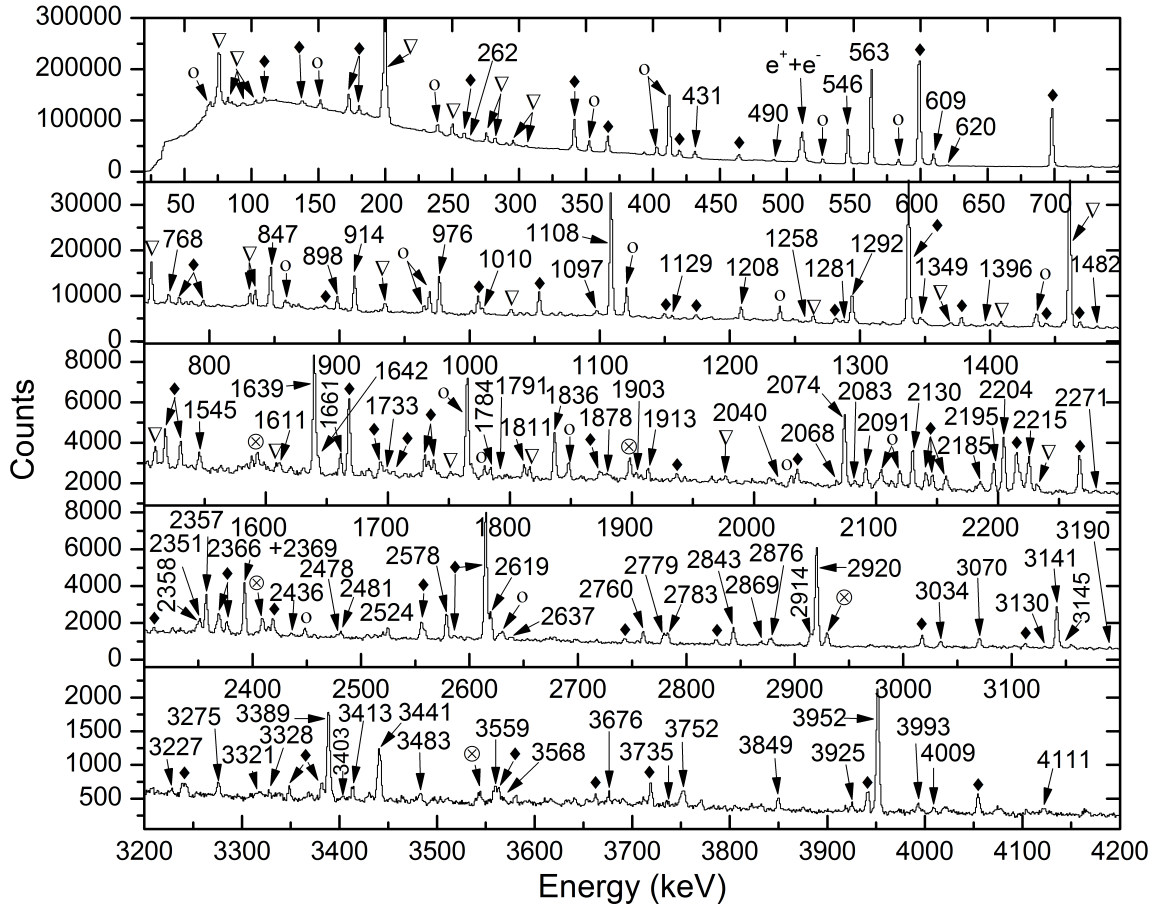

Figure 7.1: Saturation spectrum obtained with a purified ^{76}Cu beam in the energy range from 20 keV to 4.2 MeV using the Pass Through mode of the Ranging-Out setup. The γ-ray peaks associated with ^{76}Ga β decay are marked with their energy. Other members of the decay chain are indicated by symbols as ^{76}Cu: ♦ (solid diamond), ^{76}Zn: ▽ (open down-triangle), Background: ○ (circle) and Escape Peak: ⊗ (crossed bullet). The energy range focus on the γ rays associated with ^{76}Ge. Prominent γ rays from ^{76}Cu and ^{76}Zn are presented above 20 keV and below 4.2 MeV.

^{76}Cu is shown in Figure 7.1. We have determined the γ-rays intensity by fitting the peak area on the un-gated γ-singles spectrum. We analyzed the $\gamma\gamma$-coincidence and β-gated

www.manaraa.com

spectra to identify the association of all γ-rays peak seen in the γ singles spectrum to the particular element of the decay chain. The 563-keV γ ray is observed the strongest γ ray associated to the ^{76}Ga β decay and normalized the intensity of the rest of the γ rays relative to 563-keV γ ray. Coincidence information was determined from the background subtracted γ-ray gated spectra with statistical significant confidence. From the analysis, we have identified 109 γ rays associated with ^{76}Ga β decay. The details of the decay scheme development is presented in the following sections.

www.manaraa.com

Table 7.1: Energy, intensity, placement and coincidence information for γ rays associated with ^{76}Ga β decay (probable coincidences are indicated with parentheses).

Energy	**Intensity**	**Placement**	**$\gamma\gamma$-Coincidences**
262.30(11)[a]	0.66(6)	3182.40	(563), 2920
431.15(4)	5.64(7)	1539.47	546, 563, 1108, 1208, (1482), 1643, 1661, (1784), 2348, (2592)
489.86(7)[b]	1.40(7)	3182.40	562, 2129, 847
545.53(3)	36.90(11)	1108.42	431, 563, 914, (1130), 1208, 1396, 1640, (1643), (1661), 1733, 1811, 1878, 1913, (1981), 2074, (2083), 2204, 2215, 2369, (2436), 2524, (2779), 2783, 2843, (2869), (3190), 3276, 3441
562.91(3)	100.00(19)	562.93	(262), 431, 490, 546, 611, 620, 847, 913, 977, 1010, (1129), 1208, 1258, 1281, 1349, 1482, (1545), 1640, 1642, 1661, 1733, 1784, (1791), (1811), (1844), (1878), 1903, (1913), (2040), 2068, 2074, (2083), 2130, 2185, 2204, 2215, (2279), 2348, 2357, 2367, (2448), (2478), 2524, 2579, 2586, 2591, 2619, (2630), (2636), (2682), 2760, 2779, 2782, 2844, 2877, 2914, (2981), 3034, (3047), 3070, (3190),(3275), 3328, 3338, (3368), 3389, 3413, 3482, 3559, 3568, 3676, 3736, 3925, 3993, 4009
611.2(3)[b,†,*]	0.42(9)	2022.33	(563), 847
619.78(8)[a]	0.84(6)	3312.65	563, 2130
768.43(5)[a]	1.55(6)	3951.10	(546),(2074)
846.96(4)	6.58(17)	1410.15	490, 563, 611, (1258), 1281, (1578), 1611, (1791), 1903, (2068), (2187), 2478, 3034, (3131), 3146, 3403
913.9(4)[*]	0.29(7)	2022.33	546, (563), (1108)
964.64(5)[*,‡]	0.32(10)		563, (1130)
976.50(3)	7.31(8)	1539.47	563, 1208, 1482, (1608), 1643, 1661, 1784, 2348, 2592, (2697), 2846
993.5(6)[‡]	0.10(5)		(977), (1108)
1009.55(7)[a]	1.34(7)	2919.99	(1349)

Continued on next page

www.manaraa.com

Table 7.1 – Continued from previous page

Energy	Intensity	Placement	$\gamma\gamma$-Coincidences
1108.44(3)	27.13(13)	1108.42	431, 914, (1129), 1208, (1563), 1640, (1642), (1661), 1733, 1811, 1878, 1913, 2074, 2083, (2091), 2204, 2215, (2436), (2348), (2481), 2524, 2779, 2783, (2869), 2843, 3190, 3275, (3675)
1129.5(3)[b,c]	0.29(6)	2668.63	563, (1108)
1208.40(4)	2.95(7)	2747.91	431, (546), 563, 977, 1108
1258.0(3)[d]	0.32(7)	2668.63	563, 847
1281.30(7)[d]	1.53(7)	2692.36	(563), 847
1348.73(9)	1.23(7)	1910.92	563, (1010), 2040
1396.30(14)[b]	0.59(6)	2504.72	(546), (563)
1482.04(15)[d]	0.53(6)	3021.42	(431), (563), 977
1545.41(8)[d]	1.19(7)	4237.77	(563), 2129
1562.91(18)[a,†]	0.48(7)	2668.63	(1108)
1577.8(2)[a]	0.38(5)	2986.47	(847)
1601.6(4)[a]	0.38(7)	4444.15	(1733)
1608.23(18)[b]	0.46(5)	3147.70	(977)
1611.24(15)[d,*]	0.45(13)	3021.42	847
1639.50(4)	8.69(12)	2747.91	546, 563, 1108
1642.79(9)	1.25(8)	3182.40	431, (546), 563, 977, 1108
1660.92(7)[d]	1.64(7)	3200.15	431, 563, 977
1733.31(9)	1.24(7)	2841.78	546, 563, 1108, (1602)
1783.60(11)[a]	0.87(7)	3323.05	563, 977
1790.8(4)[b]	0.22(7)	3200.15	563, 847
1811.42(10)	1.08(7)	2919.99	546, (563), 1108
1844.1(4)[a]	0.29(6)	2406.99	(563)
1878.1(3)[d]	0.53(8)	2986.47	(546), (563), 1108
1903.07(18)	0.68(8)	3312.65	(563), 847
1912.96(11)[d]	1.09(8)	3021.42	546, (563), 1108
1981.0(9)[‡]	0.33(6)		(431), (546)
2040.1(3)	0.58(9)	3951.10	563, 1349
2067.7(2)[a]	0.47(7)	3477.61	563, 847
2073.95(4)	6.84(10)	3182.40	546, 563, (768), 1108
2082.53(18)[b]	0.25(10)	3190.95	(546), 1108
2091.23(9)[d]	1.84(10)	3200.15	(545), 1108
2129.73(5)	3.68(9)	2692.36	490, 563, (620), 1545
2185.33(15)	0.86(8)	2747.91	563
2186.9(5)[a]	0.38(14)	3597.06	(563), 847
2204.40(5)	5.50(15)	3312.65	546, 563, 1108

Continued on next page

www.manaraa.com

Table 7.1 – Continued from previous page

Energy	Intensity	Placement	$\gamma\gamma$-Coincidences
2214.74(6)	4.13(15)	3323.05	546, 563, 1108
2279.0(5)	0.33(9)	2841.78	(563)
2366.9(2)	0.73(11)		(546), 563
2348.4(2)	0.77(9)	3887.46	431, 563, 977, 1108
2351.32(12)[a]	1.50(10)	3890.99	431, (563), 977, 1108
2356.98(6)	4.38(10)	2919.99	262, 563
2366.9(2)[a]	0.76(11)	2929.84	563
2369.19(12)	2.09(15)	3477.61	546, 563
2435.6(3)[d]	0.35(6)	3544.01	(563), 546, 1108
2477.7(3)	0.36(6)	3887.46	(563), (847)
2481.18(15)[d]	0.73(6)	3890.99	(563), (1108)
2524.46(9)	1.33(7)	3632.87	546, 563, 1108
2578.60(6)	3.36(47)	3141.47	563
2585.84(19)[b,†]	0.69(15)	3147.70	563
2591.6(3)[d]	0.42(7)	4131.01	431, (563), 977
2619.32(7)	3.56(10)	3182.40	563
2630.37(14)	1.10(9)	3190.95	563
2636.7(5)[b]	0.35(11)	3200.15	(563)
2681.8(4)[d]	0.21(6)	3244.72	(563)
2690.3(4)[†,‡]	0.18(6)		
2696.9(3)[a,†]	0.29(6)	4237.77	(977)
2759.91(9)	1.77(8)	3323.05	563
2778.88(11)	1.54(8)	3887.46	546, 563, 1108
2782.58(10)[d]	1.62(8)	3890.99	546, 563, 1108
2843.00(12)[d]	2.42(19)	4382.47	546, 563, 1108
2846.0(5)[a,†]	0.45(16)	4382.57	(977)
2868.8(2)[d]	0.58(6)	3977.20	(546), (563), 1108
2876.5(4)[a]	0.76(18)	3439.43	563
2913.7(5)	1.73(14)	3477.61	563
2919.8(6)	15.65(14)	2919.99	262
2969.9(3)[‡]	0.25(4)		(563)
2981.1(6)[d]	0.15(7)	3544.01	563
3034.11(13)	0.93(6)	4444.15	563, (847)
3048.1(5)[a,‡]	0.19(5)		(563)
3069.94(10)	1.72(7)	3632.87	563
3130.5(5)[‡]	0.24(7)		847, 1108
3141.40(7)	6.95(11)	3141.47	
3145.5(4)[d]	0.33(7)	4555.74	847
3190.2(2)[d]	0.43(8)	4298.61	(546), 1108

Continued on next page

www.manaraa.com

Table 7.1 – Continued from previous page

Energy	Intensity	Placement	$\gamma\gamma$-Coincidences
3275.6(17)[†]	0.76(7)	4383.57	(546), 563, 1108
3321.9(12)[d]	0.14(8)	3323.05	
3327.7(4)[d]	0.20(6)	3890.99	(563)
3333.7(12)	0.13(13)	3333.66	
3337.6(4)[a]	0.19(6)	3900.52	563
3367.6(5)	0.20(5)	3930.50	(563)
3384.9(8)[a,‡]	0.28(8)		(546)
3388.57(9)	4.59(13)	3951.10	563
3403.11(4)	0.23(6)	4813.26	847
3413.22(17)[a,†]	0.7(7)	3977.2	563
3440.55(9)[a]	3.48(9)	4548.97	(546)
3482.6(3)[a]	0.65(7)	4045.57	563
3558.8(2)	0.95(8)	4121.67	563
3568.02(5)[a]	0.26(6)	4131.01	563
3675.9(3)	0.63(10)	4784.30	(546), 563, 1108
3735.6(5)[d]	0.20(6)	4298.61	563
3839.5(7)[a]	0.15(7)	3839.50	
3925.3(2)	0.58(9)	4488.27	563
3951.55(9)	7.79(11)	3951.10	
3992.9(2)	0.56(6)	4555.74	563
4008.8(4)[a]	0.29(5)	4571.69	563

[a] Newly observed γ ray.
[b] Newly observed γ ray in agreement with Mukhopadhyay *et al.* [75].
[c] Newly observed γ ray in agreement with Toh *et al.* [108].
[d] γ ray with different placement then reported in previous β-decay study [25].
[†] γ ray which is not used to calculate the β-feeding intensity due to energy tolerance issue.
[*] γ-ray energy and intensity determined from $\gamma\gamma$ coincident data.
[‡] unplaced γ ray.

7.3.1 Level Scheme

First, we placed the 563-keV γ ray de-exciting the level at 563 keV feeding the ground state which is known first excited state from several other measurements [6], then have constructed the decay scheme by placing the rest of the γ rays based on coincidence in-

www.manaraa.com

formation. Table 7.1 contains the list of γ rays assigned to ^{76}Ga β decay with their corresponding intensity, placement and the $\gamma\gamma$-coincidence information. Figure 7.2 (a) and Figure 7.3 (b) are the proposed level schemes of ^{76}Ge populated by β decay of ^{76}Ga. We have placed 100 γ rays in our proposed decay scheme with level energies occupying up to 4.81 MeV. The search for the lowest energy associated with this decay observed 262 keV.

Our proposed decay scheme is in good agreement with previous β-decay study by Camp *et al.* up to 2022 keV, i.e we firmly confirmed the levels at 563, 1108, 1410, 1539, 1911, and 2022 keV. Above this energy level, we have made significant additions and deletions as will be discussed later. Furthermore, we have compared our proposed decay scheme with the recent inelastic neutron scattering measurements by Mukhopadhyay *et al.* [75], Coulomb excitation and inelastic scattering by Toh *et al.* [108] and total absorption spectroscopy measurement by Dombos *et al.* [30].

Additional γ ray of energy 611 keV de-exciting the level at 2022 keV and feeding the level at 1108 keV is observed which was not seen in previous β-decay study [25]. The level at 2692 keV is in agreement with the previous β-decay study except for one γ-ray transition of energy 1584 keV. We identified 1584-keV γ ray in our spectra is a source background. We observed 2279-keV γ ray in probable coincidence with 563-keV γ ray leading its placement de-exciting the level at 2842 keV and represented by the dashed line in the decay scheme. Furthermore, energy levels at 2920 keV, 3313 keV and 3323 keV are further confirmed with an addition of one more γ ray each of energies 1010 keV, 620 keV, and 3322 keV respectively. All these three γ rays reported are newly observed in our measurement. We have removed a γ ray of energy 1924 keV from 3334-keV level as it

www.manaraa.com

sees nothing in coincidences. The energy level at 3478 keV is represented by dashed line in the previous study. We made it solid line as all three γ rays reported before are in strong statistical coincidences in cascade connecting the ground state. Our data agreed on the placement of level at 3622 keV and 3887 keV but removed the 1721-keV and 1613-keV γ rays from the level at 3622 keV. Furthermore, we removed the placement of γ ray of energy 3325 keV from the 3866-keV level. We established the energy level at 3951 keV which has an additional 768-keV γ ray whereas 1260-keV γ ray reported before is not observed. The energy level at 4122 keV is now confirmed with both definite γ rays de-exciting the level. The level at 4238 keV is confirmed by the placement of two γ rays of energies 1545 keV and 2697 keV and represented by a solid line in the decay scheme. Energy levels at 4784 keV and 4813 keV reported by previous β-decay study are also in agreement to our present result, but we removed the 1461-keV and 1892-keV γ rays from 4784-keV and 4813-keV levels respectively. The energy level at 4783 keV and 4812 keV are in agreement with Camp *et al.* and represented by solid lines in the decay scheme although both are proposed by the single γ-ray transition.

7.3.1.1 Description of Newly Proposed Levels

It is always important to confirm or exclude spectroscopic information reported in previous studies. Energy levels and γ rays reported in previous measurements can be removed only if we can prove previous placements of all the γ rays assigned to a level can be conclusively placed elsewhere in the decay scheme. From the present work, based on the statistically significant $\gamma\gamma$ coincidence information, we have been able to propose 24 new

www.manaraa.com

energy levels of which six are in agreement with at least one previous studies other than β decay [6]. Below 3.3 MeV, six of the newly proposed levels are in agreement with recent work by Mukhopadhyay *et al.* from the inelastic neutron scattering measurement [75]. The details of the new levels are presented below.

1. A level at 2407.0 keV is tentatively proposed by placing the 1844.1-keV γ ray feeding the 562.93-keV level. An observed 1844.1-keV γ ray shows probable coincidences with only 563-keV γ ray leading its placement as de-exciting the 2406.99-keV level, which is represented by a dashed line in the decay scheme as it is proposed from the single γ ray with probable coincidence.

2. A level at 2504.72 keV is proposed by placing the 1396.30-keV γ ray which feeds the well-established 1108.44-keV level. The 1396.30-keV γ ray which was not observed in previous β-decay study, shows the definite coincidences with 546-keV γ ray leading its placement as de-exciting the 2504.72-keV level. Although a level at 2504.72 keV is proposed by single γ ray, we have represented it by a solid line in the decay scheme as the establishment of this level agreed with recent inelastic neutron scattering measurement work by Mukhopadhyay *et al* [75] and ^{76}Ge(n, n$'\gamma$) measurement from Dostemesova *et al.* [31].

3. A level at 2668.6 keV is firmly proposed by placing the three γ rays of energies 1129.5, 1258.0 and 1562.91 keV feeding the 1539.47-, 1410.15- and 1108.42-keV levels respectively. An observed 1129.5-keV γ ray shows the probable coincidence with 1108-keV γ ray and definite coincidence with 563-keV γ ray leading its place-

www.manaraa.com

ment as de-exciting the 2668.6-keV level. Furthermore, an observed 1258.0-keV γ ray shows definite coincidences with 847-keV γ ray leading its placement as de-exciting the 2668.6-keV level. In addition, a γ ray of energy 1562.91 keV is observed in probable coincidences with 1108-keV γ ray and tentatively placed in de-exciting the 2668.6-keV level. Consequently, our data suggest that there is a level at 2668.6 keV which is in agreement with Coulomb excitation and inelastic-scattering reactions measurement by Toh *et al* [108]. The γ rays of energies 1130 keV and 1563 keV reported from this level were not observed in any previous measurements.

4. A level at 2986.5 keV is proposed by placing the two γ rays of energies 1577.8 keV and 1878.1 keV which connect the 1410- and 1108-keV levels respectively. We observed a 1577.8-keV γ ray which shows the probable coincidence with 847-keV γ ray and placed it de-exciting the 2986-keV level. A 1577.8-keV γ ray reported by this work was not observed in any previous measurements. Furthermore, an observed 1878.1-keV γ ray shows the definite coincidence with 1108-keV γ ray which leads its placement de-exciting the 2986.5-keV level. Hence, our data suggest that there is a level at 2986.5 keV, which is in agreement with neutron scattering measurement [75].

5. A level at 3021.42 keV is proposed with three γ rays of energies 1482.04, 1611.2 and 1912.96 keV which connects the well-known 1539-, 1410- and 1108-keV levels respectively. We observed a 1482-keV γ ray in definite coincidences with 977-keV γ ray leading its placement as de-exciting the level at 3021 keV. Similarly, the γ rays of

www.manaraa.com

energies 1612 keV and 1912 keV show 848-keV and 1108-keV γ rays respectively in definite coincidences leading their placement as de-exciting the level at 3021 keV. The proposed level at 3021 keV is in agreement inelastic neutron scattering measurement [75].

6. A level at 3147.70 keV is proposed with the two γ rays of energies 1608.23 keV and 2585.84 keV. A 1608-keV γ ray is observed in probable coincidences with 977-keV γ ray leading its placement as de-exciting the level at 3148 keV. Furthermore, a 2583-keV γ ray was observed in definite statistical coincidence with 563-keV γ ray and placed it as de-exciting 3148-keV level. Hence, our data suggest that there is a level at 3148 keV, which is in agreement with inelastic neutron scattering measurement [75].

7. A level at 3190.95 keV is proposed by two γ rays of energies 2082.53 keV and 2630.37 keV feeding the 1108-keV, 563-keV levels respectively. We observed a 2083-keV γ ray in definite coincidence with 1108-keV γ ray leading its placement as de-exciting the 3190-keV level. Furthermore, an observed 2630-keV γ ray shows a definite coincidence with 563-keV γ ray only and placed it as de-exciting the 3191-keV level. The proposed level at 3191 keV which is in agreement with inelastic neutron scattering measurement [75].

8. A level at 3200.15 keV is proposed by the four γ rays of energies 1660.92, 1790.8, 2091.23 and 2636.7 keV feeding the 1539-, 1410-, 1108- and 563-keV level respectively. Two γ rays of energy 1791 keV and 2637 keV we assigned to 3200-keV level

www.manaraa.com

were not observed in any previous β-decay studies. We observed a 1661-keV γ ray in definite coincidences with 431- and 976-keV γ ray which leads its placement as de-exciting the 3200-keV level. Furthermore, an observed 1791-keV γ ray shows a definite coincidence with 848-keV γ ray leading its placement as de-exciting the level at 3200 keV. Besides that, an observed 2091-keV γ ray shows a definite coincidence with 1108-keV γ ray and placed it as de-exciting the 3200-keV level. Additionally, a 2637-keV γ ray was observed in definite coincidence with 563-keV γ ray and placed it as de-exciting the level at 3200 keV. Hence, our data strongly suggest that there is a level at 3200 keV which is in agreement with inelastic neutron scattering measurement [75].

9. A level at 3439.4 keV level is proposed with two γ rays of energies 2876.5 keV and 3440.55 keV feeding the 563-keV level and ground state respectively. Both γ rays were not observed in previous β-decay measurement. We observed a 2877-keV γ ray which shows a definite coincidence only with 563-keV γ ray leading its placement as de-exciting the 3439-keV level. Furthermore, we observed a 3439-keV γ ray which shows nothing in coincidences and tentatively placed de-exciting the 3439-keV level. Thus, our data suggest that there is a level at 3439.4 keV.

10. A level at 3544 keV is proposed by placing the two γ rays of energies 2435.60 keV and 2981.1 keV feeding the 1108-keV and 563-keV levels respectively. We observed a 2435-keV γ ray in definite coincidences with 545- and 1109-keV γ ray leading its placement as de-exciting the 3544-keV level. Furthermore, an observed 2981-keV γ

www.manaraa.com

ray shows a definite coincidence with only 563-keV γ ray leading its placement as de-exciting the 3544-keV level. Consequently, our data support that there is a level at 2435.6 keV.

11. A level at 3597.1 keV is proposed by placing the single γ ray of energy 2186.9 keV which feeds the 1410-keV level in the decay scheme. We observed a 2187-keV γ ray in definite coincidences with 847-keV γ ray leading its placement as de-exciting the 3597-keV level. This energy level is represented by the dashed line in the decay scheme as it was populated by a single γ-ray transition.

12. A level at 3890.99 keV is proposed by placing the three γ rays of energies 2351.32, 2782.58 and 3327.7 keV feeding the 1539-, 1410-, 563-keV levels respectively. We observed a 2351-keV γ ray in definite coincidence with 977-keV γ ray leading its placement as de-exciting the 3891-keV level. A 2351-keV γ ray we reported for this level was not observed by any other previous measurements. Furthermore, a 2783-keV γ ray was observed in definite coincidences with 545- and 1109-keV γ ray and placed it de-exciting the 3891-keV level. Besides that, a 3328-keV γ ray shows a definite coincidence with only 563-keV γ ray leading its placement as de-exciting the 3891-keV level. Consequently, our data firmly suggest that there is a level at 3891 keV.

13. A level at 3900.5 keV is proposed from a single γ-ray transition of energy 3337.6 keV feeding the 563-keV level. We observed a 3338-keV γ ray in definite coincidence with 563-keV γ ray leading its placement as de-exciting the 3901-keV level.

www.manaraa.com

The 3336-keV γ ray is newly observed from our measurement, and the proposed level is represented by the dashed line.

14. A level at 3930.5 keV is proposed by placing a single γ ray of energy 3367.6 keV feeding the 563-keV level. we observed a 3368-keV γ ray in probable coincidences with 563-keV γ ray only, leading its placement as de-exciting the 3931-keV level. Hence, the 3930.50-keV level is represented by a dashed line in the decay scheme.

15. A level at 3977.2 keV is proposed by placing two γ rays of energies 2868.8 keV and 3413.22 keV feeding the 1108-keV and 563-keV levels respectively. The 3413-keV γ ray is newly observed in this measurement. We observed a 2869-keV γ ray in definite coincidences with 1108-keV γ ray leading its placement as de-exciting the 3976-keV level. Furthermore, a 3413-keV γ ray is observed in definite coincidences with 563-keV γ ray and placed it de-exciting the 3976-keV level. Thus, our data suggest that there is a level at 3977.2 keV.

16. A level at 4045.6 keV is proposed by placing a single γ ray of energy 3482.6 keV feeding the 563-keV level. We observed a 3483-keV γ ray which shows definite coincidence with 563-keV γ ray only leading its placement as de-exciting the 4046-keV level. The 3483-keV γ ray is newly identified to the β-decay study, and the proposed level is represented by a dashed line in the decay scheme.

17. A level at 4131.01 keV is proposed by placing the two γ rays of energies 2591.6 keV and 3568.02 keV feeding the 1539-, and 563-keV levels respectively. We observed a 2592-keV γ ray which is in definite coincidences with 431- and 977-keV γ rays

www.manaraa.com

leading its placement de-exciting the 4130-keV level. Furthermore, an observed 3568-keV γ ray shows the definite coincidences with 563-keV γ ray only leading its placement de-exiting the 4131-keV level. A 3568-keV γ ray is newly observed associated to this decay element. Hence, our data suggest that there is a level at 4131.01 keV.

18. A level at 4298.6 keV is proposed by placing the two γ rays of energies 3190.2 keV and 3735.6 keV feeding the 1108- and 563-keV levels respectively. We observed a 3190-keV γ ray in definite coincidence with 1109-keV γ ray and placed it as de-exciting the 4299-keV level. Furthermore, an observed 3736-keV γ ray shows the definite coincidences with 563-keV γ ray only leading its placement as de-exciting the 4299-keV level. Consequently, our data suggest that there is a level at 1298.6 keV.

19. A level at 4382.47 keV is proposed by placing the two γ rays of energies 2843.0 keV and 3275.6 keV feeding the 1539-, 1108-keV levels respectively. We observed a 2843-keV γ ray which shows the definite coincidences with 545- and 1108-keV γ rays leading its placement as de-exciting the 4328-keV level. Besides that, an observed 3276-keV γ ray shows a definite coincidence with 1108-keV γ ray leading its placement as de-exciting the 4382-keV level. The 2845-keV γ ray reported here is newly observed from our measurement.

20. A level at 4444.15 keV is proposed by placing three γ rays of energies 1601.6, 3034.11 and 3337.6 keV feeding the 2841-, 1410- and 1108-keV levels respectively.

www.manaraa.com

We observed a 1601-keV γ ray in probable coincidences with 1733-keV γ ray and tentatively placed it as de-exciting the 4444-keV level. Furthermore, we observed a 3034-keV γ ray in definite coincidences with 847-keV γ ray leading its placement as de-exciting the 4444-keV level. The 160-keV γ ray reported for this level is a newly observed in our present study. Additionally, we observed 3338-keV γ ray which shows probable coincidences with 546-keV γ ray and tentatively placed as de-exciting the 4444-keV level. Hence, our data suggest that there is a level at 4444.15 keV.

21. A level at 4488.3 keV is proposed by placing the γ ray of energy 3925.3 keV which feeds the well-known 563-keV level. We observed a 3925-keV γ ray in definite coincidence with 563-keV γ ray only, leading its placement as de-exciting the 4488.3-keV level.

22. A level at 4548.97 keV is proposed by placing the γ ray of energy 3440.55 keV feeding the level at 1108-keV. In this measurement, we observed that 3441-keV γ ray in definite coincidence with 545-keV γ ray leading its placement as de-exciting the 4549-keV level. The 3441-keV γ ray is newly observed from this measurement, and the level is represented by a dashed line in the decay scheme.

23. A level at 4555.75 keV is proposed by placing a γ ray of energy 3145.5 keV which connects the 1410-keV level. We observed the 3146-keV γ ray in definite coincidence with 847-keV γ ray leading its placement as de-exciting the 4556-keV level. The level 4555.75 keV is represented by a solid line in the decay scheme.

www.manaraa.com

24. Finally, a level at 4571.7 keV is proposed by placing the γ ray of energy 4008.8 keV feeding the 563-keV level. An observed 4009-keV γ ray shows the definite coincidence with 563-keV γ ray leading its placement as de-exciting the 4571-keV level. The 4009-keV γ ray reported in this study were not observed by any previous measurements.

7.3.1.2 Previously Reported Energy Levels not Observed in Current Study

From our high-efficiency, high-resolution β-decay study, our coincidence data do not observe any evidence for 19 energy levels reported by Camp *et al*, of which 9 of them were firmly proposed whereas 10 were mentioned as uncertain [25]. An explanation for each deletion is given in the following paragraph.

(i) An energy level at 2284.2 keV was proposed by placing the 1175.7-keV γ ray ($I_\gamma = 0.71(18)$) feeding the 1108.45-keV level [25] in Camp *et al.* In the present work, we observed a γ-ray peak near 1176-keV energy, but from the β-gated spectra, we identified it as a source background. Camp *et al.* reported three more 2435.6-keV ($I_\gamma = 0.56(7)$), 3465.5-keV($I_\gamma = 0.21(4)$) and 3736.9 -keV ($I_\gamma = 0.24(6)$) γ-ray feeding into the level at 2284.2 keV. A 2435.43-keV γ ray is observed in definite coincidences with 545- and 1109-keV γ ray and not the 1176-keV γ ray leading its placement as de-exciting the 3544-keV level. Furthermore, we observed a 3465-keV γ ray ($I_\gamma = 0.21(4)$) but sees nothing in coincidences and has not placed it on the decay scheme. Besides that, a 3736-keV γ ray ($I_\gamma = 0.20(6)$) is observed in definite coincidence with 563-keV γ ray leading its placement as de-exciting the 4299-keV

www.manaraa.com

level. Consequently, our data suggest that there is no level at 2284.2 keV, which is in agreement with inelastic neutron scattering measurement [75] and Coulomb excitation and inelastic-scattering reactions measurement [108].

(ii) A level at 2591.1 keV is proposed by placing the three γ rays of energies 1051.7 ($I_\gamma = 0.71(10)$), 1482.5 ($I_\gamma = 0.75(11)$) and 2591.0 keV ($I_\gamma = 0.41(7)$) feeding the 1539.46-keV, 1108.45-keV levels and the ground state respectively in previous Camp *et al.* study [25]. We observed a weak γ-ray peak of energy 1052 keV which sees nothing in coincidence and has not placed in the decay scheme. A 1482.0-keV γ ray ($I_\gamma = 0.53(6)$) was observed in definite coincidences with 976.4-keV γ ray leading its placement as de-exciting the 1539.47-keV level. Furthermore, a 2591.6-keV γ ray ($I_\gamma = 0.42(7)$) was observed in definite coincidences with 431-keV and 977-keV γ rays leading to its placement as de-exciting the 4131.01-keV level. Hence, our data do not support the existence of level at 2591.1 keV which is in agreement with recent inelastic neutron scattering measurement [75].

(iii) A level at 2654.6 keV was proposed by placing the two γ rays of energies 1546.0 keV ($I_\gamma = 0.65(13)$) and 2091.0 keV ($I_\gamma = 0.27(6)$) feeding the 1108-keV and 563-keV levels respectively by Camp *et al* [25]. In the present work, we observed a 1545.4-keV γ ray ($I_\gamma = 1.19(7)$) which is in definite coincidence with 2129-keV γ ray leading its placement as de-exciting the 4237.77-keV level. Furthermore, a 2091.23-keV γ ray ($I_\gamma = 1.84(10)$) was observed in definite coincidences with 1108-keV γ rays leading its placement as de-exciting the 3200.15-keV level. From this work,

www.manaraa.com

both γ rays are placed to higher energy levels in the decay scheme. Hence, our data do not support the existence of the level at 2654.6 keV. Rejection of this energy level is in agreement with recent inelastic neutron scattering measurement [75].

(iv) A level at 2768.76 keV was proposed by placing the two γ-ray transitions of energies 1358.9 keV ($I_\gamma = 0.28(9)$) and 1660.30 keV ($I_\gamma = 1.17(8)$) feeding the 1410.08- and 1108.45-keV levels respectively in previous study [25]. We do not observe 1359-keV γ ray in our γ-singles spectrum. Furthermore, a 1660.92-keV γ ray ($I_\gamma = 1.64(7)$) was observed in definite coincidences with 431- and 976-keV γ rays leading its placement as de-exciting the 3200.15-keV level. Consequently, our data do not support that there is a level at 2768.76 keV, which is in agreement with recent inelastic neutron scattering measurement [75].

(v) A level at 3231.8 keV was reported by a single γ-ray transition of energy 2668.8 keV ($I_\gamma = 0.24(5)$) feeding the 563-keV level and was kept question mark on previous β-decay study [25]. In the present work, we observed a very weak 2668.28-keV γ ray which shows nothing in coincidence. Hence, our data do not support the existence of the level at 3231.8 keV.

(vi) A level at 3409.2 keV was proposed by placing the single γ-rays transition of energy 661 keV ($I_\gamma = 1.12(10)$) feeding the 2727.76-keV level. Also, a 1310.6-keV γ ray ($I_\gamma = 0.40(7)$) feeds in the 3409.2-keV level [25]. In the present work, we observed a very weak 661-keV γ ray but identified associated with ^{76}Zn decay. Furthermore,

www.manaraa.com

we didn't observe a 1310.6-keV γ ray in our γ-singles spectrum. Hence, our data do not support that there is a level at 3409.2 keV.

(vii) A level at 4192.9 keV was proposed by placing the γ rays of energies 1273.1 ($I_\gamma = 1.82(11)$) and 2782.7 keV ($I_\gamma = 1.53(12)$) feeding the 2919.99- and 1410.08-keV levels respectively in previous study [25]. This level was noted uncertain too. In this present study, we don't observe a 1273.1-keV γ ray. A 2782.56-keV γ ray ($I_\gamma = 1.62(8)$) was observed which shows definite coincidences with 545- and 1108-keV γ rays and not the 847-keV γ ray, leading its placement as de-exciting the level at 3890.99 keV. Hence, our data do not support the existence of level at 4192.9 keV.

(viii) A level at 4326.5 keV was proposed by placing the γ rays of energies 1014.2 keV ($I_\gamma = 0.54(8)$) and 1634.0 keV ($I_\gamma = 0.23(6)$) feeding the 3312.33- and 2692.4-keV levels respectively from previous work [25]. This level was also mentioned uncertain. In the present work, We do not observe 1014-keV γ ray whereas 1636-keV γ ray ($I_\gamma = 0.21(6)$) was observed but sees nothing in coincidence. So, we don't have evidence to place it at 4227-keV level. Consequently, our data do not support that there is a level at 4226.5 keV.

(ix) A level at 4363.5 keV was proposed by placing the two γ rays of energies 885.8 keV ($I_\gamma = 2.00(15)$) and 1443.9 keV ($I_\gamma = 0.39(10)$) feeding the 3477.65- and 2919.99-keV levels respectively. This level was mentioned uncertain too [25]. We identified 885.8-keV γ ray is more likely associated with ^{76}Cu while do not observe

www.manaraa.com

1443.9-keV γ ray in our spectra. Hence, our data do not support the level at 1463.5 keV.

(x) A level at 4476.5 keV was proposed by placing the two γ rays of energies 843.8 keV ($I_\gamma = 1.73(17)$) and 3913.3 keV ($I_\gamma = 0.19(4)$) feeding the 3632.75- and 562.93-keV levels respectively. This level was also mentioned uncertain [25]. We didn't observe 843.8-keV γ ray in our decay spectra, observed weak 3919-keV γ-ray peak but sees nothing in coincidence and have no evidence to place it as de-exciting the 4476.5-keV level. Consequently, our data do not support the existence of level at 4476.5 keV.

(xi) A level at 4719.9 keV was firmly proposed in previous β-decay study by placing the three γ rays of energies 1310.6 keV ($I_\gamma = 0.42(7)$), 1878.3 keV ($I_\gamma = 0.55(6)$) and 2435.6 keV ($I_\gamma = 0.56(7)$) feeding the 3909.19-, 2841.57- and 2284.22-keV levels respectively [25]. In the present work, We observed a 1310-keV γ ray ($I_\gamma = 0.18(5)$) but shows nothing in coincidences and do not have evidence to place it at 4719.9-keV level. Furthermore, an observed 1878.05-keV γ ray ($I_\gamma = 0.53(8)$) shows definite coincidences with 1108-keV γ ray and placed it de-exciting the 2986.47-keV level. Besides that, we observed a 2435.59-keV γ ray ($I_\gamma = 0.35(6)$) which shows definite coincidence with 545-and 1108-keV γ rays leading its placement as de-exciting the 3544.01-keV level. Hence, our data support that there is no level at 4719.9 keV.

(xii) A level at 4814.8 keV was proposed by placing the two γ rays of energies 1182.1 keV ($I_\gamma = 0.77(11)$) feeding the 3632.72-keV level and 1502.3 keV ($I_\gamma = 0.74(10)$)

www.manaraa.com

feeding the 3312.33-keV level. This level was also mentioned mentioned uncertain by previous study [25]. In the present work, We observed both 1181-keV ($I_\gamma = 0.26(7)$) and 1502-keV ($I_\gamma = 0.30(5)$) γ rays but both of them see nothing in coincidences. Hence, we have no evidence to place them in the 4814.8-keV level.

(xiii) A level at 5122.48 keV was firmly proposed by placing the three γ rays of energies 1489.6 keV ($I_\gamma = 0.35(10)$), 1940.3 keV ($I_\gamma = 1.04(7)$) and 1980.4 keV ($I_\gamma = 0.33(6)$) feeding the 3632.75-, 3182.21- and 3141.51-keV levels respectively by previous work [25]. In the present work, we do not observe 1940-keV γ ray, observed the 1489-keV γ ray but identified as associated with ^{76}Cu, i.e. we do not observe the actual γ ray reported before. Furthermore, a weak 1981-keV γ ray was observed in singles spectra which shows 545-keV peak only in probable coincidences but do not have enough statistics to place in decay scheme. Consequently, our data do not suggest that there is a level at 5122.48 keV.

(xiv) A level at 5522.6 keV was proposed by placing the three γ rays of energies 1282.9 keV ($I_\gamma = 0.43(11)$), 2680.9 keV ($I_\gamma = 0.49(5)$) and 2868.1 keV ($I_\gamma = 0.53(7)$) feeding the 4239.4-, 2841.57- and 2654.51-keV levels respectively in previous study [25]. From the present work, we observed a 1281-keV γ ray ($I_\gamma = 1.16(5)$) which shows definite coincidences with 847-keV γ ray leading its placement as de-exciting the 2692.36-keV level. Furthermore, an observed 2681.8-keV γ ray ($I_\gamma = 0.21(5)$) shows probable coincidences with 563-keV γ rays and tentatively placed it as de-

www.manaraa.com

exciting the 3244.72-keV level. Besides that, a 2868.8-keV γ ray ($I_\gamma = 0.58(6)$) was observed in definite coincidences with 1108-keV γ rays and not any of the γ rays de-exciting the 2654-keV level leading its placement at 3977.20-keV level. Consequently, our data do not suggest that there is a level at 5522.6 keV.

(xv) A level at 5663.37 keV was proposed by placing the four γ rays of energies 2481.1 keV ($I_\gamma = 0.30(6)$), 2970.1 keV ($I_\gamma = 0.60(7)$), 3752.1 keV ($I_\gamma = 0.25(5)$) and 4253.2 keV ($I_\gamma = 0.34(5)$) feeding the 3182.21-, 2692.40-, 1911.09- and 1410.08-keV levels respectively [25]. In the present work, we did not observe 2481-, 2970- and 4253-keV γ rays in our singles spectra, whereas 3752-keV γ peak is identified as a single escape peak of 4263-keV γ ray. Hence, our data do not support the existence of the level at 5663.37 keV.

(xvi) A level at 5749.9 keV was proposed by placing the two γ rays of energies 2981.2 keV ($I_\gamma = 0.31(6)$) and 3465.2 keV ($I_\gamma = 0.21(4)$) feeding the 2768.76- and 2884.22-keV levels respectively in previous study [25], and mentioned this level uncertain. In the present measurement, we observed a 2981.07-keV γ ray ($I_\gamma = 0.12(5)$) which shows definite coincidences with 563-keV γ ray but not the any γ ray de-exciting the 2768.76-keV level, leading its placement to the 3544.01-keV level. Furthermore, an observed 3465-keV γ ray ($I_\gamma = 0.24(5)$) sees nothing in coincidence and has not placed in the decay scheme. Hence, our data do not support the existence of the level at 5749.9 keV.

www.manaraa.com

(xvii) A level at 5882.8 keV was proposed by placing the two γ rays of energies 2700.5 keV ($I_\gamma = 0.30(5)$), and 3190.6 keV ($I_\gamma = 0.32(4)$) feeding the 3182.21- and 2692.40-keV levels respectively and mentioned uncertain in previous study [25]. In the present work, we identified the 2700-keV γ ray associated with ^{76}Cu but not the ^{76}Ga. Furthermore, an observed 3190-keV γ ray ($I_\gamma = 0.43(8)$) shows definite coincidences with 1109-keV γ ray but not any of the γ rays de-exciting the 2692.40-keV level, leading its placement as de-exciting the 4298.61-keV level. Consequently, our data do not support that there is a level at 5883.0 keV.

(xviii) A level at 6021.1 keV was reported by placing the two γ rays of energies 3328.7 keV ($I_\gamma = 0.30(9)$) and 3366.5 keV ($I_\gamma = 0.22(3)$) feeding the 2692.40- and 2654.51-keV levels respectively in previous study [25]. In the present work, we didn't observe 3328-keV γ ray, whereas 3366-keV γ ray ($I_\gamma = 0.20(5)$) was observed in probable coincidences with 563-keV γ ray leading its placement as de-exciting the 3930.50-keV level. Hence, our data do not support that there is a level at 6021.1 keV.

(xix) A level at 6065.2 keV is proposed by placing the two γ rays of energies 2882.9 keV ($I_\gamma = 0.21(7)$) and 3145.3 keV ($I_\gamma = 0.45(9)$) feeding the 3182.21- and 2919.99-keV levels respectively from previous work [25]. This is the highest energy level proposed from previous β-decay measurement. We didn't observe 2883-keV γ ray in our decay spectra whereas 3145.5-keV γ ray ($I_\gamma = 0.33(7)$) was observed in definite coincidence with 847-keV γ ray and not any of the γ ray de-exciting the 2919.99-

www.manaraa.com

keV level, leading its placement as de-exciting the 4555.74-keV level. Consequently, our data do not suggest that there is a level at 6065.2 keV.

The previous β-decay study [25] has reported the ^{76}Ga-decay scheme up to 6065 keV, but our data do not support the placement of levels except above 4813 keV. Furthermore, we identified 8 γ rays which have strong coincidence information, matched in previously reported energy levels but needs energy tolerance more than 1.25 keV. These γ rays are placed in decay scheme but has not used for β-feeding intensity calculation which are listed in the table 7.1 marked with † symbol. Also, 9 γ rays which are identified associated with this ^{76}Ga decay but do not have enough coincidence information are unplaced in the decay scheme and reported Table 7.1 with symbol ‡.

www.manaraa.com

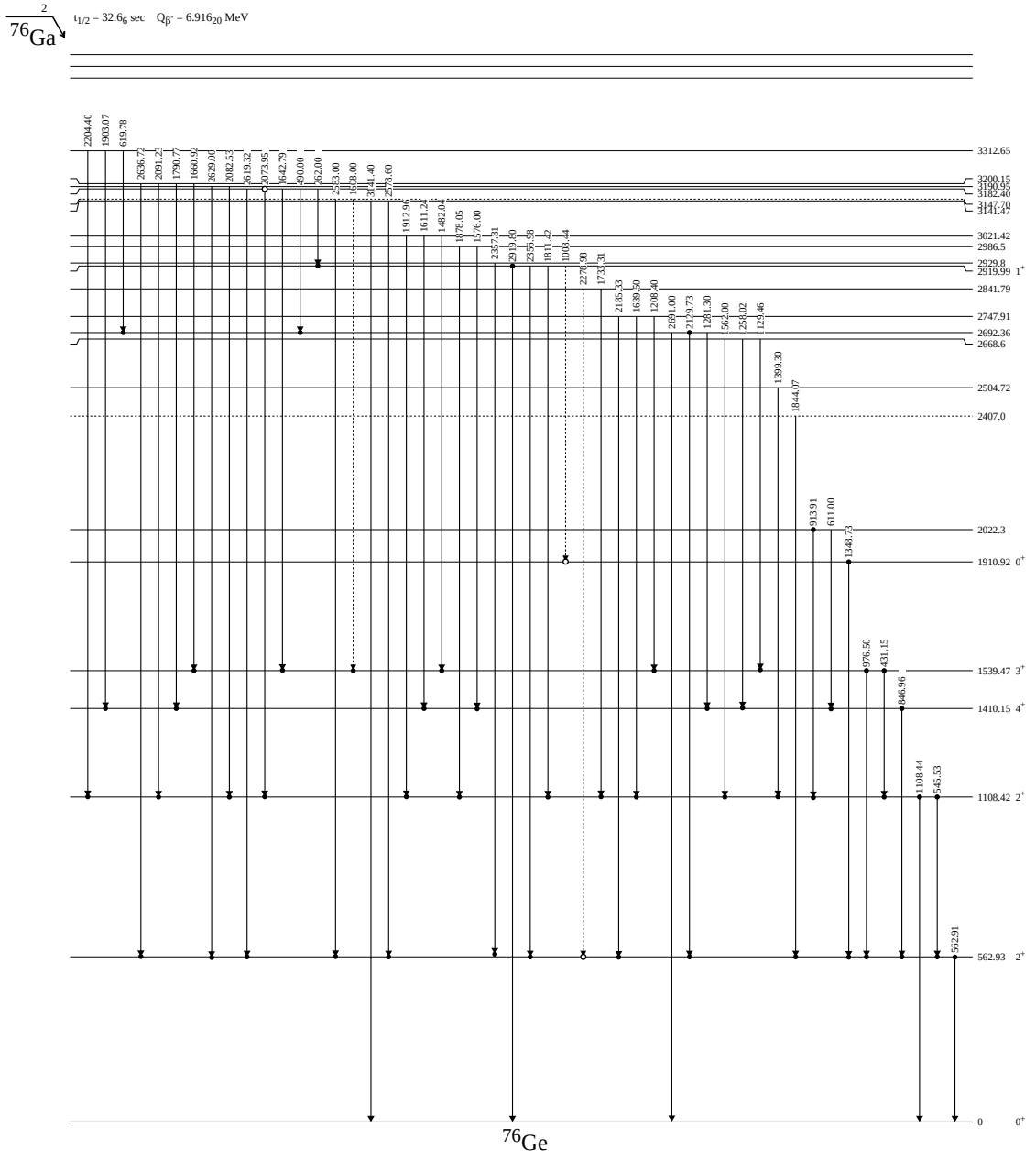

Figure 7.2: Part (a) of the proposed decay scheme for ^{76}Ga to excited states in ^{76}Ge showing low-energy transitions.

www.manaraa.com

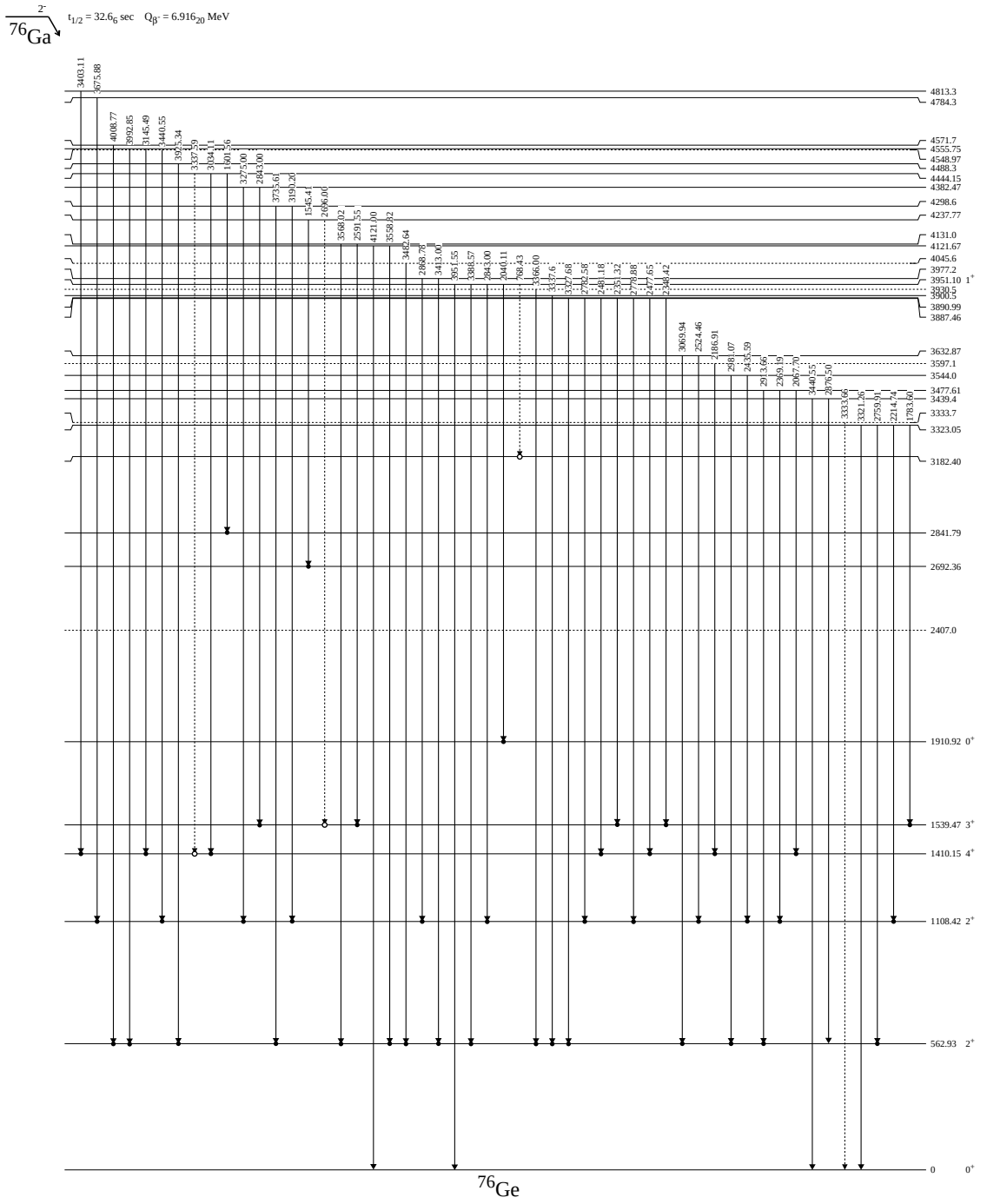

Figure 7.3: Part (b) of the proposed decay scheme for ^{76}Ga to excited states in ^{76}Ge showing high-energy transitions.

www.manaraa.com

Table 7.2: Feeding intensities ($I_{\beta-}$), lower limit $\log(ft)$ and assigned spin-parity value for ^{76}Ga β decay. The β-feeding value are given per 100 decays.

Energy Level	$\mathbf{I}_{\beta-}$	$\log(ft)$	**Spin-parity from NNDC**
0.00(0)	-	-	0^+
562.93(2)	9.6(5)	7.05	2^+
1108.42(2)	7.5(3)	6.98	2^+
1410.15(4)°	0	10.75	4^+
1539.47(3)°	0	10.70	3^+
1910.92(6)°	0	10.56	0^+
2022.3(4)	0.20(5)	8.22	4^+
2407.0(4)[a]	0.18(4)	8.10	
2504.72(15)[b]	0.40(4)	7.71	2^+
2668.6(2)[b,d]	0.43(7)	8.57	4^+
2692.36(4)	1.16(11)	7.17	3^+
2747.91(3)	8.26(11)	6.29	2^+
2841.79(9)	0.77(9)	7.28	2^+
2919.99(4)[a]	13.26(13)	6.00	$(1,2)^+$
2929.8(2)	0.49(7)	7.43	
2986.5(3)[b]	0.35(5)	7.55	$(2,3)^+$
3021.42(8)[b]	1.41(12)	6.93	$(2,3)^+$
3141.47(5)	6.24(31)	6.22	1^+
3147.70(19)	0.45(5)	7.36	$(2,3)^+$
3182.40(3)	7.98(13)	6.01	2^+
3190.95(18)[b]	0.17(6)	7.76	2^+
3200.15(6)[b]	2.70(11)	6.56	$(3)^+$
3312.65(5)	4.72(12)	6.25	3^-
3323.05(5)	4.48(12)	6.27	$2^+,3,4^+$
3333.7(12)	0.08(8)	8.00	$(2)^+$
3439.4(4)[a]	0.49(12)	7.17	
3477.61(10)	2.80(14)	6.39	1-4
3544.0(2)[a]	0.33(6)	7.28	2^+
3597.1(5)[a]	0.26(10)	7.36	
3632.87(7)	1.98(7)	6.45	$(2)^+$
3887.46(9)	1.81(9)	6.34	(3^-)
3890.99(7)[a]	2.71(10)	6.16	
3900.5(4)[a]	0.12(4)	7.51	
3930.5(5)[a]	0.20(5)	7.27	
3951.10(5)	8.99(13)	5.61	$1^- or 2^-$
3977.2(2)[a]	0.38(4)	6.96	
4045.6(3)[a]	0.42(5)	6.87	

Continued on next page

www.manaraa.com

Table 7.2 – continued from previous page

Energy Level	$\mathbf{I}_{\beta^-}$	log (ft)	**spin-parity**
4121.67(16)	0.87(6)	6.51	$(1, 2^+)$
4131.0(2)[a]	0.46(6)	6.78	
4237.77(9)	0.83(5)	6.45	
4298.6(2)[a]	0.41(6)	6.71	
4382.47(13)[a]	1.70(13)	6.04	
4444.15(12)[a]	0.91(7)	6.26	(3^-)
4488.3(2)[a]	0.37(6)	6.62	
4548.97(10)[a]	2.33(6)	5.76	
4555.75(19)[a]	0.58(6)	6.37	
4571.7(4)[a]	0.19(3)	6.85	
4784.3(3)	0.42(6)	6.33	1-4
4813.3(4)	0.15(4)	6.75	

[a] New energy level.
[b] New energy level agreed with Mukhopadhyay *et al.* [75].
[d] New energy level agreed with Dombos *et al.* [30].
°Feeding to this level was consistent with zero.

7.3.2 β-Feeding and Log(ft) Values

Figure 7.4 shows the β-feeding profile comparison of our result with previous two measurements by Camp *et al.* [25] and Dombos *et al.* [30]), which clearly shows that there is β-feeding shift to higher energy levels in our measurement specially between 2.5 to 4.5 MeV. This is due to the understanding of coincidence information and their statistically confident placements in the decay scheme. The β-feeding intensity of first excited state is observed to be 9.63% which is less than previously reported 14.4% value by Camp *et al.* [25], and greater than 7.3% reported by Dombos *et al.* [30]. We observed slightly lower feeding to 1108-keV level (Camp: 10.2%, Dombos: 11.7% and our: 7.53%). Furthermore, in the present study, almost no feeding to 1410-keV level is observed which is in good agreements with Camp *et al.* as well as Dombos *et al*. Camp *et al.* reported 10.5% β-

www.manaraa.com

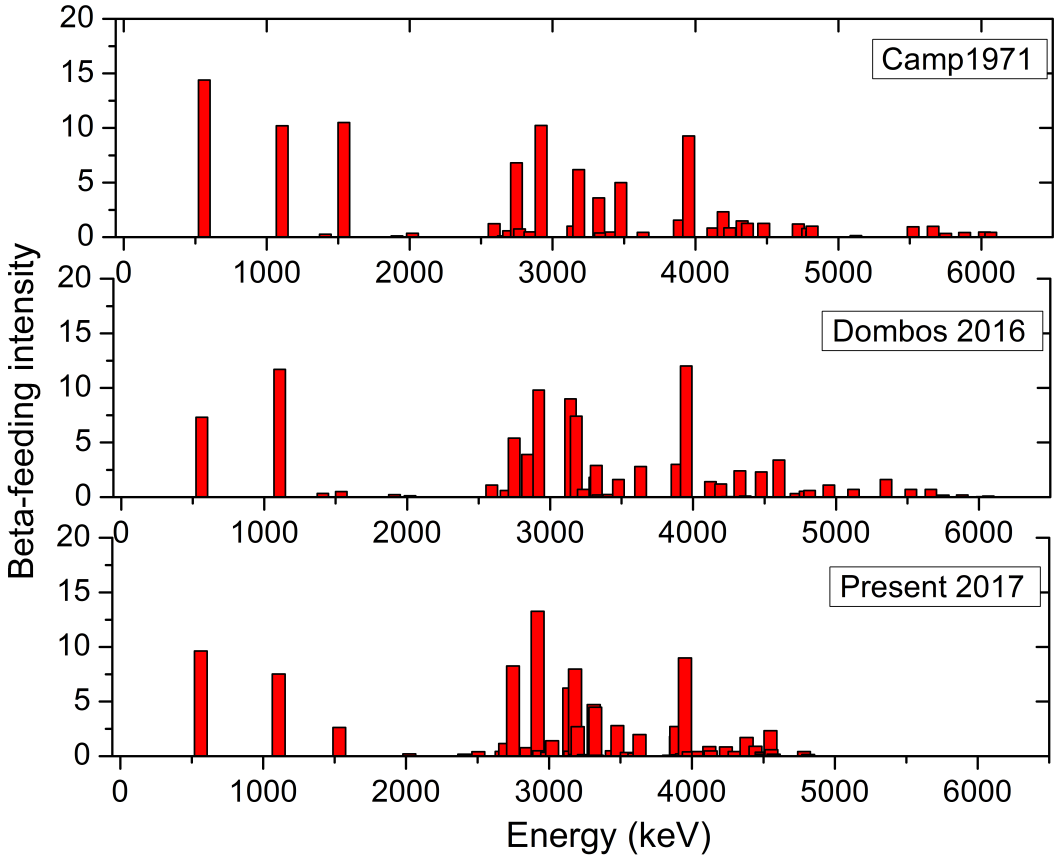

Figure 7.4: Theβ-feeding profile for ^{76}Ga β decay.

feeding to the level at 1539 keV, but we observed no feeding to this level which is in agreement with Dombos *et al.* TAS measurement. The level at 2747 and 2920 keV are observed with significantly more feeding then reported before (level 2747 keV: Camp - 6.81%, Domobs - 5.4%, present - 8.26%, level 2920 keV: Camp-10.26%, Dombos - 9.80% and present - 13.3%). The energy level at 3141 keV is reported with 1.0% β-feeding value by Camp *et al.*, but our measurement observed to be much lager feeding to this level (6.2%) which is in close agreement with Dombos *et al.* (9.8%). We observed most of the energy

www.manaraa.com

level above 3 MeV has similar β-feeding including 3951 keV (Camp - 9.70%, present - 8.99%).

We have calculated the llog (ft) [7] value for each level using the Q_{β^-} of parent ^{76}Ga - 6916.2(20) keV [112] and half-life - 32.6(6) s [6] which is listed in the Table 7.2.

7.3.3 Spin-Parity Assignment and Nushellx Result

From the level systematics of Ga nuclei, the spin-parity of the ground state of ^{76}Ga was assumed to be 3^- in the work by Camp et al. The recent work by Mane *et al.* [68] measured it to be 2^- from laser spectrsocopy. From spin-parity considerations the first two excited states should be feed by first forbidden transitions (ΔJ = 0, $\Delta\pi$ = -1). The previous measurements estabelish the first two states as 2^+ and $\log(ft)$ values we obtained are in consistent with this fact. For the 4_1^+ energy level at 1410 keV, the observed feeding is consistent with zero is also consistent with a frist frobidden unique transition(ΔJ = +2, $\Delta\pi$ = -1). Our $\log(ft)$ value support to assign 0^+ spin-parity to 1910-keV level which are in agreements with previous work [25, 75] where as 1^+ to 2920-keV and 3951-keV levels.

Further, we have calculated the theoretical prediction of ^{76}Ge states from the Nushellx@MSU [23] codes using $JJ44$ interaction and $JUN45$ model space. The obtained result is shown in Fig. 7.5. Our experimental measurement is in agreement to the theoretical value except for low energy states which are slightly stretch up by few hundred keV. Below 2 MeV, Nushellx predicts the six energy levels (0^+ and 2^+ two each, 3^+ and 4^+ one each) which is in agreement with our experimental results. It is observed that there are no negative

www.manaraa.com

Table 7.3: List of γ rays reported by previous β-decay measurement [25] which is not observed or have no coincidence information to place them in the decay scheme from the present work.

Camp *et al.*		Present work		
Energy (keV)	Intensity	Energy (keV)	Intensity	Comments
335.9(5)	8.0(20)	-	-	Not observed
661.4(2)	1.12(10)	-	-	”
843.8(2)	1.73(17)	-	-	”
885.83(10)	2(15)	885.45(23)	0.27(5)	Sees nothing in coincidences
927.05(10)	1.40(8)	927.58(20)	0.27(4)	Belongs with other decay members
1014.2(2)	0.54(8)	1014.21(39)	0.15(5)	Sees nothing in coincidences
1043.6(4)	0.45(4)	1043.87(14)	0.46(5)	”
1051.7(2)	0.71(1)	-	-	Not observed
1182.1(3)	0.77(1.1)	1181.08(45)	0.26(7)	Sees nothing in coincidences
1249.1(2)	0.97(1)	1248.05(15)	0.51(6)	”
1273.1(1)	1.82(11)	-	-	Not observed
1310.6(3)	0.42(7)	1310.05(36)	0.18(5)	”
1358.9(6)	0.28(9)	-	-	Not observed
1443.9(5)	0.39(1)	1442.82(85)	0.77(5)	Sees nothing in coincidences
1461.2(3)	0.50(1)	-	-	Not observed
1502.3(5)	0.74(1)	1502.49(22)	0.3(49)	Sees nothing in coincidences
1582.5(3)	0.75(11)	1581.17(34)	0.28(6)	”
1634(2)	1.73(8)	1636.6(5)	0.21(6)	Sees nothing in coincidences
1721.9(7)	0.22(7)	1722.46(79)	0.13(7)	Sees nothing in coincidences
1892.7(2)	0.61(4)	1891.90(69)	0.12(5)	”
1924.6(3)	0.3(4)	-	-	Not observed
1940.30(14)	1.04(7)	-	-	”
2489.6(4)	0.3(6)	-	-	”
2668.8(4)	()	0.24(5)	-	”
2882.9(9)	0.21(7)	-	-	”
3283.6(5)	0.26(6)	3283.70(129)	0.06(5)	Sees nothing in coincidences
3465.5(4)	0.21(4)	3464.28(47)	0.24(5)	”
3752.1(5)	0.25(5)	3752.90(21)	0.65(6)	”
3913.3(5)	0.19(4)	-	-	Not observed
4253.3(5)	0.34(5)	4251.50(32)	0.28(5)	Sees nothing in coincidences
Total (I_γ)	28.3(4)	Total (I_γ)	4.9(5)	

www.manaraa.com

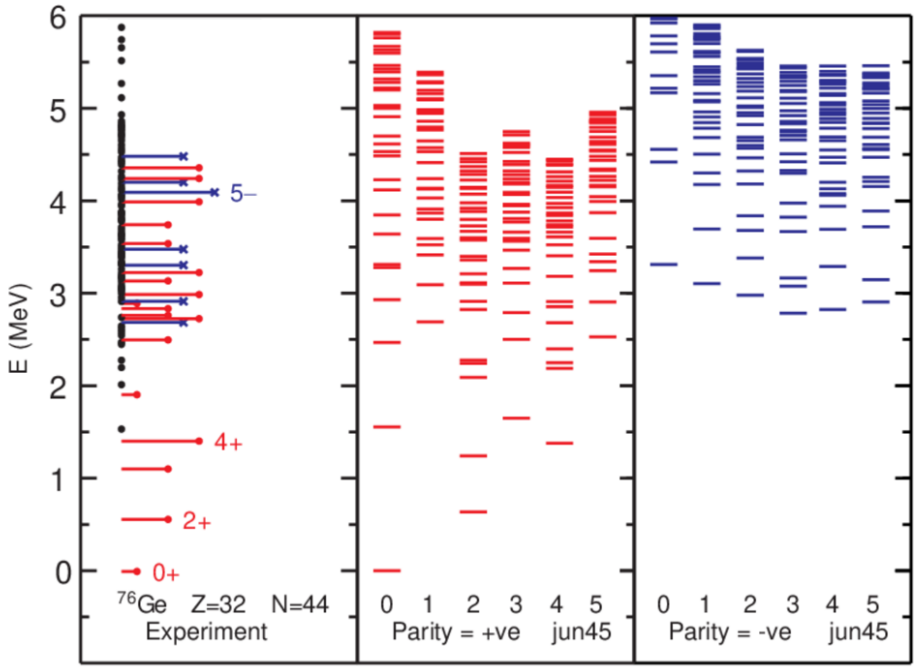

Figure 7.5: Nushellx prediction of structure of ^{76}Ge.

parity states below 3 MeV which is surprising. Also, it clearly matches both results for populating very dense states in between 3.0 to 4.5-keV range.

7.4 Discussion and Conclusion

From this high-resolution, high efficiency β-decay study of ^{76}Ga, we have been able to construct a more comprehensive and accurate decay scheme based on statistically significant $\gamma\gamma$ coincidences. We identified 109 γ rays associated with this decay and were able to place 100 γ ray into the decay scheme thus establishing 49 energy levels up to 4.812 MeV. We have observed 34 new γ rays and 24 new energy levels which were not reported in the previous β-decay measurement. We observed no evidence for 19 energy levels reported in the first β-decay study by Camp *et al.* but in agreement with more re-

www.manaraa.com

cent work [75, 108]. Out of the 107 γ rays reported by Camp *et al.*, we did not observe 30 of them (they were either very weak, not seen in the spectrum as they are beyond our detection limit, or identified as source background or escape peak, or observed but shows no coincidence information and couldn't confirm their association to ^{76}Ga decay) and are listed in the Table 7.3. Also, we found eight of the γ rays have other components as well. Form the coincidence information, we divided the intensity and assign the proper intensity to each γ rays.

From the Q_{β^-} value, we would expect there to exist energy levels up to 6 MeV as reported by Camp *et al.*, but our coincidence information doesn't allow us to place energy levels above 4.8 MeV. Our measured β-feeding profile is in close agreement with recent TAS measurement by Dombos *et al* except near 3 MeV where we have significantly more feeding. Although it looks our decay spectrum is slightly squeezed, as it is not constructed on the guess or tentative placement method, we assume we have correct understanding of ^{76}Ge structure. A total absorption spectroscopy (TAGS) study of ^{76}Ga β decay by Dombos *et al.* [30] used the previously reported decay scheme [25] which likely includes incorrect information to generate a simulation for comparison to their spectrum, and our work suggests need to revisit that calculations.

www.manaraa.com

CHAPTER VIII

THE β DECAY OF ^{77}GA

8.1 Introduction

From the classical shell model view of ^{77}Ga, it has three protons in the $\pi 2p_{3/2}$ orbitals and six neutrons in $\nu 1g_{9/2}$ orbitals. The ^{77}Ga ion produced in the decay of ^{77}Cu chain is unstable. To form the stable one, one of the neutrons from the $\nu 1g_{9/2}$ shell coverts to the proton and emits the β particles. Then the proton in the excited states emits γ rays and decay to the ground states. ^{77}Ge is not the stable nuclei, it again emits β particles and becomes the stable ^{77}As.

The primary information of the structure of ^{77}Ge populated by β decay of ^{77}Ga comes from the Aleklett *et al.* [16] from 1977, which is stored in NNDC database. They observed 14 γ rays for this decay process, placed 13 of them and established a decay scheme with nine excited states. Q_{β^-} value of ^{77}Ga is 5220.5 keV [112] and their study was only able to construct a decay scheme up to 2817-keV level. It is likely that more γ-ray transitions and high energy excited states were missed in the observation. Besides that, the main problem associated with their study did not have $\gamma\gamma$ coincidence data, and the proposed decay scheme was developed using the energy sums, differences and γ-ray intensity balances.

A recent study of excited states of ^{77}Ge by Kay *et al.* [57] from transfer-reaction observed twice as many (26) γ rays. But, they were able to establish a decay scheme only

www.manaraa.com

up to 1385 keV, and also do not observe some excited states seen by previous β-decay measurements.

The more comprehensive level scheme of the ^{77}Ge comes from the neutron capture reaction ^{76}Ge(n, γ) by Meierhofer *et al.* [71] in 2012. They have constructed the decay scheme with 68 prompt γ-ray transitions. Both of the recent experiments [57, 71] has used the coincidence information to construct the decay scheme, but still the detector efficiency widely limited the information.

From the previous knowledge of the structure of $^{74-76}$Ge, we expect to extend the decay existing decay scheme, filling the gaps as well as correct the placement of some of the γ-ray transitions reported in previous studies using very pure beam and high-efficiency detectors along with the statistical significant $\gamma\gamma$ coincidence information. The detailed structure of ^{77}Ge is important to improve the background prediction and the veto efficiency for the delayed ^{77m}Ge decay in the GERDA experiment: experiments searching the Majorana particles [71].

8.2 Experimental Technique

The experiment was performed using the Holifield Radioactive Ion Beam Facility at Oak Ridge National Laboratory. Pure ^{77}Cu ions were produced from the proton-induced fission of UC_x target following the two stages of mass separation. Pure Cu ions production mechanism was pretty similar as explained in Chapter 7. Then the two sets of experiments were performed. In the first experiment, accelerated ^{77}Cu ions of average intensity 15-ions/sec were time-tagged using the microchannel plate detector, passed through a six-

www.manaraa.com

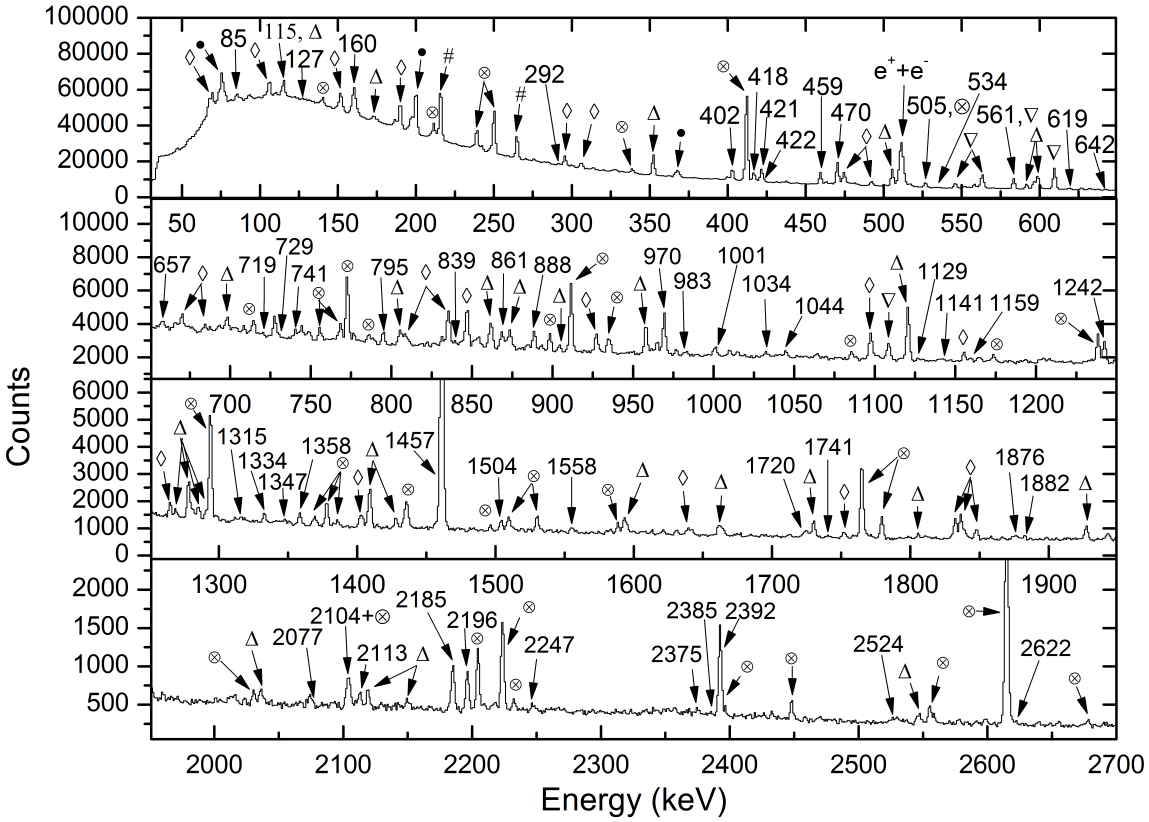

Figure 8.1: Saturation spectrum obtained in the LeRIBSS data run with a purified ^{77}Cu beam in the energy range 25 keV to 2.7 MeV. The γ-ray peaks associated with ^{77}Ga decay are marked with their energy. Other members of the decay chain are indicated by symbols as ^{77}Cu: Δ (triangle-up), ^{77}Zn: $\diamond$ (diamond), ^{77}Ge: $\#$ (hash), ^{76}Zn: $\bullet$ (solid bullet), ^{76}Ga: ∇ (triangle-down) and Background: $\otimes$ (crossed bullet). The energy range focuses on the γ ray assocaited with ^{77}Ge. The presence ^{76}Zn and ^{76}Ga in the spectra comes from 30.0(27)% β-delayed neutron emission probability [53].

segmented ion chamber (IC), and implanted on the moving tape collector (MTC) with the tape transport time 525 s. Then, data were collected in Pass-Through (PT) mode in which IC was run at a low pressure allowing the more than 99% of identified and counted ^{77}Cu

www.manaraa.com

ions exit the IC and implanted on the MTC. The MTC cycle was chosen 7-s to limit the ^{77}Ga build up in a sample ($T_{1/2}$ = 13.2 s) [53]. Then the data were collected using the triggerless data acquisition system. The second experiment was performed on the LeRIBSS setup. Average beam intensity used for this mode of the experiment was 130-ions/s and tape transport time was chosen 210 ms. As the beam was not accelerated in this mode of experiment, approximately one order of magnitude gain was observed. The 3-s growth/3-s decay MTC cycle was chosen as this experiment was intended to study ^{77}Cu decay ($T_{1/2}$ = 480ms) but it also allowed us for the decay of ^{77}Zn and ^{77}Ga study. Detail explanation of the experiment is given in Ref. [53].

The intensities of the γ ray reported for this dissertation were taken from LeRIBSS experiment which was calculated using the γ-singles spectra. We found many γ-ray peaks associated with the ^{77}Ga were suppressed with the huge backgrounds peaks and β-gated spectra were used to identify the actual γ-ray energy and corresponding intensity. Some of the peaks intensity were calculated based on the $\gamma\gamma$ coincidence information after constructing the decay scheme as explained in Chapter 4.

8.2.1 Experimental Results

Raw data from the HPGe crystals were gain matched and energy calibrated as explained in Chapter 4. Then, all the spectra were combined to generate the γ singles, $\beta\gamma$, and $\gamma\gamma$ coincidence spectra. Figure 8.1 is the summed saturation γ-singles spectra form the LeRIBSS run. From the $\gamma\gamma$ and $\beta\gamma$ coincidences information, we identified the 78 γ-ray prompts associated to the ^{77}Ga decay, of which 470-keV γ ray was the strongest one.

www.manaraa.com

Then we normalized the intensity of rest of the γ ray relative to 470-keV γ ray intensity. Table 8.1 is the list of the γ-rays associated to ^{77}Ga decay, their corresponding intensities, and coincidence information. Fig. 8.2 is the proposed level scheme of ^{77}Ge populated by the β decay of ^{77}Ge based on the statistically significant $\gamma\gamma$-coincidences. A strong 160-keV γ ray was observed which shows nothing in coincidences. Hence, as predicted by other measurements [16, 57, 71], we placed it as de-exciting the 160-keV level which feeds the ground state. This is a isomeric state, and we do not expect to see any γ ray in coincidence with 160-keV γ ray. We placed the strongest γ-ray of energy 470 keV feeding the level at 160 keV leading its placement as de-exciting the 630-keV level. Furthermore, we proposed the levels at 421 keV and 619 keV by placing the 421- and 619-keV γ rays respectively. Then, placed rest of the γ ray connecting those levels based on the $\gamma\gamma$ coincidence information. In the present work, we observed all γ rays and energy levels reported by the previous β-decay study [16]. The detail explanations of the proposed decay scheme is presented below.

8.2.2 Development of Level Scheme

In the present work, we identified 77 γ rays associated to ^{77}Ga decay, placed 67 of them in the decay scheme and established the decay scheme up to 3.14 MeV with 33 energy levels. We firmly confirmed all the energy levels at 160 keV, 421 keV, 619 keV, 630 keV, 1021 keV, 1048 keV, 1359 keV, 1664 keV and 2817 keV reported by Aleklett *et al.* [16] in previous β-decay measurement. Aleklett *et al.* has proposed 421-keV level tentatively. We confirmed this level by placing the 9 γ-ray transitions of energy 85 keV,

www.manaraa.com

198 keV, 627 keV, 1041 keV, 1242 keV, 1457 keV, 1558 keV and 2392 keV feeding into the level. The three γ rays of energies 627 keV, 1041 keV and 2392 keV are newly observed γ rays associated to ^{77}Ga decay whereas rest of them has already observed in at least one of the other measurements [16, 57, 71].

We identified three more γ rays of energies 115 keV, 127 keV and 198 keV de-exciting the 619-keV level. Besides that, 15 more γ rays were placed which feeds in the level. All three γ rays reported in this experiment de-exciting the level were also observed in other measurements [57, 71], which will be discussed in detail later. The energy level at 1021 keV is established with a γ ray of energy 392 keV de-exciting the level while two more γ rays feeds in. Furthermore, an energy level at 1359 keV has confirmed by placing the additional 729-keV γ ray de-exciting the level. Similarly, 1663-keV level is confirmed with additional 3 γ-ray transitions other than reported in previous work [16]. All the new energy levels observed other than previous β-decay study are going to discuss in detail below.

www.manaraa.com

Table 8.1: Energy, intensity, placement and coincidence information for γ rays associated with ^{77}Ga β-decay (probable coincidences are indicated with parentheses)

Energy	**Intensity**	**Placement**	**$\gamma\gamma$-Coincidences**
84.76(8)[b,*]	0.9(3)	505.37	(115), (421), (1160)
114.8(8)[b,†,*]	0.1(5)	618.71	657
126.6(2)[b,*]	0.9(5)	618.69	492
159.65(8)	43.2(9)	159.58	–
197.6(2)[b,*]	1.9(4)	618.69	(421), (1044), 2196
224.0(2)[b,†]	0.14(7)	225.00	534, 684
291.5(2)[b,*]	0.6(2)	910.27	(459)
331.7(5)	1.8(3)	491.84	
392.4(2)[b]	3.6(8)	1021.27	470, (642), 1069, 2224
402.48(7)	0.5(3)	1021.27	(459), 642
418.38(7)[b,*]	8(3)	910.27	492, (2113)
421.15(8)[b]	49.5(22)	421.18	(85), 198, 470, (627), 1041, (1159), 1242, 1315, (1414), 1457, 1555, 2113, 2392, 2385
422.5(2)	8.7(22)	1052.76	470, (1249), 1315
459.07(7)	48.5(8)	618.69	(292), 668, 741, 983, 1044, (1129), 1358, 1882, 1948, 2106, 2196, 2224, (2375), (2526)
469.97(6)	100.0(10)	629.52	392, 422, (642), 657, 729, 970, 990.5, 1034, 1249, (1315), 1347, 1358, 2185, 2247
492.03(7)[b]	22.3(8)	491.89	127, 418, 561, 795, 970, 1728, 1876, 2078, 2385, (2546)
505.11(6)[b,*]	4.4(16)	505.37	1159
534.3(3)[b,†,*]	2.6(7)	760	(224)
561.02(9)[b,*]	1.4(4)	1052.76	492
618.9(9)	12.2(8)	618.69	839, (1044), 1948
626.5(8)[a,†,*]	0.9(3)	1047.89	(421)
641.85(13)	6.5(7)	1663.33	(402), (470), 862
656.79(12)[a]	2.4(9)	1275.48	115, (470)
665.0(5)[a,*]	0.2(1)	1952.73	(795)
667.6(2)[b,*]	2.3(5)	1286.69	(459), (795), (888)
684.2(2)[b,‡]	3.9(8)		
719.24(9)[a,†]	0.39(19)	2180	(391), (470) 741
729.0(2)[a]	1.4(6)	1359.04	470
740.53(14)	6.4(8)	1359.04	459, 619, (719)
781.4(2)	3.6(7)[†]	1663.92	884
794.83(7)[b,*]	4.1(17)	1286.69	(492), (665)
831.19(15)[b,*]	3.0(8)	1878.89	888
839.4(2)[c]	3.9(8)	1458.09	(160) 619

Continued on next page

www.manaraa.com

Table 8.1 – Continued from previous page

Energy	Intensity	Placement	$\gamma\gamma$-Coincidences
861.6(11)	23(3)	1021.27	642
884.17(18)	4.9(8)	884.17	780, 2109
888.34(7)	18.5(9)	1047.89	831
970.41(5)[a]	5.3(18)	1599.93	470
990.8(5)[‡,*]	6.20(19)		(469)
983.17(19)[a,†]	4.8(7)	1598.41	459
1034.1(5)[a]	3.0(11)	1663.33	470
1041.2(2)[a]	5.8(9)	1462.36	421
1044.29(11)[a]	4.5(9)	1663.33	(198), 459, (619)
1069.0(3)	1.6(3)	2090.23	392
1129.4(7)[‡]	1.4(8)		(460)
1158.8(2)[a]	4.6(8)	1663.33	85, 421, 505
1242.21(6)	32.6(9)	1663.33	421
1249.3(3)[b]	3.4(12)	1878.89	422, 470
1315.3(4)[b]	3.5(9)	2368.18	422, 470, (492), 561
1333.1(6)	1.0(4)	1952.00	795
1347.4(4)[a,*]	2.6(8)	1977.18	470
1358.22(13)[a]	12.4(11)	1977.18	459
1414.2(3)[‡]	3.3(7)		(422)
1447.6(5)[‡,*]	1.3(4)	1952.00	(505)
1457.3(2)[b,*]	3.7(5)	1878.89	421
1503.81(11)	10.8(8)	1663.33	
1554.84(16)[b,†,*]	2.3(5)	1975.65	421
1557.7(3)[c]	3.6(9)	1977.18	421
1720.4(6)[b]	2.2(8)	1878.89	
1728.8(5)[‡,*]	7.3(3)		(492)
1741.1(18)[b]	5.8(7)	1900.68	
1876.3(2)[c]	7.0(9)	2368.18	(492)
1881.8(5)[a]	9.10(15)	2500.53	459
1948.1(4)[a]	4.0(9)	2567.36	459, (619)
2077.5(7)[a]	1.8(8)	2567.36	(492)
2105.6(7)[a]	3.0(18)	2724.26	459
2108.9(5)[‡,*]	1.53(3)		(885)
2112.72(12)[a]	12(5)	3022.99	(224), 418
2185.07(9)[b]	28.4(9)	2814.4	470
2196.25(8)[c]	10(3)	2814.4	459
2223.61(8)[a,‡,*]	2.6(14)		392, 459
2246.9(3)[a]	4.8(8)	2876.48	470
2374.6(5)[‡]	2.4(8)		459

Continued on next page

www.manaraa.com

Table 8.1 – Continued from previous page

Energy	Intensity	Placement	$\gamma\gamma$-Coincidences
2385.2(7)[a,*]	1.7(8)	2876.48	(492)
2392.44(9)	2.6(4)	2814.4	421
2525.9(4)	1.5(4)	3144.60	(459)
2545.8(5)[‡,*]	4.3(4)		(492)
2621.85(9)[‡]	1.1(5)		459

[a] Newly observed γ ray.
[b] Newly observed γ ray which is also reported by at least one other measurements [16, 57, 71].
[c] γ ray with different placement from previous β-decay measurement [16].
[†] γ ray which is not used to calculate the β-feeding intensity due to energy tolerance issue.
[*] γ-ray energy and intensity determined from $\gamma\gamma$ coincident data.
[‡] unplaced γ ray.

8.2.2.1 Description of Newly Proposed Levels Below 1664 keV

Although, the previous ^{76}Ga β-decay study by Aleklett et al. [16] was able to propose the decay scheme of ^{76}Ge up to 2717 keV, our current study is able to confirm the levels below 1664 keV only.

1. A level at 224 keV is tentatively proposed by placing a 224-keV γ ray feeding the ground state. The 224-keV γ ray is observed with very weak intensity and the level is represented by a dashed line in the decay scheme. Two γ rays of energies 534 keV and 684 keV are observed in probable coincidence with 224-keV gated γ-ray spectrum. Both γ rays were reported by Kay *et al.* [57] to this level, while only 534-keV γ ray is reported from neutron capture reaction [71]. Hence, our data show evidence for the level at 224 keV.

www.manaraa.com

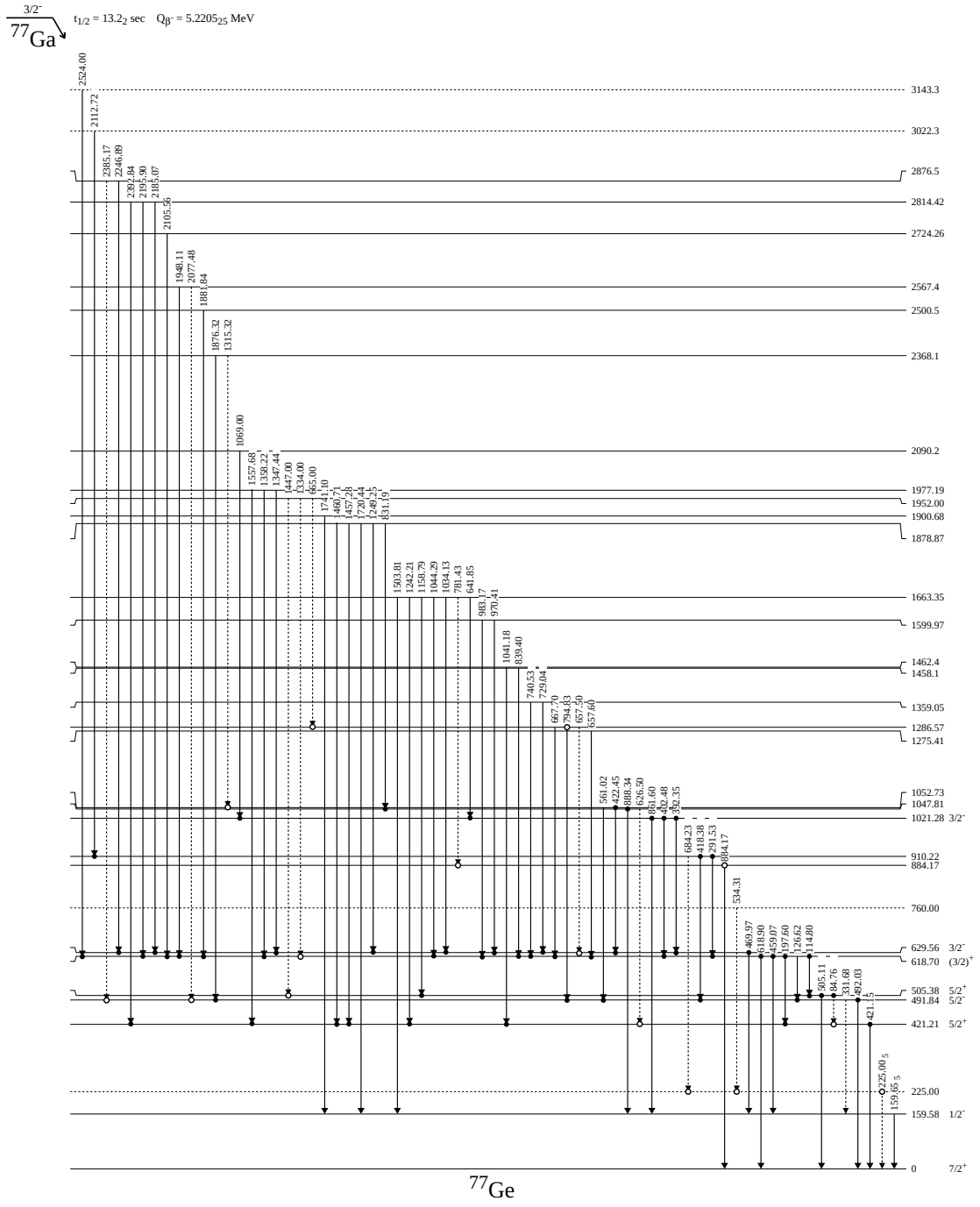

Figure 8.2: The proposed decay scheme for ^{77}Ga to excited states in ^{77}Ge.

www.manaraa.com

2. A level at 492 keV is proposed by placing the 492-keV γ ray de-exciting the level with six 127-, 332-, 418-, 1876-, 2078- and 2385-keV γ ray feeding in. This proposed level is in agreement with previous transfer reaction and neutron capture measurements [57, 71]. Out of the six γ rays feeding the level, 2077-keV and 2385-keV γ rays were not observed in any previous measurements. The 1876-keV γ ray is placed populating the level 630-keV level in neutron capture study [71], we have corrected it's placement.

3. A level at 505 keV is proposed by placing the 505-keV γ ray feeding the ground state. We observe a 505-keV γ ray in definite coincidences with 115-, 1159- and 1448-keV γ ray, and were feeds in the level. This level is in agreement with previous transfer reaction and neutron capture studies [57, 71]. The γ rays of energies 115 keV [57] and 1448 keV [71] which were reported in the early experiment were observed weak in intensity whereas 1159-keV γ ray is newly observed. Furthermore, we observe a 505-keV γ ray as a compound peak associated with ^{77}Cu and ^{77}Ga. To resolve the proper intensity of the 505-keV γ ray, we utilized the relative intensity of the γ rays of energies 421 keV (I_γ = 124(3)) and 504.8 keV (I_γ = 37(2)) from the Kay *et al.* [57] work. Our estimated intensity of 505-keV γ ray associated with ^{77}Ga decay is 8.3% of the compound peak.

4. A level at 760 keV is tentatively proposed based on 535-keV γ-ray transition feeding the 224-keV level. We observed a 534-keV γ ray in probable coincidence with 224-

www.manaraa.com

keV γ ray and placed it as de-exciting the 760-keV level which is in agreement with the transfer-reaction and neutron capture reaction studies [57, 71].

5. A level at 884 keV is proposed based on the single γ-ray transition of energy 884 keV connecting the ground state. The 885-keV γ ray was observed in definite coincidence with 781-keV γ ray and placed populating the 884-keV level. This level is in agreement with previous neutron capture study [71].

6. A level at 910 keV is firmly proposed by three γ-ray transitions of energies 292 keV, 418 keV and 684 keV. In this work, we observed a 292-keV γ ray in probable coincidence with 459-keV γ ray leading its placement as de-exciting the 910-keV level. Furthermore, an observed 418-keV γ ray shows definite coincidences with 492-keV γ ray leading its placement de-exciting the 910-keV level. Besides that, we observed a 684-keV γ ray in probable coincidence with 224-keV γ ray and placed de-exciting the 910-keV level. Moreover, an observed 2113-keV γ ray is in definite coincidence with 418-keV γ ray and placed feeding the 910-keV level. Consequently, our data suggest that there is a level at 910 keV which is in agreement with the transfer-reaction and neutron capture reaction studies [57, 71].

7. A level at 1053 keV is firmly proposed by placing the two γ rays of energies 422 keV and 561 keV feeding the 630- and 492-keV levels respectively. We observed a 422-keV γ ray in definite coincidence with 470-keV γ ray leading its placement as de-exciting the 1053-keV level. Furthermore, an observed 561-keV γ ray which shows 492-keV γ ray in definite coincidences and placed as de-exciting the 1053-

www.manaraa.com

keV level. Hence our data suggest that there is a level at 1052 keV, which is in agreement with the previous two studies [57, 71].

8. A level at 1275 keV is proposed by placing the γ ray of energy 657 keV feeding the 619-keV level. We observed a 657-keV γ ray in definite coincidence with 115-keV γ ray leading its placement as de-exciting the 1275-keV level, which is in agreement with previous transfer-reaction study [57].

9. A level at 1287 keV is firmly proposed by placing the three γ rays of energies 657 keV, 668 keV and 795 keV feeding 630-, 492- and 619-keV levels respectively. In the present work, we observed 657-keV γ ray in probable coincidences with 470-keV γ ray leading its placement as de-exciting the 1287-keV level. A 795-keV γ ray was observed in definite coincidence with 492-keV γ ray and placed it as de-exciting the 1287-keV level. Besides that, a 668-keV γ ray was observed in probable coincidences with 459-keV γ ray and placed it as de-exciting the 1287-keV level. Thus our data support the establishment of a level at 1287 keV which is in agreement with transfer-reaction study [57].

10. A level at 1458 keV is tentatively proposed with a single γ-ray transition of energy 839-keV feeding the 619-keV level. An observed 839-keV γ ray shows a 619-keV γ ray in definite coincidence leading its placement de-exciting the level at 1458 keV. The 839-keV γ ray was reported in previous transfer-reaction measurement [57] but we have corrected its placement based on $\gamma\gamma$ coincidences.

www.manaraa.com

11. A new level at 1462 keV is proposed by placing the single γ-ray transition of energy 1041 keV feeding the 630-keV level. We observed a 1041-keV γ ray in definite coincidence with 421-keV γ ray leading its placement as de-exciting the 1461-keV level. The level at 1462 keV is represented by the solid line although it is proposed by a single γ ray because the placement of 1041-keV γ ray is based on definite coincidences in both directions

12. A new level at 1600 keV is firmly proposed by placing the two γ rays of energies 970 keV and 983 keV feeding the 630- and 619-keV levels respectively. Both γ rays were not observed in any previous studies. We observed a 970-keV γ ray in definite coincidence with 470-keV γ ray and 983-keV γ ray in definite coincidences with 459-keV γ ray leading their placement as de-exiting the 1600-keV level. Hence, our data support the establishment of a level at 1600 keV.

8.2.2.2 Description of Newly Proposed Energy levels Above 1664 keV

Instead of 2817-keV γ ray proposed from Aleklett et al., we have established a 2814-keV level by placing the 2814-keV γ ray feeding the ground state. The energy levels above 1664 keV proposed from our work are going to discuss below.

13. A level at 1879 keV is firmly proposed by placing the γ rays of energies 831, 1249 and 1457 keV feeding the 1879-, 630- and 421-keV levels respectively. In the present work, we observed an 831-keV γ ray which is in definite coincidence with 888-keV γ ray leading its placement as de-exciting the 1879-keV level. Furthermore, an observed 1249-keV γ ray shows 470-keV γ rays in definite coincidence leading its

www.manaraa.com

placement as de-exciting the 1879-keV level. Besides that, we observed a 1457-keV γ ray which shows a definite coincidence with 421-keV γ ray and placed it as de-exciting the 1879-keV level. Consequently, our data support that there is a level at 1879-keV which is in agreement with previous neutron capture (n,γ) work [71].

14. A level at 1901 keV is tentatively proposed by placing the γ ray of energy 1741 keV feeding the 160-keV level. In this work, we observed a strong 1741-keV γ ray which shows nothing in the coincidences. Hence we assume it feeds the isomeric state 160-keV leading its placement as de-exciting the 1901-keV level. The proposed level at 1901 keV is in agreement with the previous (n,γ) work [71].

15. A level at 1952 keV is proposed by the placement of three weak intensity γ rays of energies 665, 1333 and 1447 keV feeding the 1287-, 619- and 505-keV levels respectively. We observed a 665-keV γ ray which is in probable coincidences 795-keV γ ray leading its placement as de-exciting the 1952-keV level. Furthermore, an observed 1333-keV γ ray shows 795-keV γ ray in definite coincidence leading its placement as de-exciting the 1952-keV level. Besides that, a 1447-keV γ ray was observed in probable coincidence with 505-keV ray and placed it as de-exciting the 1952-keV level. Hence, our data suggest that there is a level at 1952-keV, which is in agreement with the previous (n,γ) study [71]. The 1334-keV γ ray reported for this level was not observed by any previous measurements.

16. A level at 1977 keV is proposed by placing the three 1347-, 1358- and 1558-keV γ rays feeding the 630-, 619- and 421-keV levels respectively. All these three γ rays

www.manaraa.com

are newly observed in this measurement. A 1347-keV γ ray is observed in definite coincidence with 470-keV γ ray leading its placement as de-exciting the 1977-keV level. Furthermore, a 1358-keV γ ray was observed in definite coincidence with 459-keV γ ray and placed it as de-exciting the 1977-keV level. Besides that, we observed 1558-keV γ ray in definite coincidence with 421-keV γ ray and placed it as de-exciting the 1977-keV level. Thus, our data support that there is a level at 1977 keV.

17. A level at 2090 keV is tentatively proposed by the placing the single γ ray of energy 1069 keV feeding the 1021-keV level. We observed a 1069-keV γ ray which is in definite coincidence with 392-keV γ ray leading its placement as de-exciting the 2090-keV level. The level at 2090 keV is represented by the solid line in the decay scheme (although it is proposed from a single γ ray) because the placement of 1069-keV γ ray is based on definite coincidences in both directions.

18. A level at 2368 keV firmly proposed by placing the two γ rays of energies 1315 keV and 1876 keV feeding the 1053- and 492-keV levels respectively. We observed a 1315-keV γ ray in probable coincidence with 422-keV γ ray leading its placement as de-exciting the 2368-keV level. Furthermore, an 1876-keV γ ray was observed in definite coincidence with 492-keV γ ray and placed it as de-exciting the 2368-keV level. Thus our data support that there is a level at 2368-keV which is in agreement with previous work [71]. We have corrected the placement of 1876-keV γ ray to the 2368-keV level and not the 2507-keV level as reported by Meierhofer *et al.* [71].

www.manaraa.com

19. A level at 2501 keV is proposed by placing the γ ray of energy 1882 keV feeding the 619-keV level. We observed a 1882-keV γ ray which shows definite coincidence with 459-keV γ ray leading its placement as de-exciting the 2501-keV level. The level at 2501 keV is represented by the solid line although it is proposed by a single γ ray because the placement of 1882-keV γ ray is based on definite coincidences in both directions.

20. A level at 2567 keV is firmly proposed by placing the two γ rays of energies 1948 keV and 2078 keV feeding the 619 keV and 492 keV levels respectively. Both γ rays were not observed in any previous studies. We observed a 1948-keV γ ray in definite coincidence with 459-keV γ ray leading its placement as de-exciting the 2576-keV level. Furthermore, an observed 2078-keV γ ray shows definite coincidence with 492-keV γ ray and placed it as de-exciting the 2567-keV level. Hence, our data suggest that there is a level at 2567 keV.

21. A level at 2724 keV is proposed by placing the γ-ray transition of energy 2106 keV feeding the 2105-keV level. In this measurement, we observed a 2106-keV γ ray which shows a definite coincidence with 459-keV γ ray leading its placement as de-exciting the 2723-keV level. The level at 2724 keV is represented by the solid line although it was proposed by the single γ ray as the placement of 2105-keV γ ray is based on definite coincidences in both directions.

22. A level at 2814 keV is firmly proposed by placing the three 2185-, 2196- and 2392-keV γ rays feeding the 630-, 619- and 421-keV levels respectively. We observed

www.manaraa.com

a 2185-keV γ ray is in definite coincidence with 470-keV γ ray only leading its placement as de-exciting the 2814-keV level. Furthermore, an observed 2196-keV γ ray shows definite coincidence with 459-keV γ ray leading its placement as de-exciting the 2814-keV level. Besides that, a 2392-keV γ ray was observed which is in definite coincidence with 421-keV γ ray and have placed as de-exciting the 2814-keV level. Thus our data strongly support that there is a level at 2814-keV which is in agreement with neutron capture study [71]. We have corrected the placement of γ ray of energy 2196 keV reported from neutron capture reaction study [71] whereas 2392-keV γ ray is newly observed in our measurement.

23. A level at 2877 keV is proposed by placing the two γ rays of energies 2247 keV and 2385 keV feeding the 630-keV and 492-keV levels respectively. We observed a 2247-keV γ ray in definite coincidence with 470-keV γ ray leading its placement as de-exciting the 2877-keV level. Furthermore, an observed 2385-keV γ ray shows definite coincidence with 492-keV γ ray and have placed it as de-exciting the 2877-keV level. Both γ rays which are placed de-exciting the level at 2876 keV are newly observed in this measurement. Consequently, our data suggest that there is a level at 2877 keV.

24. A level at 3023 keV is proposed by placing the γ ray of energy 2113 keV feeding the 910-keV level. We observed a 2113-keV γ ray which shows definite coincidences with 418-keV γ ray leading its placement as de-exciting the 3023-keV level. We

www.manaraa.com

represented this level with a dashed line in the decay scheme as is new level proposed from a single γ ray.

25. Finally, a level at 3143 keV is tentatively proposed by placing the γ ray of energy 2526 keV feeding the 619-keV level. We observed a 2526-keV γ ray in probable coincidence 459-keV γ ray leading its placement at 3143-keV level. This γ rays and corresponding level both are new information observed in our experiment. The level at 3143 keV is represented by a dashed line in the decay scheme. This is the highest energy level proposed by our measurement.

From our closer observation, we identified 18 γ rays associated with the ^{77}Ga β decay contains the components of other decay elements. Some of them are from the background whereas some of them from the other daughter elements of the decay chain. These γ rays are of energy: 115, 127, 198, 292, 418, 505, 534, 561, 627, 665, 668, 795, 831, 1347, 1447, 1457, 1555 and 2385 keV. We used the coincidence technique explained in Chapter 4 to find their proper intensity associated with ^{77}Ga. Furthermore, we used the ratio of γ single spectra to the β-gated spectra of the all observed γ-ray peaks to identify the association of the γ ray to the proper elements in the decay chain.

www.manaraa.com

Table 8.2: Feeding intensities (I_{β^-}), lower limit $\log(ft)$ and assigned spin-parity value for ^{77}Ga β decay. The β-feeding value are given per 100 decays.

Energy Level	$\mathbf{I}_{\beta^-}$	$\log(ft)$	**Spin-parity from NNDC**
0.00°	0	8.5	$7/2^+$
159.58(5)	40(25)	5.6	$1/2^-$
225.0(5)‡	-	-	-
421.21(5)°	0	>9.09	$5/2^+$
491.84(6)‡°	0	>9.1	$5/2^-$
505.38(5)‡°	0	>9.1	$5/2^-$
618.70(5)°	0	>9.0	$(3/2^+)$
629.56(6)	6.8(8)	6.17	$3/2^-$
760.5(5)‡	-	-	-
884.17(18)‡	0.92	6.93	
910.22(9)‡	0.61(17)	7.09	
1021.28(7)	2.8(6)	6.38	
1047.81(7)	3.1(2)	6.33	
1052.73(10)‡	3.3(7)	6.30	
1286.57(8)‡	1.7(4)	6.47	
1359.05(13)	1.47(18)	6.5	
1458.1(2)†	0.73(15)	6.75	
1462.4(2)†	1.09(16)	6.58	
1599.97(8)†	1.0(4)	6.54	
1663.35(6)	11.7(4)	5.44	$3/2^-$
1878.87(12)‡	2.3(3)	6.03	
1900.68(19)‡	1.10(14)	6.34	
1952.7(5)‡	0.55(5)	6.6	
1977.19(13)†	3.5(3)	5.79	
2090.2(3)†	0.60(14)	6.49	
2368.1(2)‡	2.0(2)	5.80	
2500.5(5)†	1.7(3)	5.77	
2567.4(3)†	1.1(2)	5.92	
2724.3(7)†	0.6(3)	6.07	
2814.42(7)‡	7.7(6)	4.89	
2876.5(2)†	1.2(2)	5.64	
3022.3(5)†	2.0(5)	5.3	
3143.3(9)†	1.5(5)	5.34	

° Feeding to this level was consistent with zero.

† Newly established energy level.

‡ Newly established energy level agreed with at least one other measurements [57, 71].

www.manaraa.com

8.2.3 β-Feeding and Log(ft) Value

After constructing the decay scheme, we attempted to find the β-feeding to the each level using the MASTER program. But, we cannot directly calculate the β-feeding intensity and branching ratio of this decay as it's first excited state (160 keV) is a isomeric state. We have taken the spin-parity consideration to assign the tentative β-feeding to the ground level and the isomeric state 160 keV. The ground state of parent nuclei ^{77}Ga has the spin-parity $3/2^-$ form its upaired proton in the $\pi 2p_{3/2}$ states which is confromed from several studies [100]. It decays to ^{77}Ge through the β decay. The ground state of ^{77}Ge has $7/2^+$ spin-parity confirmed from other measurements [100], which create the scenario of unique first forbidden transition form $3/2^-$ to $7/2^+$ (ΔJ = 2, $\Delta\pi$ = -1) and should have low $\log(ft)$ value in range 8 to 9 [62]. We assume it to be 8.5(2) which gives the almost zero β feeding (0.05(2) $\%$) to the ground state. Spin-parity of isomeric state 160 keV has assigned 1/2$^-$ from several studies [100]. Decay from $3/2^-$ to $1/2^-$ crates the scenario of allowed transition (ΔJ = 1, $\Delta\pi$ = +1) and should have low $\log(ft)$ value. We assume the $\log(ft)$ value for 160-keV level to be 5.6(3), which estimates the β-feeding value 40(25)$\%$, which is shown in Figure 8.3. This shows that the rest of around 60$\%$ only feeds the other states in the decay scheme.

Our rough estimate for the β-feeding to level 160 keV comes in perfect agreement with the results obtained using a coefficient of Internal Conversion (IT) reported by Kibedi *et al.* [58]. From our proposed decay scheme, summed intensity feeding the 160-keV level is 208.78(341)$\%$. The intensity of 160-keV γ ray is observed to be 43.24(93)$\%$. We calculated the actual intensity using the internal coefficient (α = 0.836) [6] and equation:$(1 +$

www.manaraa.com

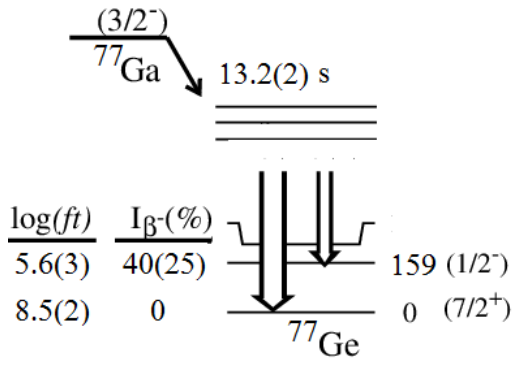

Figure 8.3: Un-observed β-feeding for ^{77}Ga β decay. The estimated β-feeding intensities are shown on the left next to the energy levels. (See text for details.)

$\alpha)I_{160}$. It comes to be 79.39(93) %. As only 19(2)% of 160-keV level undergoes the Internal Conversion, the actual intensity of the 160-keV γ peak is calculated to be 417.8(442)%. Then the calculated absolute β-feeding to 160-keV level appeared to be 39.6(91)%. Furthermore, based on the above assumption, we have calculated the absolute β-feeding intensity for each proposed levels which are listed in Table 8.2.

Lower limit $\log(ft)$ values for all the proposed levels shown in Table 8.2 is calculated using the NNDC website [6]. We have used the Q_{β^-} value 5220.5(24) keV and $T_{1/2}$ = 13.2(2) s taken from AME2012 calculations [112].

8.2.4 Spin-Parity Assignment and Nushellx Result

Our calculated $\log(ft)$ value is not conclusive to assign the spin-parity of most of the states. We have calculated the level structure of ^{77}Ge using the Nushellx [23] using the $JUN45$ effective interactions and $JJ44$ model space which is shown in Figure 8.4. We have compared our decay scheme with theoretical results and found that the Nushellx

www.manaraa.com

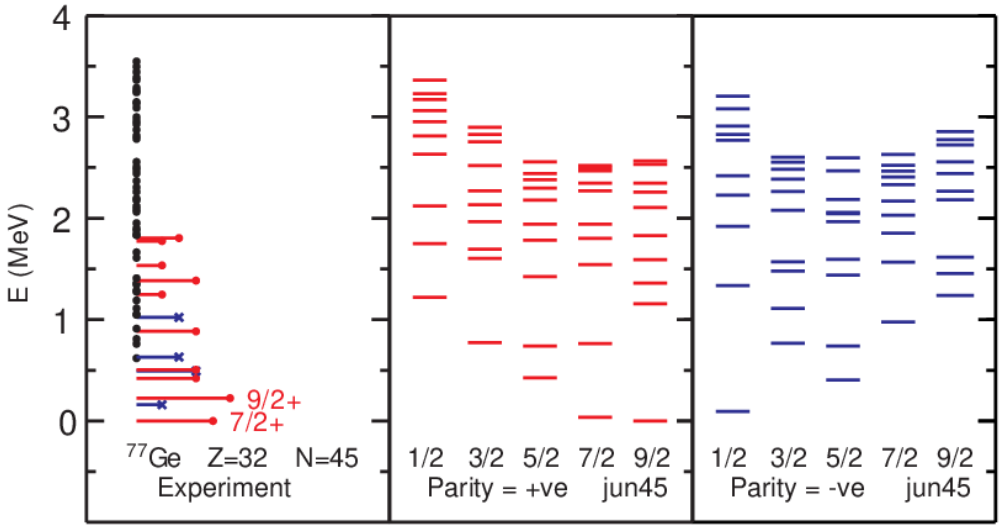

Figure 8.4: Nushellx predictions of structure of ^{77}Ge.

calculation is not in agreement with our experimental results. Nushellx predicts the ground state to be $9/2^+$ but we assigned to be $7/2^+$. This assignment is consistent with several other measurements [100].

8.3 Discussion and Conclusion

Using the pure beam and high-efficiency clover detectors, we have been able to identify 77 γ rays associated with the ^{77}Ga β decay and established the decay scheme up to 3.24 MeV based on statistically significant $\gamma\gamma$ coincidences. We observed all 13 γ rays reported in previous β-decay study. Out of the 77 γ rays we observed, 30 of them are in agreement with other studies than β decay and are already listed in NNDC, whereas rest of the γ rays are totally new observed from this measurement associated with this decay. Our proposed decay scheme contains 33 energy levels of which 9 are reported in previous β-decay work,

www.manaraa.com

13 agreed with other measurements, while 11 are newly populated form the new γ-ray transitions. We have identified 18 γ rays having the components form other elements in the decay chain and room background. We used the β-gated spectra and coincidence information to divide their proper intensities associated with this decay. Furthermore, we have calculated the β-feeding intensity and $\log(ft)$ values for all the proposed level, and have compared our proposed decay scheme with the Nushellx theoretical calculations. From the present measurement, we have extended the decay scheme with a better understanding of the coincidence information and filled the decay scheme with a lot more γ rays.

www.manaraa.com

CHAPTER IX

CONCLUSION

Starting from an isobarically purified $^{74-77}$Cu beam at the Holifield Radioactive Ion Beam Facility of Oak Ridge National Lab, we have performed a detailed β-decay studies of $^{74-77}$ Ga nuclei using the four clovers HPGe detectors. From the careful analysis of four-sets of $^{74-77}$Ga β-decay data, we have established a more comprehensive decay scheme for all corresponding Germanium nuclei based on $\gamma\gamma$ coincidences. We have introduced the statistical significant factor (S) which adds the confidence on the placement of the γ ray to a new level along with removing the experimental biases. In most of the cases, we have extended the energy levels to cover more energy window available for β decay, confirmed the placement of γ rays assigned in the previous studies, corrected the placement of some incorrectly placed γ rays and energy levels. The previous experiment failed to observe the weak γ rays due to the poor detection efficiency of the detector, beam production rate and source contamination. From the expended level scheme, β-feeding intensity and corresponding $\log(ft)$ values were calculated and tentative or firm spin-parity assignments were made whenever possible for all proposed levels. Finally, shell model-calculations are used for comparison to the observed level density.

www.manaraa.com

Although $^{74-77}$Ga is not considered as a major contributor of the decay heat, the present studies will provide us with a better understanding of the pandemonium effect and how it is related to other nuclei which need to be studied. Present β-decay spectroscopy studies definitely have improved our understanding of the nuclear structure near/far from stability for some nuclei and can be used to improve the modeling of nucleosynthesis process, which will affect the prediction of r-process path.

Still, we have limitations of detecting all the γ rays due to the efficiency of the detector although recent experiment utilized a detector whose efficiency was much higher compared to previous studies, we expect to revisit some of the nuclei with Total Absorption Spectroscopy (TAS) or Modular Total Absorption Spectroscopy (MTAS) technique [88, 118] in the future.

www.manaraa.com

REFERENCES

[1] "BC-404 plastic scintillator," *http://www.crystals.saint.gobain.com/uploadedFiles/SG-Crzystals/Documents/SG27*.

[2] "ENERGY FOR THE FUTURE, The Nuclear Option, a position paper of the European Physical Society, Nuclear Physics Division, 2010," .

[3] "Experimental K-alpha X-ray Energies," *http://hyperphysics.phy-astr.gsu.edu/hbase/Tables/kxray.html*.

[4] "Isotope Seperator Online in HRIBF at ORNL," *https://www.phy.ornl.gov*.

[5] "Low energy Radioactive Ion Beam Spectroscopy Station," *http:/www.phy.ornl.gov/leribss.*

[6] "National Nuclear Data Center," *https://www.nndc.bnl.gov*.

[7] "National Nuclear Data Center LOGFT web program," *http://www.nndc.bnl.gov/logft/*.

[8] "Nuclear Energy Research and Development Roadmap, Report to Congress, U.S. Department of Energy, 2010," *http://www.ne.doe.gov/pdfFiles/NuclearEnergy_Roadmap_Final.pdf*.

[9] "Technology Roadmap, Nuclear Energy, International Energy Agency, 2010," *http://www.ica.org/papers/2010/nuclear_roadmap.pdf*.

[10] N. Abgrall, E. Aguayo, F. T. Avignone, A. S. Barabash, F. Bertrand, M. Boswell, V. Brudanin, M. Busch, A. Caldwell, Y.-D. Chan, et al., "The majorana demonstrator neutrinoless double-beta decay experiment," *Advances in High Energy Physics*, vol. 2014, 2014.

[11] D. Abriola, A. Nichols, and J. Tuli, *Summary Report of an IAEA Technical Meeting on Co-ordination of the International Network of Nuclear Structure and Decay Data Evaluators*, Tech. Rep., International Atomic Energy Agency, 2011.

[12] D. Abriola and A. Sonzogni, "Nuclear Data Sheets for A= 72," *Nuclear Data Sheets*, vol. 111, no. 1, 2010, pp. 1–140.

www.manaraa.com

[13] K. Abusaleem and B. Singh, "Nuclear Data Sheets for A= 71," *Nuclear Data Sheets*, vol. 112, no. 1, 2011, pp. 133–273.

[14] K.-H. Ackermann, M. Agostini, M. Allardt, M. Altmann, E. Andreotti, A. Bakalyarov, M. Balata, I. Barabanov, M. B. Heider, N. Barros, et al., "The GERDA experiment for the search of $0\nu\beta\beta$ decay in ^{76}Ge," *The European Physical Journal C*, vol. 73, no. 3, 2013, p. 2330.

[15] M. F. M. Al-Shudifat, "Beta decay of neutron-rich isotopes of zinc and gallium," 2015.

[16] K. Aleklett, E. Lund, G. Nyman, and G. Rudstam, "Total β-decay energies and masses of short-lived isotopes of zinc, gallium, germanium and arsenic," *Nuclear Physics A*, vol. 285, no. 1, 1977, pp. 1–18.

[17] A. Algora, D. Jordan, J. L. Taín, B. Rubio, J. Agramunt, A. B. Perez-Cerdan, F. Molina, L. Caballero, E. Nácher, A. Krasznahorkay, M. D. Hunyadi, J. Gulyás, A. Vitéz, M. Csatlós, L. Csige, J. Äysto, H. Penttilä, I. D. Moore, T. Eronen, A. Jokinen, A. Nieminen, J. Hakala, P. Karvonen, A. Kankainen, A. Saastamoinen, J. Rissanen, T. Kessler, C. Weber, J. Ronkainen, S. Rahaman, V. Elomaa, S. Rinta-Antila, U. Hager, T. Sonoda, K. Burkard, W. Hüller, L. Batist, W. Gelletly, A. L. Nichols, T. Yoshida, A. A. Sonzogni, and K. Peräjärvi, "Reactor Decay Heat in ^{239}Pu: Solving the γ Discrepancy in the 4–3000-s Cooling Period," *Phys. Rev. Lett.*, vol. 105, Nov 2010, p. 202501.

[18] G. Alton, Y. Liu, and D. Stracener, "High-efficiency target ion sources for radioactive ion beam generation," *Review of scientific instruments*, vol. 77, no. 3, 2006, p. 03A711.

[19] F. T. Avignone III, S. R. Elliott, and J. Engel, "Double beta decay, Majorana neutrinos, and neutrino mass," *Reviews of Modern Physics*, vol. 80, no. 2, 2008, p. 481.

[20] C. M. Baglin, "Nuclear data sheets for A= 81," *Nuclear Data Sheets*, vol. 109, no. 10, 2008, pp. 2257–2437.

[21] J. R. Beene, D. W. Bardayan, A. G. Uribarri, C. J. Gross, K. Jones, J. F. Liang, W. Nazarewicz, D. W. Stracener, B. A. Tatum, and R. Varner, "ISOL science at the Holifield radioactive ion beam facility," *Journal of Physics G: Nuclear and Particle Physics*, vol. 38, no. 2, 2011, p. 024002.

[22] S. Brant, N. Yoshida, and L. Zuffi, "β decay of odd-A As to Ge isotopes in the interacting boson-fermion model," *Physical Review C*, vol. 70, no. 5, 2004, p. 054301.

[23] B. Brown and W. Rae, "The shell-model code NuShellX@ MSU," *Nuclear Data Sheets*, vol. 120, 2014, pp. 115–118.

www.manaraa.com

[24] D. C. Camp, D. R. Fielder, and B. P. Foster, "Energy levels in ^{74}Ge from the decay of ^{74}Ga," *Nuclear Physics A*, vol. 163, no. 1, 1971, pp. 145–160.

[25] D. C. Camp and B. P. Foster, "Energy levels in ^{76}Ge from the decay of ^{76}Ga," *Nuclear Physics A*, vol. 177, no. 2, 1971, pp. 401–417.

[26] M. Chacko, L. Dorikens-Vanpraet, and M. Dorikens, "The decay of ^{75}Ga to levels in ^{75}Ge," *Zeitschrift für Physik*, vol. 267, no. 5, 1974, pp. 359–365.

[27] B. Cheal, E. Mané, J. Billowes, M. Bissell, K. Blaum, B. Brown, F. Charlwood, K. Flanagan, D. Forest, C. Geppert, et al., "Nuclear spins and moments of Ga isotopes reveal sudden structural changes between N = 40 and N = 50," *Physical review letters*, vol. 104, no. 25, 2010, p. 252502.

[28] B. P. Crider, E. E. Peters, J. Allmond, M. T. McEllistrem, F. M. Prados-Estévez, T. Ross, J. Vanhoy, and S. W. Yates, "Inelastic neutron scattering cross sections for ^{76}Ge relevant to background in neutrinoless double-β decay experiments," *Physical Review C*, vol. 92, no. 3, 2015, p. 034310.

[29] J. Dobaczewski, N. Michel, W. Nazarewicz, M. Płoszajczak, and J. Rotureau, "Shell structure of exotic nuclei," *Progress in Particle and Nuclear Physics*, vol. 59, no. 1, 2007, pp. 432–445.

[30] A. Dombos, D.-L. Fang, A. Spyrou, S. Quinn, A. Simon, B. Brown, K. Cooper, A. Gehring, S. Liddick, D. Morrissey, et al., "Total absorption spectroscopy of the β decay of ^{76}Ge," *Physical Review C*, vol. 93, no. 6, 2016, p. 064317.

[31] G. Dostemesova, D. Kaipov, and Y. G. Kosyak, "Study on ^{70,72,74,76}Ge nucleus excited states in the (n, n'γ) reaction," 1987.

[32] B. Ekström, B. Fogelberg, P. Hoff, E. Lund, and A. Sangariyavanish, "Decay Properties of $^{75-80}$Zn and Qβ-values of Neutron-Rich Zn and Ga Isotopes," *Physica Scripta*, vol. 34, no. 6A, 1986, p. 614.

[33] S. R. Elliott and J. Engel, "Double-beta decay," *Journal of Physics G: Nuclear and Particle Physics*, vol. 30, no. 9, 2004, p. R183.

[34] A. R. Farhan and B. Singh, "Nuclear data sheets for A= 78," *Nuclear Data Sheets*, vol. 110, no. 9, 2009, pp. 1917–2080.

[35] R. Firestone, "Nuclear Data Sheets for A=22," *Nuclear Data Sheets*, vol. 106, no. 1, 2005, pp. 1 – 88.

[36] R. Firestone, V. Shirley, C. Baglin, S. Chu, and J. Zipkin, "Table of isotopes,", 1996.

www.manaraa.com

[37] K. T. Flanagan, P. Vingerhoets, M. Avgoulea, J. Billowes, M. L. Bissell, K. Blaum, B. Cheal, M. De Rydt, V. N. Fedosseev, D. H. Forest, C. Geppert, U. Köster, M. Kowalska, J. Krämer, K. L. Kratz, A. Krieger, E. Mané, B. A. Marsh, T. Materna, L. Mathieu, P. L. Molkanov, R. Neugart, G. Neyens, W. Nörtershäuser, M. D. Seliverstov, O. Serot, M. Schug, M. A. Sjoedin, J. R. Stone, N. J. Stone, H. H. Stroke, G. Tungate, D. T. Yordanov, and Y. M. Volkov, "Nuclear Spins and Magnetic Moments of ^{71,73,75}Cu: Inversion of $\pi 2p_{3/2}$ and $\pi 1f_{5/2}$ Levels in ^{75}Cu," *Phys. Rev. Lett.*, vol. 103, Oct 2009, p. 142501.

[38] R. Fournier, J. Kroon, T. Hsu, B. Hird, and G. Ball, "The neutron particle structure of the germanium isotopes," *Nuclear Physics A*, vol. 202, no. 1, 1973, pp. 1–29.

[39] L. Gaudefroy, O. Sorlin, D. Beaumel, Y. Blumenfeld, Z. Dombrádi, S. Fortier, S. Franchoo, M. Gélin, J. Gibelin, S. Grévy, et al., "Reduction of the spin-orbit splittings at the N= 28 shell closure," *Physical review letters*, vol. 97, no. 9, 2006, p. 092501.

[40] C. Gross, K. Rykaczewski, D. Shapira, J. Winger, J. Batchelder, C. Bingham, R. Grzywacz, P. Hausladen, W. Krolas, C. Mazzocchi, et al., "A novel way of doing decay spectroscopy at a radioactive ion beam facility," *The European Physical Journal A-Hadrons and Nuclei*, vol. 25, no. 1, 2005, pp. 115–116.

[41] R. Grzywacz, "Applications of digital pulse processing in nuclear spectroscopy," *Nuclear Instruments and Methods in Physics Research Section B: Beam Interactions with Materials and Atoms*, vol. 204, 2003, pp. 649–659.

[42] R. Grzywacz, C. J. Gross, A. Korgul, S. Liddick, C. Mazzocchi, R. Page, and K. Rykaczewski, "Rare isotope discoveries with digital electronics," *Nuclear Instruments and Methods in Physics Research Section B: Beam Interactions with Materials and Atoms*, vol. 261, no. 1-2, 2007, pp. 1103–1106.

[43] W. Gudowski, "Accelerator-driven transmutation projects. The importance of nuclear physics research for waste transmutation," *Nuclear Physics A*, vol. 654, no. 1-2, 1999, pp. C436–C457.

[44] L. Guo, J. Maruhn, and P.-G. Reinhard, "Triaxiality and shape coexistence in germanium isotopes," *Physical Review C*, vol. 76, no. 3, 2007, p. 034317.

[45] G. Gürdal and E. McCutchan, "Nuclear Data Sheets for A= 70," *Nuclear Data Sheets*, vol. 136, 2016, pp. 1–162.

www.manaraa.com

[46] G. Gürdal, E. A. Stefanova, P. Boutachkov, D. A. Torres, G. J. Kumbartzki, N. Benczer-Koller, Y. Y. Sharon, L. Zamick, S. J. Q. Robinson, T. Ahn, V. Anagnostatou, C. Bernards, M. Elvers, A. Heinz, G. Ilie, D. Radeck, D. Savran, V. Werner, and E. Williams, "Measurements of $g(4_1^+, 2_2^+)$ in ^{70,72,74,76}Ge: Systematics of low-lying structures in $30 \leq Z \leq 40$ and $30 \leq N \leq 50$ nuclei," *Phys. Rev. C*, vol. 88, Jul 2013, p. 014301.

[47] K. Hara, T. Kin, M. Oshima, S. Nakamura, A. Kimura, M. Koizumi, and Y. Toh, "Prompt gamma rays emitted from the neutron capture reaction of ^{74}Ge," *Journal of the Korean Physical Society*, vol. 59, no. 23, 2011, pp. 1832–1835.

[48] J. Hardy, B. Jonson, P. Hansen, and L. Carraz, "The essential decay of pandemonium: gamma-ray spectroscopy," *Phys. Lett. B*, vol. 71, 1977, p. 307.

[49] K. Heyde and J. L. Wood, "Publisher's Note: Shape coexistence in atomic nuclei," *Reviews of Modern Physics*, vol. 83, no. 4, 2011, p. 1655.

[50] S. Hofmann, "On beyond Uranium Science Spectra," 2002, p. 044331.

[51] S. Ilyushkin, J. Winger, K. Rykaczewski, C. Gross, T. Mendez, D. Shapira, D. Stracener, R. Grzywacz, J. Hamilton, J. Batchelder, et al., "THE β AND β-DELAYED NEUTRON DECAY STUDIES OF ^{75}Cu AND ^{77}Cu," *Fission and Properties of Neutron-Rich Nuclei*, World Scientific, 2014, pp. 460–464.

[52] S. Ilyushkin, J. Winger, K. Rykaczewski, C. Gross, D. Stracener, R. Grzywacz, S. Liddick, I. Darby, S. Padgett, J. Batchelder, et al., "The beta decays of ^{75,77}Cu," 2008.

[53] S. V. Ilyushkin, J. A. Winger, C. J. Gross, K. P. Rykaczewski, J. C. Batchelder, L. Cartegni, I. G. Darby, C. Goodin, R. Grzywacz, J. H. Hamilton, A. Korgul, W. Królas, S. N. Liddick, C. Mazzocchi, S. Padgett, A. Piechaczek, M. M. Rajabali, D. Shapira, and E. F. Zganjar, "β decay of the $\pi f_{5/2}$ ground state of ^{77}Cu studied with 225 MeV and 0.2 MeV purified radioactive beams," *Phys. Rev. C*, vol. 80, Nov 2009, p. 054304.

[54] S. V. Ilyushkin, J. A. Winger, K. P. Rykaczewski, C. J. Gross, J. C. Batchelder, L. Cartegni, I. G. Darby, R. Grzywacz, J. H. Hamilton, A. Korgul, W. Królas, S. N. Liddick, C. Mazzocchi, T. Mendez, S. Padgett, M. M. Rajabali, D. Shapira, D. W. Stracener, and E. F. Zganjar, "β-decay studies of the transitional nucleus ^{75}Cu and the structure of ^{75}Zn," *Phys. Rev. C*, vol. 83, Jan 2011, p. 014322.

[55] Y. Ishikawa, N. Kato, S. Suematsu, and T. Kuroyanagi, "The level structure of ^{75}Ge by the ^{74}Ge (d, pγ) reaction," *Nuclear Physics A*, vol. 403, no. 2, 1983, pp. 396–420.

www.manaraa.com

[56] K. Kaneko, T. Mizusaki, Y. Sun, and S. Tazaki, "Systematical shell-model calculation in the pairing-plus-multipole Hamiltonian with a monopole interaction for the $pf_{5/2}g_{9/2}$ shell," *Phys. Rev. C*, vol. 92, Oct 2015, p. 044331.

[57] B. P. Kay, C. J. Chiara, J. P. Schiffer, F. G. Kondev, S. Zhu, M. P. Carpenter, R. V. F. Janssens, T. Lauritsen, C. J. Lister, E. A. McCutchan, D. Seweryniak, and I. Stefanescu, "Properties of excited states in ^{77}Ge," *Phys. Rev. C*, vol. 80, Jul 2009, p. 017301.

[58] T. Kibedi, T. Burrows, M. Trzhaskovskaya, P. M. Davidson, and C. Nestor Jr, "Evaluation of theoretical conversion coefficients using BrIcc," *Nuclear Instruments and Methods in Physics Research Section A: Accelerators, Spectrometers, Detectors and Associated Equipment*, vol. 589, no. 2, 2008, pp. 202–229.

[59] H. Klapdor-Kleingrothaus, I. Krivosheina, A. Dietz, and O. Chkvorets, "Search for neutrinoless double beta decay with enriched ^{76}Ge in Gran Sasso 1990–2003," *Physics Letters B*, vol. 586, no. 3-4, 2004, pp. 198–212.

[60] G. F. Knoll, "Radiation detection and measurement," 2010.

[61] A. Korgul, K. P. Rykaczewski, R. K. Grzywacz, C. R. Bingham, N. T. Brewer, C. J. Gross, C. Jost, M. Karny, M. Madurga, C. Mazzocchi, A. J. Mendez, K. Miernik, D. Miller, S. Padgett, S. V. Paulauskas, M. Piersa, D. W. Stracener, M. Stryjczyk, M. Woli ńska Cichocka, and E. F. Zganjar, "Experimental study of the β decay of the very neutron-rich nucleus ^{85}Ge," *Phys. Rev. C*, vol. 95, Apr 2017, p. 044305.

[62] K. S. Krane, "*Introductory Nuclear Physics*," *Wiley*, 1988.

[63] K.-L. Kratz, H. Gabelmann, P. Möller, B. Pfeiffer, H. Ravn, A. Wöhr, I. Collaboration, et al., "Neutron-rich isotopes around the r-process "waiting-point" nuclei $^{79}_{29}$Cu$_{50}$ and $^{80}_{30}$Zn$_{50}$," *Zeitschrift für Physik A Hadrons and Nuclei*, vol. 340, no. 4, 1991, pp. 419–420.

[64] R. Lecomte, M. Irshad, S. Landsberger, G. Kajrys, P. Paradis, and S. Monaro, "Coulomb-excitation studies of ^{70}Ge, ^{72}Ge, ^{74}Ge, and ^{76}Ge," *Phys. Rev. C*, vol. 22, Dec 1980, pp. 2420–2423.

[65] S. N. Liddick, *Beta-Decay Studies of Neutron-Rich Nuclides and the Possibility of an N = 34 Subshell Closure*, doctoral dissertation, PhD thesis, Michigan State University, 2004.

[66] M. Lipoglavšek, A. Likar, M. Vencelj, T. Vidmar, R. Bark, E. Gueorguieva, F. Komati, J. Lawrie, S. Maliage, S. Mullins, et al., "Measuring high-energy γ-rays with Ge clover detectors," *Nuclear Instruments and Methods in Physics Research Section A: Accelerators, Spectrometers, Detectors and Associated Equipment*, vol. 557, no. 2, 2006, pp. 523–527.

www.manaraa.com

[67] R. Lüttke, E. A. McCutchan, V. Werner, K. Aleksandrova, S. Atwater, H. Ai, R. J. Casperson, R. F. Casten, A. Heinz, A. F. Mertz, J. Qian, B. Shoraka, J. R. Terry, E. Williams, and R. Winkler, "Collectivity in ^{66}Ge and ^{68}Ge via lifetime measurements," *Phys. Rev. C*, vol. 85, Jan 2012, p. 017301.

[68] E. Mané, B. Cheal, J. Billowes, M. Bissell, K. Blaum, F. Charlwood, K. Flanagan, D. Forest, C. Geppert, M. Kowalska, et al., "Ground-state spins and moments of ^{72,74,76,78}Ga nuclei," *Physical Review C*, vol. 84, no. 2, 2011, p. 024303.

[69] M. G. Mayer and J. H. D. Jensen, "Elementary theory of nuclear shell structure," 1955.

[70] E. McCutchan, "Nuclear data sheets for A= 83," *Nuclear Data Sheets*, vol. 125, 2015, pp. 201–394.

[71] G. Meierhofer, P. Grabmayr, L. Canella, P. Kudejova, J. Jolie, and N. Warr, "Prompt γ rays in ^{77}Ge and ^{75}Ge after thermal neutron capture," *The European Physical Journal A*, vol. 48, no. 2, 2012, p. 20.

[72] S. Michimasa, S. Shimoura, H. Iwasaki, M. Tamaki, S. Ota, N. Aoi, H. Baba, N. Iwasa, S. Kanno, S. Kubono, et al., "Proton single-particle states in the neutron-rich ^{23}F nucleus," *Physics Letters B*, vol. 638, no. 2-3, 2006, pp. 146–152.

[73] K. Miernik, K. P. Rykaczewski, R. Grzywacz, C. J. Gross, M. Madurga, D. Miller, D. W. Stracener, J. C. Batchelder, N. T. Brewer, L. Cartegni, A. Fijałkowska, M. Karny, A. Korgul, W. Królas, C. Mazzocchi, A. J. Mendez II, S. W. Padgett, S. V. Paulauskas, J. A. Winger, M. Woli ńska Cichocka, and E. F. Zganjar, "β-decay study of ^{94}Kr," *Phys. Rev. C*, vol. 94, Aug 2016, p. 024305.

[74] S. Mordechai, H. Fortune, R. Middleton, and G. Stephans, "^{74}Ge (t, p) ^{74}Ge Reaction," *Physical Review C*, vol. 18, no. 6, 1978, p. 2498.

[75] S. Mukhopadhyay, B. Crider, B. Brown, S. Ashley, A. Chakraborty, A. Kumar, M. McEllistrem, E. Peters, F. Prados-Estévez, and S. Yates, "Nuclear structure of ^{76}Ge from inelastic neutron scattering measurements and shell model calculations," *Physical Review C*, vol. 95, no. 1, 2017, p. 014327.

[76] A. Negret and B. Singh, "Nuclear Data Sheets for A= 75," *Nuclear Data Sheets*, vol. 114, no. 8-9, 2013, pp. 841–1040.

[77] C. D. Nesaraja, "Nuclear data sheets for A= 69," *Nuclear Data Sheets*, vol. 115, 2014, pp. 1–134.

[78] T. Otsuka, T. Suzuki, R. Fujimoto, H. Grawe, and Y. Akaishi, "Evolution of Nuclear Shells due to the Tensor Force," *Phys. Rev. Lett.*, vol. 95, Nov 2005, p. 232502.

www.manaraa.com

[79] D. Radford, "http://www.tlabs.ac.za/wp-content/uploads/pdf/Radford˙SA2a.pdf," *ORNL Physic Division*.

[80] D. Radford, "Notes on the use of program gf3," *http://radware.phy.ornl. gov/gf3*, 2000.

[81] S. Raman and N. B. Gove, "Rules for Spin and Parity Assignments Based on Logft Values," *Phys. Rev. C*, vol. 7, May 1973, pp. 1995–2009.

[82] B. Ramstein, R. Tamisier, L. Rosier, P. Avignon, and J. Delaroche, "States of ^{76}Ge via (p, p) inelastic scattering at 22 MeV," *Nuclear Physics A*, vol. 411, no. 2, 1983, pp. 231–247.

[83] P. Reeder, R. Warner, R. Liebsch, R. Gill, and A. Piotrowski, "Delayed neutron precursor ^{75}Cu," *Physical Review C*, vol. 31, no. 3, 1985, p. 1029.

[84] U. Rizwan, A. Garnsworthy, C. Andreoiu, G. Ball, A. Chester, T. Domingo, R. Dunlop, G. Hackman, E. Rand, J. Smith, et al., "Characteristics of GRIFFIN high-purity germanium clover detectors," *Nuclear Instruments and Methods in Physics Research Section A: Accelerators, Spectrometers, Detectors and Associated Equipment*, vol. 820, 2016, pp. 126–131.

[85] A. Roberts, A. Howard, J. Kolata, A. Villano, F. Becchetti, P. A. DeYoung, M. Febbraro, S. Freeman, B. Kay, S. McAllister, et al., "Proton pair correlations and the neutrinoless double-β decay of ^{76}Ge," *Physical Review C*, vol. 87, no. 5, 2013, p. 051305.

[86] C. Rouki, A. Domula, J. Drohé, A. Koning, A. Plompen, and K. Zuber, "γ production and neutron inelastic scattering cross sections for ^{76}Ge," *Physical Review C*, vol. 88, no. 5, 2013, p. 054613.

[87] B. Rubio and W. Gelletly, "β decay of exotic nuclei," *Lect. Notes Phys.*, vol. 764, 2009, p. 044331.

[88] B. Rubio, W. Gelletly, E. Nácher, A. Algora, J. Taín, A. Pérez, and L. Caballero, "Beta decay studies with the total absorption technique: past, present and future," *Journal of Physics G: Nuclear and Particle Physics*, vol. 31, no. 10, 2005, p. S1477.

[89] K. P. Rykaczewski, "Conquering nuclear pandemonium," *Physics*, vol. 3, 2010, p. 94.

[90] J. Schiffer, S. Freeman, J. Clark, C. Deibel, C. Fitzpatrick, S. Gros, A. Heinz, D. Hirata, C. Jiang, B. Kay, et al., "Nuclear Structure Relevant to Neutrinoless Double β Decay: ^{76}Ge and ^{76}Se," *Physical review letters*, vol. 100, no. 11, 2008, p. 112501.

www.manaraa.com

[91] J. P. Schiffer, S. J. Freeman, J. A. Caggiano, C. Deibel, A. Heinz, C.-L. Jiang, R. Lewis, A. Parikh, P. D. Parker, K. E. Rehm, S. Sinha, and J. S. Thomas, "Is the Nuclear Spin-Orbit Interaction Changing with Neutron Excess?," *Phys. Rev. Lett.*, vol. 92, Apr 2004, p. 162501.

[92] M. Schumaker, G. Hackman, C. Pearson, C. Svensson, C. Andreoiu, A. Andreyev, R. Austin, G. Ball, D. Bandyopadhyay, A. Boston, et al., "Measured and simulated performance of Compton-suppressed TIGRESS HPGe clover detectors," *Nuclear Instruments and Methods in Physics Research Section A: Accelerators, Spectrometers, Detectors and Associated Equipment*, vol. 570, no. 3, 2007, pp. 437–445.

[93] B. Schürmann, D. Rychel, B. van Krüchten, J. Speer, and C. Wiedner, "Inelastic alpha-scattering from the stable even germanium isotopes," *Nuclear Physics A*, vol. 475, no. 2, 1987, pp. 361–379.

[94] U. Silwal, S. Ilyushkin, J. Winger, K. Rykaczewski, C. Gross, J. Batchelder, L. Cartegni, I. Darby, R. Grzywacz, J. Hamilton, et al., "Detailed β-Decay Study of Neutron Rich ^{76}Cu and Structure of ^{76}Zn Isotope," *APS Division of Nuclear Physics Meeting Abstracts*, 2017.

[95] B. Singh, "Nuclear data sheets," *Nuclear Data Sheets*, vol. 74, no. 63, 1995.

[96] B. Singh, "Nuclear data sheets for A= 73," *Nuclear Data Sheets*, vol. 101, no. 2, 2004, pp. 193–323.

[97] B. Singh, "Nuclear data sheets for A= 80," *Nuclear data sheets*, vol. 105, 2005, pp. 223–418.

[98] B. Singh, "Nuclear Data Sheets for A= 79," *Nuclear Data Sheets*, vol. 135, 2016, pp. 193–382.

[99] B. Singh and A. R. Farhan, "Nuclear data sheets for A= 74," *Nuclear Data Sheets*, vol. 107, no. 7, 2006, pp. 1923–2102.

[100] B. Singh and N. Nica, "Nuclear Data Sheets for A= 77," *Nuclear Data Sheets*, vol. 113, no. 5, 2012, pp. 1115–1314.

[101] P. Srivastava and M. Ermamatov, "Structure of odd Ge isotopes with 40¡ N¡ 50," *Physics of Atomic Nuclei*, vol. 76, no. 6, 2013, pp. 692–701.

[102] I. Stefanescu, W. Walters, R. Janssens, S. Zhu, R. Broda, M. Carpenter, C. Chiara, B. Fornal, B. Kay, F. Kondev, et al., "Identification of the g 9/2-proton bands in the neutron-rich ^{71,73,75,77}Ga nuclei," *Physical Review C*, vol. 79, no. 6, 2009, p. 064302.

www.manaraa.com

[103] D. Stracener, "Status of radioactive ion beams at the HRIBF," *Nuclear Instruments and Methods in Physics Research Section B: Beam Interactions with Materials and Atoms*, vol. 204, 2003, pp. 42–47.

[104] J. Sun, Z. Shi, X. Li, H. Hua, C. Xu, Q. Chen, S. Zhang, C. Song, J. Meng, X. Wu, et al., "Spectroscopy of ^{74}Ge: From soft to rigid triaxiality," *Physics Letters B*, vol. 734, 2014, pp. 308–313.

[105] B. A. Tatum, J. R. Beene, and D. T. Dowling, "The Oak Ridge Isochronous Cyclotron: Enhancements to ORNL's HRIBF driver accelerator," *AIP Conference Proceedings*. AIP, 2001, vol. 600, pp. 148–150.

[106] H. Taylor, R. Schulte, P. Tivin, and H. Ing, "The Decay of 8.0 min ^{74}Ga," *Canadian Journal of Physics*, vol. 53, no. 2, 1975, pp. 107–116.

[107] D. Tilley, H. Weller, and C. Cheves, "Energy levels of light nuclei A= 16–17," *Nuclear Physics A*, vol. 564, no. 1, 1993, pp. 1–183.

[108] Y. Toh, C. Chiara, E. McCutchan, W. Walters, R. Janssens, M. Carpenter, S. Zhu, R. Broda, B. Fornal, B. Kay, et al., "Evidence for rigid triaxial deformation at low energy in ^{76}Ge," *Physical Review C*, vol. 87, no. 4, 2013, p. 041304.

[109] J. Tracy, James L., "A binding energy study of the Atomic Mass Evaluation 2012 and an updated beta-decay study of neutron-rich ^{76}Cu," *PhD diss., Mississippi State University*, 2016, p. 10243335.

[110] J. L. Tracy, J. A. Winger, B. C. Rasco, U. Silwal, D. P. Siwakoti, K. P. Rykaczewski, R. Grzywacz, J. C. Batchelder, C. R. Bingham, N. T. Brewer, L. Cartegni, A. A. Ciemny, A. Fijałkowska, C. J. Gross, C. Jost, M. Karny, K. Kolos, A. Korgul, W. Królas, Y. Liu, M. Madurga, C. Mazzocchi, A. J. Mendez, K. Miernik, D. Miller, S. Padgett, S. V. Paulauskas, D. W. Stracener, M. Woli ńska Cichocka, M. M. Rajabali, and E. F. Zganjar, "Updated β-decay measurement of neutron-rich ^{74}Cu," *Phys. Rev. C*, vol. 98, Sep 2018, p. 034309.

[111] J. Van Roosbroeck, H. De Witte, M. Gorska, M. Huyse, K. Kruglov, D. Pauwels, J.-C. Thomas, K. Van de Vel, P. Van Duppen, S. Franchoo, J. Cederkall, V. N. Fedoseyev, H. Fynbo, U. Georg, O. Jonsson, U. Köster, L. Weissman, W. F. Mueller, V. I. Mishin, D. Fedorov, A. De Maesschalck, N. A. Smirnova, and K. Heyde, "Evolution of the nuclear structure approaching ^{78}Ni : β decay of $^{74-78}$Cu," *Phys. Rev. C*, vol. 71, May 2005, p. 054307.

[112] M. Wang, G. Audi, A. Wapstra, F. Kondev, M. MacCormick, X. Xu, and B. Pfeiffer, "The AME2012 atomic mass evaluation," *Chinese Physics C*, vol. 36, no. 12, 2012, p. 1603.

المنارة للاستشارات
www.manaraa.com

[113] J. Winger, "β-decay Spectrosocpy Studies of Exotic Nuclei," *Priv. Communication*, 2015.

[114] J. Winger, S. Ilyushkin, A. Korgul, C. J. Gross, K. P. Rykaczewski, J. Batchelder, C. Goodin, R. Grzywacz, J. Hamilton, W. Krolas, et al., "DECAY STUDIES OF VERY NEUTRON RICH NUCLEI NEAR ^{78}Ni.," *Acta Physica Polonica B*, vol. 39, no. 2, 2008.

[115] J. A. Winger, "Shell model studies of the N= 50 isotones in the 78Ni'doubly magic'region," 1987.

[116] J. A. Winger, S. V. Ilyushkin, K. P. Rykaczewski, C. J. Gross, J. C. Batchelder, C. Goodin, R. Grzywacz, J. H. Hamilton, A. Korgul, W. Królas, S. N. Liddick, C. Mazzocchi, S. Padgett, A. Piechaczek, M. M. Rajabali, D. Shapira, E. F. Zganjar, and I. N. Borzov, "Large β-Delayed Neutron Emission Probabilities in the ^{78}Ni Region," *Phys. Rev. Lett.*, vol. 102, Apr 2009, p. 142502.

[117] J. A. Winger, K. P. Rykaczewski, C. J. Gross, R. Grzywacz, J. C. Batchelder, C. Goodin, J. H. Hamilton, S. V. Ilyushkin, A. Korgul, W. Królas, S. N. Liddick, C. Mazzocchi, S. Padgett, A. Piechaczek, M. M. Rajabali, D. Shapira, E. F. Zganjar, and J. Dobaczewski, "New subshell closure at $N = 58$ emerging in neutron-rich nuclei beyond ^{78}Ni," *Phys. Rev. C*, vol. 81, Apr 2010, p. 044303.

[118] M. Wolińska-Cichocka, K. P. Rykaczewski, A. Fijałkowska, M. Karny, R. Grzywacz, C. J. Gross, J. Johnson, B. Rasco, and E. Zganjar, "Modular Total Absorption Spectrometer at the HRIBF (ORNL, Oak Ridge)," *Nuclear Data Sheets*, vol. 120, 2014, pp. 22–25.

[119] T. Yoshida, "Estimation of nuclear decay heat for short-lived fission products," *Nuclear Science and Engineering*, vol. 63, no. 4, 1977, pp. 376–390.

www.manaraa.com